Aus dem Adolf-Butenandt-Institut der
Ludwigs-Maximilians-Universität München
Lehrstuhl für Molekularbiologie
Vorstand: Prof. Dr. Peter B. Becker
Arbeitsgruppe: PD Dr. Philipp Korber

Dissection of Nucleosome Positioning Mechanisms by Genome-Wide *In Vitro* Reconstitution

Dissertation zum Erwerb des Doktorgrades der
Naturwissenschaften (Dr. rer. nat.) an der Medizinischen Fakultät
der Ludwig-Maximilians-Universität München

vorgelegt von
Dipl. Biol. Nils Krietenstein
aus Paderborn (Nordrhein-Westfalen)
2017

Gedruckt mit der Genehmigung der Medizinischen Fakultät der Ludwig-Maximilians-Universität München

Betreuer: Prof. Dr. Peter B. Becker

Zweitgutachterin: Prof. Michaela Smolle, PhD

Dekan: Prof. Dr. med. dent. Reinhard Hickel

Tag der mündlichen Prüfung: 15.05.2017

Eidesstattliche Versicherung

Ich erkläre hiermit an Eides statt, dass ich die vorliegende Dissertation mit dem Thema **„Dissection of Nucleosome Positioning Mechanisms by Genome-Wide *In Vitro* Reconstitution**“ selbständig verfasst, mich außer der angegebenen keiner weiteren Hilfsmittel bedient und alle Erkenntnisse, die aus dem Schrifttum ganz oder annähernd übernommen sind, als solche kenntlich gemacht und nach ihrer Herkunft unter Bezeichnung der Fundstelle einzeln nachgewiesen habe.

Ich erkläre des Weiteren, dass die hier vorgelegte Dissertation nicht in gleicher oder in ähnlicher Form bei einer anderen Stelle zur Erlangung eines akademischen Grades eingereicht wurde.

Eidesstattliche Versicherung

_____ _____

Ort, Datum Nils Krietenstein

This thesis is dedicated to my parents, Ingrid and Rainer Krietenstein.

Table of contents

Preface

The results of this work stem from the collaborative efforts of the labs from PD Dr. Philipp Korber, Prof. B. Franklin Pugh, PhD., Prof. Craig L. Peterson, PhD., and Prof. Dr. Karl-Peter Hopfner. We studied effects of purified factors, chromatin remodelers and DNA binding factors, as well as whole cell extracts on genome-wide nucleosome positioning *in vitro*. Chromatin remodeling complexes were purified and their activities validated and quantified by Shinya Watanabe, PhD., (yeast endogenous remodelers) and Dr. Sebastian Eustermann (recombinant INO80 complexes). I purified the DNA binding factors Reb1 and Abf1. Further, I performed all other experiments described in the work here, except Abf1-ChIP-exo and the Chd1 activity assay. Samples for deep sequencing were also prepared by myself and sequenced either at LMU Munich (LaFuGa) or at Pennsylvania State University. Bioinformatics were done by Megha Wal, PhD., for the collaboration with the Pugh and Peterson labs (Krietenstein et al., 2016, Cell), and by myself for the collaboration with the Hopfner lab. The results discussed in this work will be published in at least two primary research papers. The principal technique of reconstituting nucleosome positioning with salt gradient dialysis and *trans*-factors on a genome-wide scale was published by myself and others with PD Dr. Korber as corresponding author (Krietenstein et al., 2012, Methods of Enzymology).

Further, I contributed to publications that studied remodeler contributions *in vivo*. These results are not included in this work, since respective lead authors contributed the most of the work. In addition, together with the members of the Korber lab, I published a review article on genome-wide nucleosome positioning in yeast, with focus on available techniques, nucleosome positioning maps, and current models of nucleosome positioning mechanisms, in a collaborative effort.

Publications covered in this thesis (descending chronological order):

Krietenstein, N.*, Wal, M.*, Watanabe, S., Park, B., Peterson, C.L., Pugh, B.F[§]., and Korber, P[§]. (2016). Genomic Nucleosome Organization Reconstituted with Pure Proteins. Cell *167*, 709–721.e12.

Krietenstein, N., Wippo, C.J., Lieleg, C., and Korber, P[§]. (2012). Chapter Nine - Genome-Wide In Vitro Reconstitution of Yeast Chromatin with In Vivo-Like Nucleosome Positioning. In Methods in Enzymology, Carl Wu and C. David Allis, ed. (Academic Press), pp. 205–232.

Contributions to other manuscripts (chronological order):

Lieleg, C., **Krietenstein, N.**, Walker, M., and Korber, P[§]. (2014). Nucleosome positioning in yeasts: methods, maps, and mechanisms. Chromosoma *124*, 131–151.

Musladin, S., **Krietenstein, N.**, Korber, P[§]., and Barbaric, S[§]. (2014). The RSC chromatin remodeling complex has a crucial role in the complete remodeler set for yeast PHO5 promoter opening. Nucleic Acids Res. 42, 4270–4282.

Pointner, J.*, Persson, J.*, Prasad, P.*, Norman-Axelsson, U., Strålfors, A., Khorosjutina, O., **Krietenstein, N.**, Svensson, J.P., Ekwall, K[§]., and Korber, P[§]. (2012). CHD1 remodelers regulate nucleosome spacing in vitro and align nucleosomal arrays over gene coding regions in S. pombe.

*Co-first authors

[§]corresponding author(s)

Summary

In eukaryotes, nuclear DNA is organized as chromatin, where the nucleosome represents the basic unit. Nucleosomes restrict the accessibility of other DNA binding factors to DNA. Thereby, DNA templated processes, like transcription, DNA replication, and DNA repair, can be influenced by positioned nucleosomes. Genome-wide mapping of nucleosomes in cells showed highly defined rather than random positioning. In particular, a stereotypical pattern of nucleosomal organization was observed at transcription start sites (TSSs) in baker's yeast, *Saccharomyces cerevisiae*, as well as in most other eukaryotes. Upstream of the TSSs there are nucleosome depleted regions (NDRs) that bear regulatory elements, for example transcription factor binding sites and TATA-like elements. The NDRs are flanked by well positioned nucleosomes, the -1 nucleosome upstream and the +1 nucleosome downstream. Over the gene body, an array of equally spaced nucleosomes is aligned to the +1 nucleosomes with its regularity decreasing with distance to the +1 nucleosome. In mutant cells, where the regularity of these genic arrays is disturbed, cryptic promoters within genes become activated leading to the appearance of erroneous transcripts. This is a clear example of nucleosome positioning regulating transcription.

In general, to understand the regulatory impact of chromatin on DNA templated processes, it is essential to study how nucleosome positioning is regulated.

Nucleosome remodeling enzymes ("remodelers") and sequence-specific DNA binding factors of the general regulatory factor (GRFs) class are implicated in the organization of nucleosome positions. In *S. cerevisiae*, the GRFs Abf1 and Reb1 as well as the remodeler RSC are suggested to establish NDRs, while remodelers of the CHD and ISWI families are shown to regularly space nucleosomes *in vitro* and probably are involved in establishing and maintaining nucleosomal arrays *in vivo*. So far, only the simultaneous deletion of multiple and/or all ATPases of the CHD and ISWI families affected the arrays *in vivo*. Therefore, redundant mechanisms appear to exist within a cell.

In vitro, near physiological *S. cerevisiae* nucleosome positioning can be reconstituted by yeast whole cell extracts (WCEs). In such experiments, plasmid libraries containing the entire yeast genome are chromatinized by classical salt gradient dialysis. Nucleosome positions taken after this dialysis do not reflect physiological positions. Only upon incubation with yeast whole cell extracts nucleosomes are positioned to their physiological positions in an ATP-dependent manner, i.e. they adopt the stereotypic NDR-array pattern. This reconstitution experiment demonstrates that nucleosome positioning follows an active mechanism driven by *trans*-factors and provides an *in vitro* system to dissect nucleosome positioning mechanisms despite the *in vivo* redundancy.

Here in this work, we used this *in vitro* system to study the effect of purified remodelers and GRFs on nucleosome positioning, either together with or in absence of mutant yeast whole cell extracts. This allowed the distinction between specific and unspecific, direct and indirect, and sufficient and insufficient nucleosome positioning activities of individual factors. We could identify four stages for the establishment of the NDR-array pattern and the responsible factors for each stage: Stage 1) Generation of NDRs by RSC. This is mediated either by RSC reading poly(dA:dT) elements or by the GRFs Reb1 and Abf1. Stage 2) Positioning of the +1 and -1 nucleosomes by INO80 and/or ISW2. INO80 itself has the intrinsic ability to position +1 nucleosomes, potentially by recognizing DNA shapes. In contrast to INO80, ISW2 on its own is not capable to position +1 nucleosomes but requires GRFs, like Reb1 or Abf1. Stage 3) Both INO80 as well as ISW2 align further nucleosomes to +1 nucleosomes, but with a non-physiologically too wide spacing. Stage 4) ISW1a adjusts a physiological spacing between these array nucleosomes.

Elaborating on the surprising role of INO80 in +1 positioning (stage 2), we purified and tested recombinant INO80 and recombinant histone octamers to establish a purely recombinant system with no factors prepared from *S. cerevisiae*. As the INO80-specified nucleosome positioning was still observed in this entirely recombinant system, we concluded that neither histone variants nor modifications are required to reconstitute INO80-specific nucleosome positioning by INO80 or physiological nucleosome positions by yeast whole cell extract. Catalytically inactivating mutations in the Rvb1 and Rvb2 ATPases did not disturb INO80 to position nucleosomes, suggesting that the activity of these Rvb1/2 ATPases are not involved in nucleosomes remodeling and +1 nucleosome positioning. Additionally, we could show that the spacing generated by INO80 is independent of nucleosome density, demonstrating that INO80 has nucleosome clamping activity. Surprisingly, even though it was reported previously that the deletion of histone tails did not affect INO80 remodeling activity in sliding assays, we found that it did inhibit +1 nucleosome positioning by INO80. Thus, nucleosome positioning by INO80 can be uncoupled from nucleosome remodeling.

Overall, in this work we present the first *in vitro* reconstitution of an *in vivo*-like structure on a genome-wide scale with only purified factors. Biochemistry allowed us to confirm known and to identify new activities of chromatin remodelers or DNA binding factors contributing to genome-wide nucleosome organization. We could identify four mechanistic stages that lead to a physiological nucleosomal NFR-+1-array organization. In a further advancement, we used only recombinant factors that allow more detailed mechanistic studies. This demonstrates that this *in vitro*-system is a powerful tool to study a novel aspect of nucleosome remodeling by different remodelers, i.e. genome-wide nucleosome positioning on physiological DNA sequences.

Zusammenfassung

In Eukaryonten ist die nukleäre DNA als Chromatin organisiert, wobei eine erste Einheit das Nukleosom darstellt. Nukleosomen verhindern den Zugang zu DNA für andere DNA-bindende Faktoren. Daher können DNA geleitete Prozesse, wie die Transkription, DNA-Replikation und DNA-Reparatur, durch positionierte Nukleosomen beeinflusst werden. Die genomweite Kartierung von Nukleosomen zeigte, dass Nukleosomenpositionen eher klar definiert als zufällig sind. Insbesondere wurde ein stereotypisches Nukleosomenmuster an Transkriptionsstartstellen (TSSs) in der Bäckerhefe *Saccharomyces cerevisiae* sowie in den meisten anderen Eukaryonten gefunden. Stromaufwärts von diesen TSSs befinden sich nukleosomenarme Regionen (NDRs). Diese enthalten regulatorische Elemente, wie zum Beispiel Transkriptionsfaktorbindestellen und TATA-ähnliche Elemente. Die NDRs werden von gut positionierten Nukleosomen flankiert, den -1 Nukleosomen stromaufwärts und den +1 Nukleosomen stromabwärts. Ausgerichtet am +1 Nukleosom befindet sich eine Array abstandsgleicher Nukleosomen über dem Strukturgen, wobei die Regularität der Abstände mit der Entfernung zum +1 Nukleosom nachlässt. In Mutantenzellen, in denen die Regularität dieser nukleosomaler Arrays gestört ist, werden kryptische Promotoren aktiviert. Das führt zum Auftreten fehlerhafter Transkripte und ist ein eindeutiges Beispiel für die Regulation der Transkription durch Nukleosomenpositionierung.

Um den regulatorischen Einfluss von Chromatin auf DNA-Matrizenprozesse zu verstehen, ist es entscheidend zu untersuchen, wie die Nukleosomenpositionierung reguliert wird.

Unter anderem wurden Nukleosomen-Remodulierungsenzyme („Remodelers“) und sequenzspezifische DNA-bindende Faktoren aus der Klasse der generellen regulatorischen Faktoren (GRFs) in den Zusammenhang mit der Organisation von Nukleosomenpositionen gebracht. Für *S. cerevisiae* wurde eine Beteiligung der GRFs Reb1 und Abf1 sowie des Remodelers RSC an der NDR-Formierung nahegelegt, während die *In vivo*- und *In vitro*-Beteiligung der Remodeler aus den CHD- und ISWI-Familien an der Etablierung und Erhaltung abstandsgleicher nukleosomaler Arrays aufgezeigt wurde. Bislang führte nur die simultane Abwesenheit mehrerer oder aller ATPasen der CHD- und ISWI-Familien zu Effekten dieser Arrays *in vivo*. Deshalb erschien es, als ob redundante Mechanismen in einer Zelle existierten.

Durch Hefeganzzellextrakte konnten annähernd physiologische *S. cerevisiae* Nukleosomenpositionen *in vitro* rekonstituiert werden. In solchen Experimenten wurden Plasmidbanken, die das ganze Hefegenom abdecken, durch klassische Salzgradientendialyse chromatinisiert. Nukleosomenpositionen, die hierdurch eingestellt wurden entsprachen nicht physiologischen Positionen. Erst durch die Inkubation mit Hefeganzzellextrakten wurden

Nukleosomen ATP-abhängig zu ihren physiologische Positionen repositioniert, d. h. sie bildeten das stereotypische NDR-array Muster. Dieses Rekonstitutionsexperiment zeigte, dass die Nukleosomenpositionierung einem aktiven und durch *trans*-Faktoren getriebenen Mechanismus folgt, und bietet somit ein *In vitro*-System, das die mechanistische Analyse der Nukleosomenpositionierung ermöglicht, unabhängig von deren *In vivo*-Redundanz.

In dieser Arbeit nutzten wir dieses *In vitro*-System, um die Effekte von aufgereinigten Remodelern und GRFs mit oder ohne Mutantenhefeganzzellextrakten zu studieren. Das erlaubt die Unterscheidung zwischen spezifischen und unspezifischen, direkten und indirekten und hinreichenden oder unzulänglichen Aktivitäten der Faktoren. Wir konnten vier Phasen zur Etablierung des NDR-array-Musters und die verantwortlichen Faktoren identifizieren: Phase 1) Ausbildung der NDR durch RSC. Dieses wird durch direkt von RSC gelesenen poly(dA:dT) Elementen oder durch die GRFs Reb1 und Abf1 vermittelt. Phase 2) Positionierung der +1 und -1 Nukleosomen durch INO80 und/oder ISW2. INO80, hat die intrinsische Eigenschaft +1 Nukleosomen zu positionieren, möglicherweise durch die Erkennung von Formen der DNA. Im Gegensatz zu INO80 ist ISW2 nicht in der Lage selbstständig +1 Nukleosomen zu positionieren, sondern benötigt hierfür GRFs, wie Reb1 oder Abf1. Phase 3) Beide, sowohl INO80 als auch ISW2, setzen weitere Nukleosomen neben das bereits positionierte +1 Nukleosom, jedoch mit einem nicht-physiologischen, zu weitem Abstand. Phase 4) ISW1a stellt den physiologischen Abstand in diesen nukleosomaler Arrays ein.

Um die überraschende Rolle von INO80 bei der +1-Positionierung weiterzuverfolgen, reinigten und testeten wir rekombinanten INO80-Komplex und rekombinante Histonoktamere, sodass wir ein rein rekombinantes System, ohne einen aus *S. cerevisiae* gereinigten Faktor, erzeugten. Mittels diesen rekombinanten Systems konnten wir zeigen, dass weder Histonvarianten noch Modifikationen für die Rekonstitution INO80-spezifischer Nukleosomenpositionen durch INO80 oder physiologischer Nukleosomenpositionen durch einen Hefeganzzellextrakt benötigt wurden. Katalytisch inaktive Mutanten der Rvb1- und Rvb2-ATPasen störten INO80 nicht, Nukleosomen zu positionieren. Das lässt vermuten, dass die Rvb1/Rvb2 ATPase-Aktivität nicht an der Nukleosomenremodulierung und an der +1-Nukleosomenpositionierung beteiligt ist. Zusätzlich konnten wir zeigen, dass der durch INO80 generierte Abstand unabhängig von der Nukleosomendichte war, was demonstrierte, dass INO80 clamping Aktivität besitzt. Überraschenderweise inhibierte die Beseitigung von Histonschwänzen die +1-Positionierung durch INO80, obwohl es bekannt war, dass es nicht die Remodulierungsaktivität von INO80 betrifft.

Zusammengefasst betrachtet konnten wir in dieser Arbeit die erste *In vitro*- Rekonstitution einer Struktur im genomweiten Maßstab mit ausschließlich aufgereinigten Faktoren präsentieren. Diese biochemische Herangehensweise erlaubte es uns, bekannte Aktivitäten, die zur genomweiten Nukleosomenorganization beitragen, von Chromatin-Remulierungsenzymen und DNA-Bindefaktoren zu bestätigen und neue zu identifizieren. Wir konnten vier mechanistische Phasen, die zur physiologischen NFR-+1-array Nukleosomenorganization führen, identifizieren. In einer Weiterentwicklung benutzten wir ausschließlich rekombinanten Faktoren, was detailliertere Studien erlaubt. Das demonstriert, dass dieses *In vitro*-System ein wirkmächtiges Werkzeug ist, um eine neue Eigenschaft von Remodelers zu studieren, nämlich die genomweite Nukleosomenpositionierung auf physiologischen DNA-Sequenzen.

1 Introduction

In eukaryotic cells chromosomes are organized into chromatin to accommodate extremely long DNA molecules, for example, 2 m DNA in diploid human cells, into a nucleus with a few micron in diameter. The most basic unit of DNA packaging is the nucleosome, where DNA is wrapped around a histone octamer (Richmond et al., 1984). Arrays of nucleosomes were described as beads on a string when first visualized by electron microscopy (EM) (Olins et al., 1975). These nucleosomal arrays can be further condensed by other proteins, like linker histone H1 (Thoma et al., 1979; Zhou et al., 1998) or corepressor complexes (Fan et al., 2004; Francis et al., 2004; Sekiya and Zaret, 2007), and by packing of nucleosomes against each other into higher order structures (Schwarz and Hansen, 1994). Through histone DNA interactions in a nucleosome, a substantial part of DNA surface becomes deeply engulfed (Luger et al., 1997), which leads to restricted accessibility of DNA to binding proteins, like transcription factors (TF) (Hahn and Young, 2011; Rando and Winston, 2012; Yu and Morse, 1999). Therefore chromatin represses DNA templated processes, like transcription, replication, and DNA repair (Schones et al., 2008; Siriaco et al., 2009; Weiner et al., 2015). In consequence, the degree of DNA compaction into chromatin also offers a level of regulating these processes.

1.1 Organization and structure of chromatin

1.1.1 The primary structure of chromatin

In the 19th century, Walter Flemming discovered a stainable substance in the nucleus and termed it chromatin. Decades later, nucleosomes were identified to form regular structures that confer resistance of distinctly sized DNA fragments – and multiples of it – to nuclease digestion (Hewish and Burgoyne, 1973). These regular nucleosome structures were later identified to consist of four stoichiometric proteins (Kornberg, 1974), the histones, that form the nucleosomes and appear as “beads-on-a-string” in electron micrographs (Olins et al., 1975). In 1997, the first nucleosome high resolution structure was solved (Luger et al., 1997) that confirmed low resolution structures (Arents et al., 1991; Richmond et al., 1984) and extended previous models: The histone octamer is composed of four, relatively small (20-25 kDa), spirally arranged core (“canonical”) histones H2A, H2B, H3, and H4 with two copies each (Figure 1.1 A). 147 bp of DNA are wrapped around a histone octamer in 1.65 left-handed super-helical turns. 80% of the histone proteins contribute to the barrel- or disc-like structure of the core nucleosome while the other 20%, the so called histone tails, remain rather unstructured (Luger et al., 1997). This nucleo-protein complex has a mass of 206 kDa, a height of 5.5 nm, and a diameter of 11 nm (Richmond et al., 1984).

The central base pair of the 147 bp DNA fragment defines the nucleosome dyad and is located at the pseudo-symmetrical axis of the histone octamer (Luger et al., 1997). At this position, the DNA major groove faces the histone core and is defined as superhelix location zero (SHL0). Each successive DNA helical turn is then counted as negative or positive superhelix location, depending on its position relative to the dyad axis. Thus, the location number increases from -7 to 0 SHL for the first 73 bp and from 0 to +7 SHL for the second 73 bp with respect to the DNA entry site. Wrapping DNA on the histone octamer surface causes a decrease in helical twist, from 10.5 to 10.2 bp per helical turn (Tolstorukov et al., 2007). The relative orientation of a DNA base pair to the histone core is described as the rotational positioning (Drew and Travers, 1985). As the relative orientation of major and minor groove towards the histone auto-correlates with a 10 bp periodicity, also the rotational positioning recurs along a nucleosome with 10 bp periodicity. *In vivo*, a 10 bp periodic distribution of AT and GC dinucleotides was observed on average for DNA that is incorporated into nucleosomes (Albert et al., 2007). GC dinucleotides were preferentially found at rotational positions where the major groove faces the histone core and AT dinucleotides where the minor groove faces the histone core (Figure 1.1 B). The primary structure of chromatin resembles "beads-on-a-string" (Olins et al., 1975), where nucleosome core particles are linked by short stretches of DNA, the linker DNA (van Holde, 1989). In general, the term nucleosome describes the nucleosome core particle plus linker DNA. In this work the term nucleosome is used to describe the core nucleosome particle without linker DNA.

These nucleosomal arrays represent the primary structure of chromatin, the so called 10 nm fiber. The average distance between these core particles is called spacing or nucleosomal repeat length (NLR). The spacing within cells of the same type is largely constant, but it can vary between species or between tissue cell types within one species (van Holde 1998). For the budding yeast *S. cerevisiae*, the model organism used in this study, the average linker length is 18 bp (Jiang and Pugh, 2009a; Thomas and Furber, 1976).

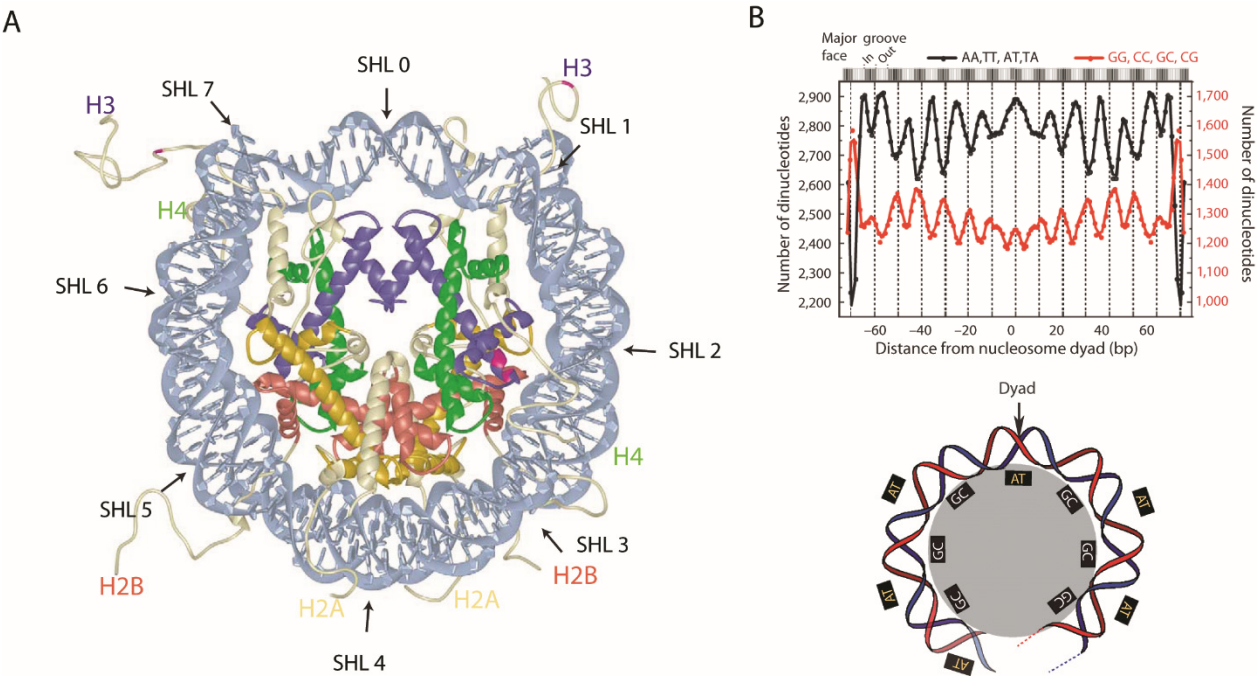

Figure 1.1 Overview of the nucleosome core particle structure. (A) Scheme of the nucleosome high-resolution crystal structure published by Luger et al., Nature 1997, showing the wrapping of DNA (light blue) around the histone octamer (two copies of each H2A shown in yellow, H3 shown in blue, H4 shown in green, and H2B shown in red) in 1.65 left-handed helical turns. Super helical locations (SHL) 1-7 are indicated for the view side of the nucleosome. [Adapted and reprinted with permission from Elsevier (Luger, 2003)]. (B) Smoothed frequency distribution of AA, TT, AT and TA or GC, CC, GC, and CG along 147 bp nucleosomal DNAs from yeast (BY4741)(top). Schematic representation of preferred dinucleotide distribution within a nucleosome (bottom)[Adapted and reprinted with permission from Nature Publishing Group (Albert et al., 2007)]

Another feature of the primary chromatin structure are nucleosome free regions (NFRs), alternatively called nucleosomes depleted regions (NDR) (Jiang and Pugh 2009b; Struhl and Segal 2013), which are typically 150-200 bp in length. Originally, these regions were termed hypersensitive sites (Wu, 1980), since they are especially sensitive to digestion by nucleases. Often these hypersensitive sites contain regulatory elements, like promoters, enhancers, and origins of replication (Almer and Hörz, 1986; Bell et al., 2011; Berbenetz et al., 2010; Eaton et al., 2010; Elgin, 1981), and are often modulated in response to signals. For example, hormone inducible enhancers become hypersensitive upon hormone induction (Reik et al., 1991) or promoters of the *PHO* regulon become hypersensitive to nuclease digestion upon phosphate starvation (Almer et al., 1986), correlating in increased transcription of downstream genes. Such NDRs are often flanked by highly positioned nucleosomes (Hughes and Rando, 2014; Lieleg et al., 2014). In *S. cerevisiae*, for example, most promoters correlate with NDRs and show a stereotypical nucleosomal NDR-+1-array organization (Lee et al., 2007; Yuan et al., 2005) (Figure 1.2). Here, the NDRs are flanked by two highly positioned nucleosomes, the -1 and +1 nucleosomes. Over the gene bodies, nucleosomal arrays with regularly spaced nucleosomes are aligned to +1 nucleosomes. The regularity of nucleosomal arrays decreases with distance to NDRs.

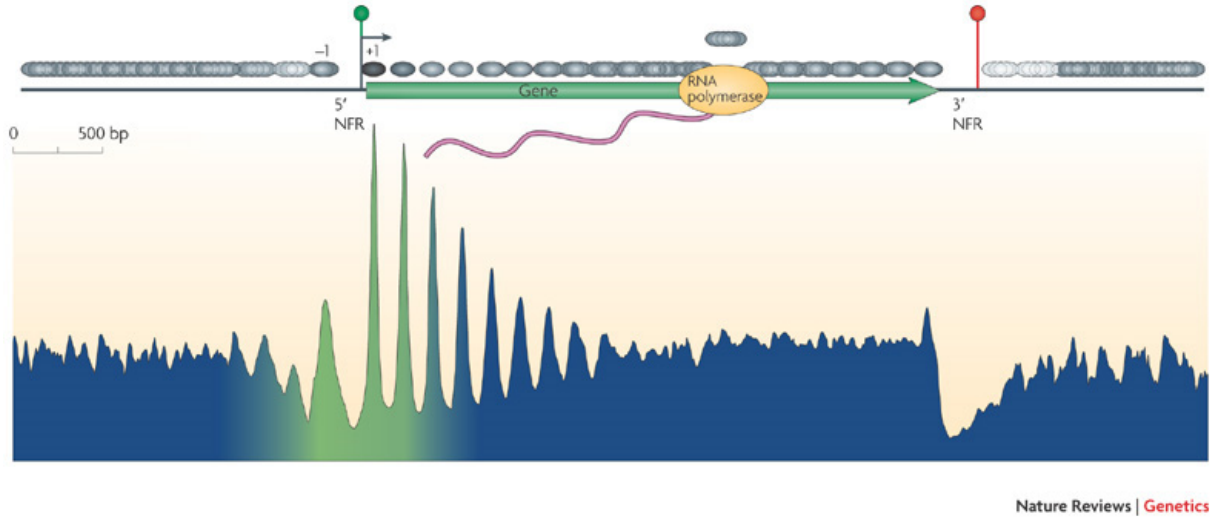

Figure 1.2 Stereotypical NDR-array organization in S. cerevisiae. Average nucleosome dyad density distribution as a composite of all genes aligned at transcription start sites (TSS)(indicated by arrow). Actively transcribed genes (green lollipop) display a stereotypical NDR-array pattern. NDRs are flanked by highly positioned -1 and +1 nucleosomes. The +1 nucleosome is flanked by a regularly spaced nucleosomal array. [Adapted and reprinted with permission from Nature Publishing Group *(Jiang and Pugh, 2009b)*]

1.1.2 Histone variants and modifications

The nucleosome composition can be varied by incorporation of histone variants. Histone variants are non-allelic isoforms of the canonical histones (reviewed in: Hake and Allis, 2006; Henikoff and Ahmad, 2005; Szenker et al., 2011; Weber and Henikoff, 2014). These histone variants are incorporated into chromatin by chromatin remodelers and histone chaperones (Drane et al., 2010; Goldberg et al., 2010; Tagami et al., 2004; Torigoe et al., 2011). The incorporation of such variants is often site-specific. *S. cerevisiae*, for example, has two histone variants: Htz1 (Santisteban et al., 2000) and Cse4 (Meluh et al., 1998). Htz1 is the homolog of H2A.Z in other species, which is enriched at the +1 nucleosome positions at transcribed and untranscribed genes (Guillemette et al., 2005; Raisner et al., 2005; Zhang et al., 2005). Therefore, it is thought to be involved in transcriptional regulation. Cse4 is the centromere-specific H3 variant, a homologue to the human CenH3 (Amor et al., 2004). Centromeric variants are specifically incorporated at centromeres. A curiosity in *S. cerevisiae* is that there is only one centromeric nucleosome, which is very precisely positioned (Cole et al., 2011a), while most other eukaryotes have regional centromeres encompassing many nucleosomes. In contrast to *S. cerevisiae*, almost 20 histone variants are known for humans that can be expressed in a cell cycle or cell type-specific way.

Besides the incorporation of histone variants, chromatin composition can be altered by post translational modifications (PTMs) (reviewed in: Bannister and Kouzarides, 2011; Kouzarides, 2007). PTMs are small chemical modifications to amino acids that are set and removed in histones by specific histone modifying enzymes. Histone modifications mostly occur at specific amino acids at histone tails but can also occur in the globular histone domains (Jack and Hake, 2014).

Such histone modifications are most common at serine, lysine, arginine and threonine and include phosphorylation, acetylation, methylation, ubiquitylation, and more. Histone modifications can alter the biophysical properties of chromatin, e.g., by adding or neutralizing charges. Further, and maybe more important, many chromatin factors have histone modification-specific binding domains that allow site-specific targeting to modified histones. The variety of chemical modifications in combination with the multitude of histone modification sites led to the proposal of the histone code (Jenuwein and Allis, 2001). Here, chromatin factors are recruited to sites specified by histone marks and thereby confer specific functionalities to specific regions of the genome. It is still under debate if such a mechanism amounts to a real code in the sense that there is multivalent binding to distinct combinations of histone marks and not mainly one-to-one relations of PTMs and readers as typical of signaling pathways (Rando, 2012). There are numerous examples that distinct modifications correlate with distinct DNA template processes, like histone H3 lysine 9 methylation correlates with constitutive heterochromatin and histone H4 lysine 4 methylation at promoters with transcriptional activity (Weiner et al., 2015). Nonetheless, extensive genome-wide ChIP-seq mapping of histone PTMs and principal component analysis revealed that many histone modifications correlate with similar affects, which suggests that a possible histone code would be rather redundant (Sadeh et al., 2016; Weiner et al., 2015).

In summary, chromatin is decorated by histone modifications and histone variants. The site-specific integration of histone variants and the correlation of histone modifications with distinct DNA templated processes as well as the correlation of miss-regulation of such chromatin features with disease states (Zink and Hake, 2016) underscore that histone variants and PTMs have regulatory functions.

1.1.3 Chromatin higher order structure

Through packaging of DNA into chromatin the negative charge of DNA is neutralized to some extent by basic histone proteins, which facilitates compaction. However, simply wrapping the DNA around the histone core is not sufficient to fit the DNA into the small nucleus. In theory, the level of compaction has to be five times higher than predicted for the 10-nm fiber (reviewed in Maeshima et al., 2014). So there have to be higher order structures, even more for the case of mitotic chromosomes where chromatin is most compacted. Indeed, by EM a chromatin fiber with 30 nm diameter was detected in preparations from rat liver cells (Finch and Klug, 1976). Initially, the existence of this so-called “30 nm fiber” was interpreted by the “solenoidal model” for superstructure in chromatin. Today, there are two prominent models that could describe the repeating structure within a 30 nm fiber: the “one-start” and the “two-start” helix model (reviewed

in Grigoryev and Woodcock, 2012). The "one-start" or solenoid model describes a tube or spiral that is formed by approximately 6 nucleosomes per turn (Figure 1.3 A) (Finch and Klug, 1976). Alternatively, the "two-start" model suggests a "zig-zag" structure, where the first nucleosome (N1) is close to the third nucleosome (N3) and the second nucleosome (N2) to the fourth nucleosome (N4) (Figure 1.3 B). Such a latter structure was first observed in chromatin isolated from chicken erythrocytes (Woodcock et al., 1984). Crystal and cryo-EM structures of *in vitro* reconstituted chromatin fibers with four (tetramer) and 12 (dodecamer) nucleosomes support the "two-start" model (Schalch et al., 2005; Song et al., 2014). Crosslinking of *in vitro* reconstituted chromatin fibers with 12 or 10 nucleosomes and subsequent cleavage of inter-nucleosomal DNA resulted in SDS-PAGE migration patterns of 6 and 5 nucleosomes respectively, suggesting spatial relations of two independent groups and therefore supporting the zig-zag organization (Dorigo et al., 2004). However, most evidence for structures of the 30 nm fiber were derived from (cryo-) EM and crystal structures. Both methods involve harsh sample preparation conditions, like artificial salt conditions or sample drying, which can strongly impact chromatin compaction and higher order folding.

Recently, nucleosome-nucleosome interactions were mapped on a genome-wide scale *in vivo* by Micro-C and Micro-C XL (Hsieh et al., 2015, 2016). There, abundant interactions of nucleosomes within one gene ("gene-crumple") were observed. This is consistent with so called "clutches" detected by super high resolution microscopy (Ricci et al., 2015) that were interpreted as structures consisting of few nucleosomes. Nonetheless, none of this would supports either the one-start (solenoid) nor the two-start (zig-zag) model (Hsieh et al., 2015). Most experiments that aimed to visualize the 30 nm fiber *in vivo* failed (Maeshima et al., 2016a), except for chicken erythrocytes that are mostly transcriptionally inactive (Woodcock, 1994). Therefore, the *in vivo* existence and relevance of the 30 nm fiber is still under debate. Alternatively, the chromatin higher order structure may mainly consist of rather undefined aggregations of nucleosomes, which has been called a "liquid-like state" of chromatin (Maeshima et al., 2016b).

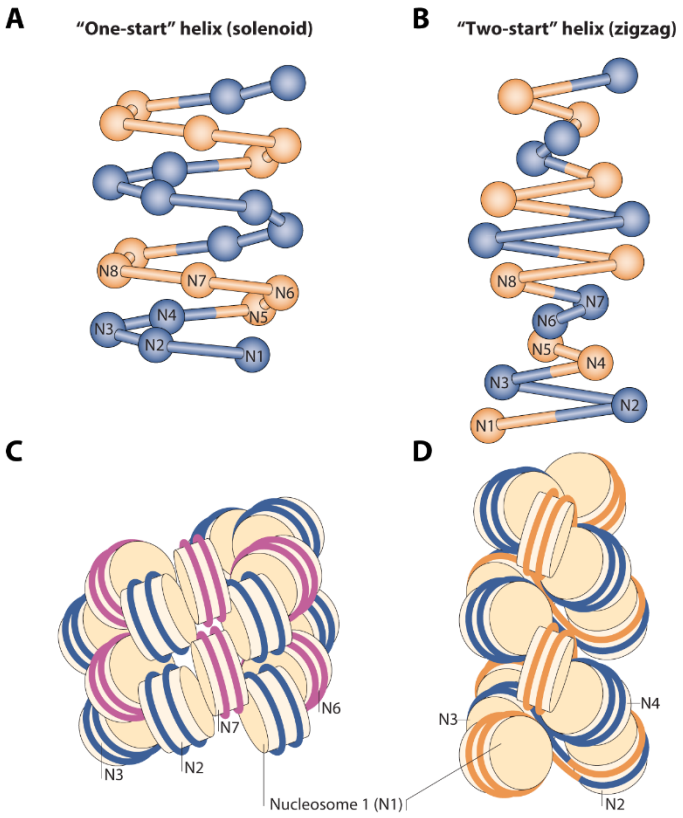

Figure 1.3 "One-start" and "Two-start" models for the 30 nm fiber. *(A/C) "One-start" helix or solenoid model. Nucleosomes (N) follow a helical trajectory with bending of the linker DNA. (B/D) "Two-start" helix or zigzag model. Straight linkers are formed between neighboring nucleosomes aligning two rows (N1, N3, N5, ... and N2, N4, N6, ...) in a zigzag conformation.* [Adapted and reprinted with permission from Nature Publishing Group *(Luger et al., 2012)*]

1.2 Nucleosome positioning: Organization and mechanisms

In the most basic view, regulation of DNA template processes by chromatin is imparted by differential DNA accessibility. Either DNA is free and accessible to binding by regulatory factors or access is restricted because the DNA is incorporated into a nucleosome (Li et al., 2005). Therefore, it is essential to understand where and how nucleosomes are positioned at genomic features, like genes, as mainly this decides which DNA stretch is accessible and which one is not. Most techniques to determine nucleosome positions use nucleases, like DNaseI and MNase (Elgin, 1981; Keene and Elgin, 1981; Wu, 1980; Wu et al., 1979). DNA that is wrapped around a histone octamer is more protected against nuclease digestion compared to free DNA (Hewish and Burgoyne, 1973). Detection of the protected DNA with single locus-specific probes (indirect end-labeling) or at genome scale (micro array or next-generation sequencing) allows the determination of nucleosome positions at single loci or across an entire genome (Lee et al., 2007; Yuan et al., 2005). This way, nucleosome positioning studies revealed that nucleosomes are not randomly distributed throughout genomes but are highly positioned relative to genomic features.

1.2.1 Terminology of nucleosome positioning

Most nucleosome positioning techniques study nucleosome positions in a population of DNA molecules. Therefore, a nucleosome position is in general an average derived from many nucleosomes at different DNA molecules. The distribution of the nucleosome position population is usually Gaussian (Cole et al., 2012). Terms to describe different aspects of nucleosome positioning are: translational and rotational positioning, nucleosome occupancy, and nucleosomal repeat length (NRL) or spacing (Figure 1.4) (reviewed in Lieleg et al., 2014).

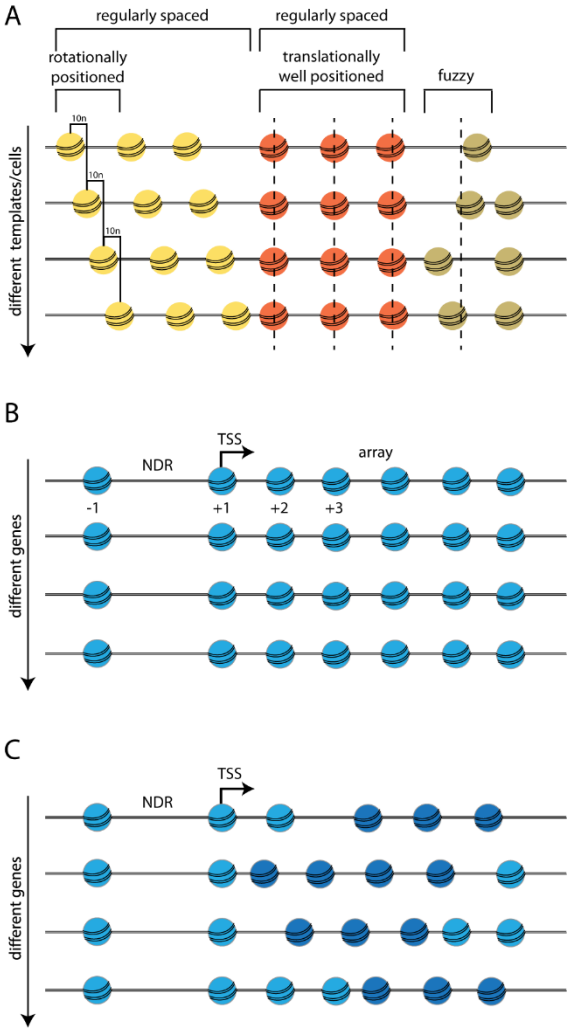

Figure 1.4 Concepts of nucleosome positioning. (A) Illustration of terms defined in "Terminology of nucleosome positioning" (1.2.1). (B) Stereotypical NDR-array organization of different genes aligned at a common reference point (TSS). The first nucleosome downstream of the TSS is termed +1 nucleosome, the following nucleosomes subsequently +2, +3, etc. The +1 nucleosome of many genes is located at a fixed distance for many genes. Upstream of the +1 nucleosome is the NDR located, which contains the promotor. Nucleosome downstream of the +1 nucleosome display cell type-specific spacing. Alignment points, such as the TSS are used for composite representations, e.g., Figure 1.2. (C) Light blue nucleosomes have unchanged positions compared to B, dark blue nucleosomes have altered positions, but are regularly spaced to each other. Such a nucleosomal rearrangement would lead less observed regularity in composite representation but would yield regularly spaced patterns in bulk "MNase ladders". [Adapted and reprinted with permission from Chromosoma (Lieleg et al., 2014)]

"Translational positioning" describes a nucleosomal position relative to a genomic coordinate. Usually the nucleosome dyad position is used as reference point within the nucleosome as only

one base pair coincides with the nucleosomal dyad (1.1.1)(Luger et al., 1997). Translationally well positioned nucleosomes occupy the same position at the same genomic coordinate for all cells in the population. In contrast, "fuzzy" nucleosomes have a broader distribution of nucleosome dyad positions around a given base pair within the population (Figure 1.4). "Nucleosome positioning" is most commonly understood as translational positioning and also used as such in this work.

"Rotational positioning" describes the position of a given DNA base pair relative to the histone octamer within the nucleosome. As described in 1.1.1, the DNA helix is wrapped around the histone octamer with periodic contacts. About every 10 bp the DNA binds to the histone octamer surface. At the nucleosome dyad, the major groove of a DNA helix faces the histone octamer and the minor groove faces to the outside. This pattern repeats for SHL -7 to 7 (1.1.1). If the major or minor groove faces to the outside affects DNA accessibility for binding factors. As the relative orientation of major and minor groove auto-correlates with a 10 bp periodicity, also the rotational positioning recurs along a nucleosome with 10 bp periodicity. In other words, nucleosomes with translational positions that are offset by multiples of 10 bp have the same rotational positioning. Hydroxyl radical nucleosome mapping, a method that allows nucleosome mapping at base pair resolution, showed that the Gaussian distributions of nucleosome positions have a 10 bp periodic substructure (Brogaard et al., 2012). Therefore, most translationally fuzzy nucleosomes nonetheless largely maintain the same rotational positioning.

The probability of a given base pair to be incorporated in any nucleosome is called "nucleosome occupancy". This metric is uncoupled from the question of high versus fuzzy translational positioning. For example, there can be highly positioned nucleosomes with low occupancy, if only few cells show a nucleosome at this position, and all other combinations of these terms.

The NRL or nucleosome spacing describes the average distance between nucleosomes in regular arrays and is mostly defined as dyad-to-dyad distance. The NRL can be measured by MNase ladders or as the average distance of nucleosome peaks in genome-wide sequencing. Whereas the MNase ladder directly gives the distribution of fragment sizes originating from one, two, three, …, next neighbor nucleosomes on the same molecule, the latter infers the NRL from positions of mapped mono-nucleosomes. In any case, the NRL reflects an average of many nucleosomes rather than a property of individual nucleosomes.

1.2.2 Nucleosome positioning patterns

The nucleosome positioning patterns (maps) throughout the whole genome for more than 30 species are known (reviewed Lieleg et al., 2014). In addition, tissue-specific maps for multicellular organisms and maps of chromatin factor mutants, especially for yeasts, are available. In all maps, the depletion of nucleosomes from regulatory elements, such as promoter and terminator regions, replication origins, enhancers and insulators, is observed (Givens et al., 2012; Lantermann et al., 2010; Lee et al., 2007; Mavrich et al., 2008a; Nishida et al., 2013; Schones et al., 2008; Tsankov et al., 2010; Valouev et al., 2008; Yuan et al., 2005).

In budding yeast, most of the genome consists of genes. Therefore, understanding how nucleosomes are organized at promoters and over coding regions will help to understand the vast majority of nucleosomes in yeast. Broadly, two general types of nucleosome positioning patterns at promoters are observed in *S. cerevisiae*: stereotypical (also called canonical) and non-stereotypical organization (Cairns, 2009; Hughes and Rando, 2014; Jiang and Pugh, 2009b; Tirosh and Barkai, 2008).

1.2.2.1 Promotors with stereotypical nucleosome organization

Constitutively expressed and mainly TFIID-dependent genes (Huisinga and Pugh, 2007) are those that show a stereotypical or canonical promoter chromatin organization and are the majority in yeast. Such a nucleosomal organization is characterized by an NDR-+1-array organization (Figure 1.2). The region just upstream of the TSS corresponds to an NDR, contains the promotor, is enriched with TF- binding sites, depleted for TATA elements, but contains TATA-like elements (Lee et al., 2007; Rhee and Pugh, 2012). In *S. cerevisiae*, these NDRs have an average size of 150 bp and are flanked by two well positioned nucleosomes, the -1 and +1 nucleosomes (Jiang and Pugh, 2009a). The +1 nucleosome is positioned such that the TSS is located on average 12 bp within the +1 nucleosome upstream border, i.e. this border is at -12 bp relative to the TSS (Lee et al., 2007; Mavrich et al., 2008b). A regular nucleosomal array with an NRL of 165 bp is aligned to the +1 nucleosome. The +1 and +2 nucleosomes have the highest degree of translational positioning, which decreases along the nucleosomal array with distance to the NDR (Jiang and Pugh, 2009a; Yuan et al., 2005). With minor variations, this stereotypical NDR-+1-array nucleosome organization is conserved through evolution from yeast to man. The main differences are the distance between the TSS and the +1 nucleosome and the NRLs. For example, in *H. sapiens* the 5' border of the +1 nucleosome is located at +40 bp for active and at +10 bp for inactive promoters relative to the TSS (Schones et al., 2008), and these distances vary also for other species, like *C. elegans*, *D. melanogaster* as well as other yeasts (Mavrich et al., 2008a; Tsankov et al.,

2010; Valouev et al., 2008). Regarding the NRL, it ranges from 154 bp in *S. pombe* and *Aspergillus nidulans* (Givens et al., 2012; Lantermann et al., 2010; Moyle-Heyrman et al., 2013; Nishida et al., 2013) to 177 bp in *Kluyveromyces lactis* (Tsankov et al., 2010) to 197 bp in *D. melanogaster* (Becker and Wu, 1992). In *H. sapiens* the NLR depends on the cell type (Mavrich et al., 2008a; Valouev et al., 2011).

1.2.2.2 Promoters with a non-stereotypical nucleosome organization

Genes that have a non-stereotypical promoter organization are the so-called "stress" or "environmentally responsive" genes (Cairns, 2009; Hughes and Rando, 2014)(Figure 1.5). Such genes are often transcriptionally repressed at normal, unstressed growth conditions. Their promoters often contain TATA boxes and TF binding sites, which are broadly distributed over the promoter (Basehoar et al., 2004; Venters et al., 2011) and are often occupied by nucleosomes under repressed conditions. On average, these genes do not show stereotypical nucleosome organization but have a unique, gene-specific promoter nucleosome positioning profile. Notably, such genes do have translationally well positioned nucleosomes, like the well-studied *PHO5* (reviewed in Korber and Barbaric, 2014). Such genes show high nucleosome turnover (Dion et al., 2007) that may allow TF binding for gene activation. These genes become conditionally induced, e.g., upon stress, like DNA-damage, or altered nutrient supply, e.g., change of carbon source or phosphate starvation. Upon induction, the promoter chromatin structure is remodeled, which depends on chromatin co-factors, like chromatin remodeler ATPases or histone modifying enzymes. This not constitutive but regulated class of genes is more prominent in multicellular organisms than in yeasts, e.g., tissue-specific genes often show non-stereotypical promoter chromatin in their repressed states.

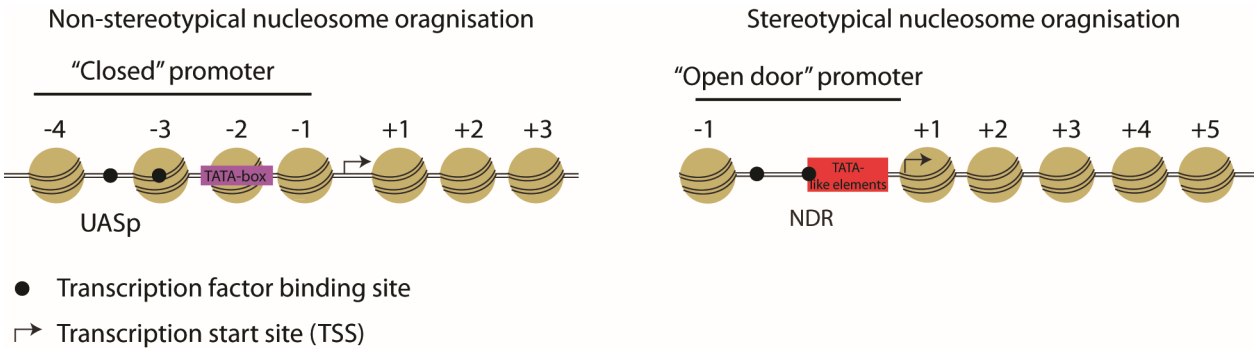

Figure 1.5 Non-stereotypical and stereotypical nucleosome positioning in S. cerevisiae. Illustration of non-stereotypical (left) and stereotypical (right) nucleosome positioning patterns. Non-stereotypical, or "closed" promoters, often display nucleosome covering promoter elements, like TATA-boxes and TF binding sites, upstream of the TSS. Promoters with stereotypical nucleosome organization most often have an "open" promoter that contains TATA-like elements and TF binding sites. Further, nucleosomes downstream of the TSS show regularly spaced arrays.

1.2.3 The relationship between chromatin structure and transcription

The relationship between transcription and chromatin structure was at first mostly studied for genes with non-stereotypical nucleosome organization as these genes are inducible and thus allow a clear comparison between low and high levels of transcription. The chromatin structure at promoters of the budding yeast *PHO* regulon is among the best characterized in this regard. Genes of this regulon are regulated by intracellular phosphate levels. Among these, the *PHO5* locus served as model for pioneer studies on nutrition-dependent gene activation and chromatin-transitions (reviewed in Korber and Barbaric, 2014). In the repressed state, the promoter is bound by 5 positioned nucleosomes, the -1 to -5 nucleosomes. The -1 nucleosome occludes the TATA-box and the -2 nucleosome the UASp2 (phosphate regulated TF binding site). Upon induction, nucleosomes at the promotors are remodeled so that the promoter opens and becomes hypersensitive to nucleases. This promoter opening correlates with an increase in transcription and production of acid phosphatase activity, the gene-product of *PHO5* (Almer et al., 1986). Genetic studies showed that promoter opening is possible without transcriptional activation (Fascher et al., 1993), whereas the opposite was not observed so far, indicating that chromatin is a regulator of transcription. Many chromatin factors, like the chromatin remodeling enzymes SWI/SNF, RSC, INO80, Isw1, and Chd1, the histone acetylases Gcn5 and Rtt109, the histone methylase Set1, as well as histone chaperones are shown to be involved in *PHO5* promoter chromatin remodeling (reviewed Korber and Barbaric, 2014). This and similar observations at heat shock genes (Shen et al., 2001), *CUP1* (Shen et al., 2001) and GAL genes shaped the view on transcriptional regulation by chromatin (reviewed in Rando and Winston, 2012).

However, this correlation between chromatin remodeling and transcription activation is not so obvious on the genome-wide scale. Various stress conditions, like a carbon source shift, heat shock, drug treatment or oxidative stress lead to a transcriptional change at many genes but without much chromatin reorganization (Cole et al., 2011b; Huebert et al., 2012; Kaplan et al., 2009; Shivaswamy et al., 2008; Soriano et al., 2013; Zawadzki et al., 2009). Also the correlation between transcription rate and nucleosome depletion at NDRs is not as pronounced on the genome-wide scale as the *PHO5* paradigm might have suggested (Lantermann et al., 2010). Nonetheless, highly expressed genes tend to have highly nucleosome depleted promoter regions. In the most extreme cases, like for induced heat shock genes, nucleosomal depletion is observed over the entire gene body (Reja et al., 2015; Zhao et al., 2005).

Another type of relationship between transcription and chromatin structure regards the question if not only chromatin remodeling regulates transcriptional output but if transcription shapes chromatin structure, particularly nucleosome positioning. For one, transcription elongation may

affect nucleosome spacing. Transcription through nucleosomes *in vitro* shows that PolII passage causes a repositioning of the nucleosome "backwards" (Kulaeva et al., 2007; Studitsky et al., 1997). This is in accordance with tighter spacing observed at highly transcribed genes (Valouev et al., 2011) as well as wider spacing upon conditional depletion of PolII *in vivo* (Weiner et al., 2010). Also, the extent of nucleosomal arrays over gene bodies increases with expression levels, at least in human cells (Schones et al., 2008). Second, ChIP-exo mapping of individual pre-initiation complex (PIC) subunits revealed that most subunits bind at a fixed distance to +1 nucleosome positions, TFIID even at the same relative position at TFIID regulated genes (Rhee and Pugh, 2012). In human cells, PolII co-localizes with +1 nucleosomes at elongating and stalled genes, even though the +1 nucleosomes are positioned at non-uniform distances to TSSs (Schones et al., 2008). All has been argued to suggest that there may be a causal relationship between PIC/PolII occupancy and +1 nucleosome positions.

1.2.4 Mechanisms of nucleosome positioning

The vast majority of genes in yeast show a stereotypical nucleosome organization. To explain the mechanism of this organization would elucidate the positioning mechanism for the majority of yeast genes. The NDR-+1-array formation can be mechanistically subdivided into several stages: 1) NDR formation, 2) positioning of the +1 nucleosome, 3) generation of nucleosomal array, and 4) alignment of this array to the NDR/+1 nucleosome. These stages can be influenced by many factors, the most prominent are: 1) histone-DNA interaction, 2) non-histone DNA binding factors, 3) chromatin remodelers, and 4) DNA templated processes, such as transcription.

Several attempts have been made to mechanistically explain the NDR-+1-array organization. The most prominent are statistical nucleosome positioning, *cis*-factor or "intrinsic" nucleosome positioning, and *trans*-factor induced nucleosome positioning. The terms *cis*- and *trans*-factors are defined from a nucleosome-centric view, i.e. *cis*-factors comprise only histones and DNA and *trans*-factors all other factors in addition.

1.2.4.1 Statistical nucleosome positioning

Statistical nucleosome positioning was first proposed in 1988 (Kornberg and Stryer, 1988). It assumes that nucleosomes are freely mobile in a linear space and behave as spheres that exclude each other. Given a limited space, the occupancy probability of such spheres would be high at barriers and decrease with distance to the barriers. Just by statistical movement the nucleosome occupancy would oscillate and the spacing of this oscillation would depend on the density. One

way to think of this is a can of tennis balls. The more balls are stored in the can, the tighter and more precise are the average positions of balls in this can (Rando and Winston, 2012). Therefore, a combination of barriers, corresponding to NDRs, and high nucleosome density would be sufficient to explain NDR-+1-array organization (Möbius and Gerland, 2010). The beauty of this model is its simplicity. Differences in NRL observed between species and cell types could be explained solely by differences in nucleosome concentration. In addition, nucleosome positioning would be independent of underlying DNA sequences, which would allow evolutionary freedom to evolve DNA sequences.

However, a prediction of this model is that nucleosome spacing would increase with decreased nucleosome density. Genome-wide *in vitro* reconstitution experiments showed that largely unaltered spacing was maintained at 50% nucleosome density (Zhang et al., 2011). The same was shown *in vivo* upon reduction of nucleosome density, either by the deletion of genes encoding the FACT components Nhp6a/b in *S. cerevisiae* (Celona et al., 2011) or Pob3 in *S. pombe* (Hennig et al., 2012), or by shutdown of histone expression (van Bakel et al., 2013; Gossett and Lieb, 2012), as well as in aged cells (Hu et al., 2014). Therefore, the original statistical positioning model is not sufficient to explain the observed nucleosomal organization.

An expansion of this model includes a *trans*-factor that binds two neighboring nucleosomes at once and sets a fixed distance between them is more suitable to describe the observed nucleosomal organization also at lower histone densities (Möbius et al., 2013). Such an activity is proposed for remodelers, which could either function as molecular rulers (Yamada et al., 2011) or have clamping activity (Lieleg et al., 2015), or for the linker histone H1 (Öberg et al., 2012). These factors and potential mechanisms are discussed below (1.2.4.3).

1.2.4.2 Cis-factor driven nucleosome positioning

Cis-factor or intrinsically driven nucleosome positioning describes the idea that nucleosome positions are solely determined by histone-DNA interactions and not by *trans*-factors. Indeed, the 147 bp DNA in a nucleosome can be viewed as a particularly long binding site for a DNA binding factor, here the histone octamer (Struhl and Segal, 2013). Incorporation of DNA into a nucleosome drastically distorts DNA structure (Luger et al., 1997). Thus, nucleosome positioning preferences could be a function of the cumulative binding energy costs and gains upon forming a nucleosome with a given DNA sequence and could reflect, for example, sequence-dependent DNA flexibility. Indeed, *in vitro* selection of DNA sequences that are more prone to nucleosome formation than were others identified as very high affinity DNA and called the “Widom 601” sequence (Lowary and Widom, 1998). This sequence outcompetes other sequences when nucleosomes are

reconstituted with limiting amount of histones by salt gradient dialysis (SGD) and is used for many chromatin *in vitro* e.g., (Klinker et al., 2014a). Nevertheless, this nucleosome forming preference seems to be specific to the SGD conditions as it did not result in permanently positioned nucleosomes inside of cells (Gracey et al., 2010).

In vivo analysis of highly positioned nucleosomes in budding yeast revealed a 10 bp AT and GC dinucleotide frequency that correlates with rotational orientation of DNA within a nucleosome (Figure 1.2 B). AT and GC dinucleotides are located at positions where the DNA minor or major groove, respectively, faces the histone octamer, suggesting intrinsic preferences for rotational positioning (Albert et al., 2007; Satchwell et al., 1986; Segal et al., 2006). Indeed, such a 10 bp dinucleotide periodicity is observed for all eukaryotic species and is most pronounced when nucleosome positions are mapped with base pair resolution and without MNase bias by hydroxyl-radical cleavage (Brogaard et al., 2012; Moyle-Heyrman et al., 2013; Voong et al., 2016). This periodicity probably explains the rotational positioning of fuzzy nucleosomes (1.2.1).

However, budding yeast genome-wide *in vitro* reconstitutions by SGD revealed that pure histone DNA interactions were not sufficient to generate *in vivo*-like nucleosome positions, especially the NDR-+1-array organization (Kaplan et al., 2009; Zhang et al., 2009, 2011). Only upon incubation with whole cell extracts (WCEs), *in vivo*-like positions were generated in an ATP-dependent manner (Zhang et al., 2011). This argues for *trans*-factor driven nucleosome positioning. Further, introduction of large genomic fragments from *K. lactis* via yeast artificial chromosomes (YACs) into *S. cerevisiae* resulted in nucleosome positions on these YACs that were different than the endogenous ones observed in *K. lactis* (Hughes et al., 2012). This demonstrates that the same DNA sequence is interpreted differently in *S. cerevisiae* and *K. lactis* with regard to nucleosome positioning, also arguing for *trans*-factor driven nucleosome positioning.

Even though the DNA sequence is not sufficient to translationally position nucleosomes to the degree seen *in vivo*, poly(dA:dT) elements did account for NDR formation on a genome-wide scale *in vitro* (Kaplan et al., 2009; Zhang et al., 2009, 2011) and are clearly enriched at budding yeast promoters *in vivo* (Lee et al., 2007; Yuan et al., 2005) and can strongly influence transcription levels (Raveh-Sadka et al., 2012). It is suggested that these elements are intrinsically stiff, which disfavors incorporation into nucleosomes both *in vitro* and *in vivo*. Even though this may be true biophysically, such a nucleosome exclusion mechanism cannot be universal. Comparative analysis of NDR organization of 12 different yeast species showed that such poly(dA:dT) elements are widely but not universally used through evolution (Tsankov et al., 2011, 2010). For example, NDRs in *S. pombe* are not enriched for poly(dA:dT) elements (Lantermann et al., 2010; Tsankov

et al., 2011), and hydroxyl-radical nucleosome mapping identified that poly(dA/dT) were even enriched around nucleosomal dyads and not in NDRs in this yeast (Moyle-Heyrman et al., 2013). In summary, translational nucleosome positioning *in vivo* cannot be solely driven by histone-DNA interactions alone. Biophysical properties may influence nucleosome positioning also *in vivo*, potentially if they discriminate against nucleosome formation due to intrinsical stiffness or if they regulate rotational nucleosome positioning based on dinucleotide frequency, but both *in vivo* and *in vitro* studies argue that translational positioning is mainly regulated by *trans*-factors.

1.2.4.3 Trans-factor driven nucleosome positioning

Trans-factor driven nucleosome positioning seems to be indeed the most important regulator of global nucleosome positions. In yeast, mutations of genes encoding several factors influenced nucleosomal organizations, including DNA binding factors, chromatin remodelers, histone concentration, histone deposition factors, like *nhp6a/b* or *spt6* mutations, and transcription (reviewed in Lieleg et al., 2014). Overall, most mutations had only mild effects on global NDR-+1-array formation if at all. The most severe effects were observed when global histone deposition was impaired, either by shut down of histone expression (van Bakel et al., 2013; Gossett and Lieb, 2012) or by interfering with histone deposition (Celona et al., 2011; Hennig et al., 2012). An increased nucleosome occupancy at NDRs was observed for depletion of general regulatory factors (GRFs), e.g., Reb1 and Abf1, or the remodeler RSC (Badis et al., 2008; van Bakel et al., 2013; Hartley and Madhani, 2009; Kubik et al., 2015; Parnell et al., 2008). Cloning of a Reb1 binding site in combination with a poly(dA) stretch resulted in *de novo* NDR formation that was dependent on RSC and Reb1 (Hartley and Madhani, 2009). Noteworthy, all these factors are essential, suggesting that NDR formation is a global and essential process, presumably because it regulates transcription. In contrast, the shutdown of transcription itself is less disturbing to chromatin structure (van Bakel et al., 2013; Weiner et al., 2012). Further, there seems to be considerable redundancy of nucleosome positioning mechanisms *in vivo*. Nucleosome occupancy at the yeast *CLN2* promoter was increased upon combined deletion of GRF and TF binding sites (Bai et al., 2011). The individual depletion of other remodelers besides RSC, such as Isw1, Isw2 and, Chd1, led only to minor nucleosome rearrangements, such as upstream shifts of nucleosomal arrays including the +1 nucleosome (van Bakel et al., 2013; Tirosh et al., 2010; Whitehouse et al., 2007; Yen et al., 2012). Only the combined ablation of the remodelers Isw1 and Chd1 in *S. cerevisiae* (Gkikopoulos et al., 2011; Ocampo et al., 2016) or Hrp1 and Hrp3 in *S. pombe* (Hennig et al., 2012; Pointner et al., 2012; Shim et al., 2012) led to severe effects on nucleosomal array formation. In such mutants, NDRs and +1 nucleosomes are comparable to those of the wild type, but the genic

nucleosomal arrays were largely disturbed. However, nucleosome spacing of bulk chromatin in MNase ladders was maintained (Pointner et al., 2012), suggesting that the alignment of regularly spaced nucleosomes was impaired in these mutants. This demonstrates that *in vivo* NDR formation and +1 nucleosome positioning is distinct from nucleosomal array formation and/or alignment. Of note, *S. pombe* does not have a member of the ISWI remodeler family and Hrp1 and Hrp3 belong to the CHD remodeler family (1.3.1). Thus, the simultaneous ablation of all ISWI- and CHD-type remodelers caused impaired nucleosomal array formation in two widely diverged yeast species, suggestion that the use of these remodeler families in general is conserved through evolution but which remodeler type is involved in particular is diverged (Pointner et al., 2012). Not only the mechanism but also the biological role of genic nucleosome arrays seems to be conserved as disturbance of the nucleosomal array over the gene body leads to increased cryptic transcription, but not too much changes of sense transcript levels, in both budding and fission yeast (Hennig et al., 2012; Pointner et al., 2012; Shim et al., 2012; Smolle et al., 2012).

Collectively, these mutant studies demonstrated that *trans*-factors, especially GRFs and chromatin remodelers, are engaged in establishing features of nucleosomal organization. However, it is difficult to distinguish if remodelers and GRFs have direct or indirect, specific or generic, sufficient or necessary roles *in vivo*. Mutation of genes encoding remodelers or GRFs may lead to transcriptional changes which then affect nucleosome positioning. Especially in the case of combined deletions, it is difficult to dissect the contribution of individual factors.

1.2.4.4 Direct and specific roles of trans-factors indicated by reconstitution in vitro

The laboratory of Dr. Philipp Korber developed an *in vitro* reconstitution system that recapitulates physiological nucleosome positioning (Hertel et al., 2005; Korber and Horz, 2004; Krietenstein et al., 2012; Zhang et al., 2009) and allows dissecting if a factor's role is direct or indirect, necessary and/or sufficient, and specific or unspecific. Individual plasmids with genomic inserts or plasmid libraries containing the entire yeast genome are assembled by SGD (Figure 2.1 A). Nucleosome positions after SGD are solely driven by histone-DNA interactions and considered "intrinsic" nucleosome positions (Kaplan et al., 2009; Zhang et al., 2009, 2011). Such nucleosome positions do not reflect physiological nucleosome positions, e.g., +1 nucleosome positions or arrays over coding regions with physiological spacing. However, NDRs over poly(dA:dT) elements are partially reconstituted, even though not with physiological width. Upon incubation with yeast WCEs physiological NDR-+1-array nucleosome organization was reconstituted for most genes (Zhang et al., 2011). Importantly, this was strictly dependent on ATP and in absence of

transcription, demonstrating that nucleosome positioning *in vitro* is an active, transcription-independent process. *In vitro* reconstitution at single loci, like *PHO8*, with RSC-depleted extract showed that RSC had a direct, necessary, but not sufficient role in promoter NDR formation (Wippo et al., 2011). Moreover, this NDR formation at *PHO8* was specific to RSC, since only RSC, but not ISW2 or SWI/SNF, conferred the ability to properly position nucleosomes at this promoter in RSC depleted extracts. This demonstrated that remodelers have specific functions in nucleosome positioning and that this *in vitro* reconstitution system is a powerful tool to study nucleosome positioning mechanisms of individual remodelers.

1.2.5 An integrative model for nucleosome positioning mechanisms

We suggested an integrative model that combines proposed mechanisms that lead to *in vivo* NDR-+1-array formation (Lieleg et al., 2014)(Figure 1.6). NDRs are kept free of nucleosomes by nucleosome excluding sequences, like poly(dA:dT) elements and/or *trans*-factors, like GRFs, TFs in combination with remodelers. +1/-1 nucleosomes are positioned by remodelers to define the borders of NDRs, maybe in connection with nucleosome positioning sequences (NPSs). This could either be guided by other *trans*-factors, like GRFs or probably PIC assembly, or by nucleosome positioning sequences. Such an NDR/+1 nucleosome organization could serve as a barrier in the sense of statistical positioning (1.2.4.1). However, array formation is independent of nucleosome density (Celona et al., 2011; Zhang et al., 2011) and an active process (Zhang et al., 2011), suggesting that nucleosomal array formation is mediated by remodelers with clamping activity (Lieleg et al., 2015). Remodelers can be recruited at organizing centers, like NDRs (Zentner et al., 2013; Zhang et al., 2011), and exert their effects from there and/or bind to genic nucleosomes, maybe mediated by histone PTMs. Remodeling will then lead to regular spacing, either by "length sensing" or "clamping" (Lieleg et al., 2015), and to array alignment at the +1 nucleosome. This model is much related to another "unified" model (Hughes and Rando, 2014; Struhl and Segal, 2013), but we emphasize the role of transcription-independent and remodeler driven nucleosome positioning, since NDR-+1-array formation can be reconstituted *in vitro* in absence of transcription (Zhang et al., 2011).

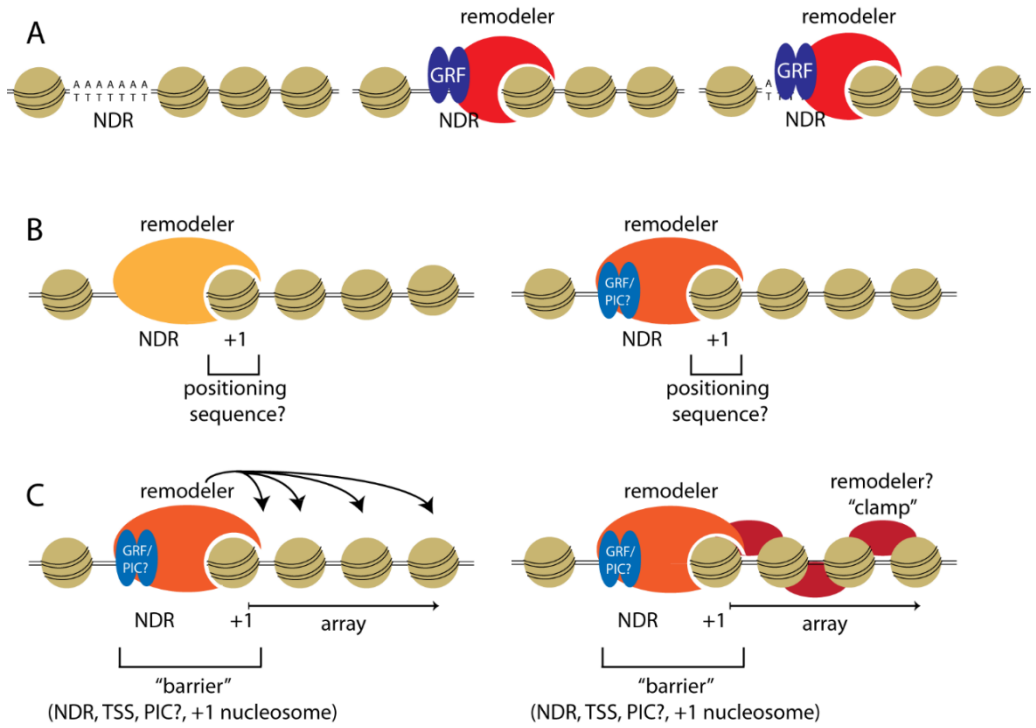

Figure 1.6 Integrative model for NDR-array formation. (A) NDR formation guided by intrinsically nucleosome repelling poly(dA:dT) elements, GRF guided NDR formation by remodelers, or a combination of both, (B) +1 nucleosome positioning through remodelers, either guided by nucleosome positioning sequences or by DNA binding factors and/or PIC assembly. (C) Nucleosomal array regularity and alignment through active nucleosome spacing, packaging and/or clamping. [Adapted and reprinted with permission from Chromosoma (Lieleg et al., 2014)]

1.3 ATP-dependent chromatin remodeling complexes alter chromatin structure

ATP-dependent chromatin remodeling complexes can alter the structure of chromatin (reviewed in Bartholomew, 2014; Becker and Workman, 2013; Clapier and Cairns, 2009; Flaus and Owen-Hughes, 2011; Narlikar et al., 2013). The first chromatin remodeler was genetically identified as a mating-type switch regulator and regulator of the sucrose fermentation pathway in *S. cerevisiae*, hence it was called SWI/SNF (switch defective/sucrose non-fermenting) (Winston and Carlson 1992) reviewed in (Rando and Winston, 2012). First biochemical evidence for chromatin regulation as an active process came from chromatin *in vitro* reconstitutions with *Drosophila melanogaster* embryonic extracts (Becker and Wu, 1992). Such extracts reconstituted chromatin with physiological spacing on DNA and generated DNaseI hypersensitivity upon TF binding in an ATP-dependent manner (Tsukiyama et al., 1994). Indeed, biochemical purification of SWI/SNF and other remodeling complexes, like the ACF and CHRAC complexes from the fly (Fyodorov and Kadonaga, 2002; Ito et al., 1996; Varga-Weisz et al., 1997) demonstrated that these complexes generate hypersensitivity to nuclease digestion in an ATP-dependent way. Therefore, DNA accessibility can be regulated by this class of enzymes.

1.3.1 Families of chromatin remodelers

The ATPase subunit Swi2/Snf2 displays homology to helicases of the SF2 superfamily. The corresponding subgroup of SF2 helicases was named after Snf2. Snf2-type ATPases do not unwind DNA but translocate on it. All other nucleosome remodeling ATPases were later on identified through sequence homology to Snf2, i.e. belong to the Snf2-type, and most of them have biochemically verified nucleosome remodeling activity.

The domain structure of Snf2-typ ATPases is used to further classify different remodeler families (Flaus, 2006), of which the four major are the SWI/SNF, ISWI, CHD, and INO80 families. For example, two characteristic domains, the DExx and HELICc domains, are separated by an insertion of variable length and the INO80 family is characterized by a rather long insertion (Figure 1.7). Further, the presence and position of additional domains, like bromo, chromo, HSA or SANT/SLIDE domains, discriminate between the remodeler subfamilies.

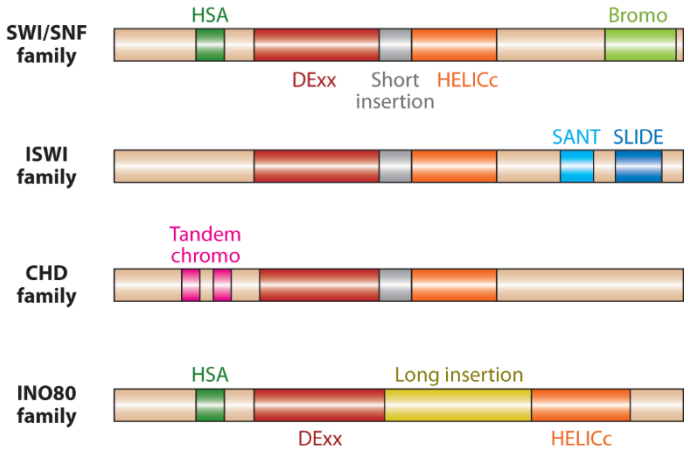

Figure 1.7 Domain organization of ATPase subunits of the four major ATP-dependent chromatin remodeler families. The DExx and HELICc domains are shared through all chromatin remodeler families (red and orange, respectively). Compared to other families, remodelers of the INO80 family (SWR and INO80 in yeast) have a long insertion (yellow) between these domains. Remodelers of the SWI/SNF and INO80 families have a N-terminal HSA (helicase-SANT associated) domain (dark green). In addition, SWI/SNF remodelers have an C-terminal Bromo domain (light green). ISWI family members show a C-terminal HAND-SANT-SLIDE domain (light and dark blue). CHD family members carry two chromo-domains that are tandemly arranged (pink). [Adapted and reprinted with permission from Annual Reviews (Clapier and Cairns, 2009)]

Beyond the ATPase domain structure, remodelers are further diversified by association with different subunits into large complexes. This may alter the activity of the remodeling complex, even if the same ATPase is incorporated. For example, the yeast Isw1 ATPase is incorporated into the ISW1a and ISW1b complexes and both have clearly different properties *in vitro* (Vary et al., 2003). All this leads to a huge diversity of chromatin remodelers (Rippe et al., 2007). In human, for example, more than 100 remodeling complexes were found. In yeast, two representatives each of remodeler ATPases of the INO80, SWI/SNF and ISWI families are found. The CHD family has only one representative in yeast, Chd1 (Flaus, 2006).

In general, remodelers display all or some of the following basic properties: (A) binding affinity to nucleosomes, (B) domains that recognize covalent histone modifications, (C) domains and/or

proteins that regulate the ATPase activity, especially in contact with DNA or nucleosomes, and (D) domains and/or proteins that mediate interactions with other chromatin components or TFs (Clapier and Cairns, 2009).

1.3.2 Basic chromatin remodeler functions

There are mainly four basic reactions remodelers can catalyze (Figure 1.8). They can slide nucleosomes, exchange histones, e.g., for histone variants, evict histones (= disassemble nucleosomes), or assemble nucleosomes.

Nucleosome sliding involves translocation of nucleosomes along DNA such that nucleosomes at the end of the sliding reaction are still canonical nucleosomes but at altered translational positions. Nucleosome sliding may be monitored by various experimental procedures (Varga-Weisz et al., 1997). In one procedure, changes in DNA accessibility are measured by DNA cleavage through site-specific restriction enzymes (RE). Nucleosomes are positioned *in vitro* by nucleosome positioning sequences and RE sites located within these sequences or on neighboring linker DNA will show differential cutting efficiency prior and after the remodeling reaction. Sites occluded by a nucleosome will be less accessible than linker sites, but sliding of a nucleosome by the remodeling enzyme will change the relative accessibilities. It is important to monitor at least two sites that are initially occluded and accessible, respectively. If just an increase of accessibility at one site is monitored, this cannot discriminate between sliding or eviction. In contrast, if accessibility of an RE sites that was initially located in the linker shows decreased accessibility after remodeling, this is indicative of nucleosome sliding (Klinker et al., 2014a). Another procedure is the nucleosome mobility shift assay (Längst et al., 1999). Short (< 250 bp) linear DNA fragments that harbor one single nucleosome at an end position show different electrophoretic mobility compared to the same DNA fragment with a more centrally located nucleosome. Yet another migration position in the gel is seen with free DNA. So changes in electrophoretic mobility upon remodeling indicate either nucleosome sliding or eviction.

Such mono-nucleosome sliding assays may reveal, at least indirectly, also another kind of nucleosome remodeling, the nucleosome spacing activity. Nucleosome spacing refers to the establishment of regular nucleosomal arrays with uniform linker lengths, i.e. nucleosomes are not only translocated but positioned with respect to each other in a regular way. Remodelers with spacing activity are thought to equalize the linker DNA on both sides of a nucleosome. This amounts to centering of mono-nucleosomes on short DNA fragments. Note that this readout is sufficient but not necessary for remodelers with spacing activity as the fly remodeler CHRAC

centers mono-nucleosomes, but the corresponding ATPase subunit ISWI does not (Längst et al., 1999) even though it displays spacing activity in a different assay type (Lieleg et al., 2015). One possible model to explain such spacing activity is the "length sensor model". Here, the ATPase activity of a remodeler is stimulated by increasingly long linker DNA such that the nucleosome is preferentially translocated towards the longer linker. Repeated sensing of linker lengths on both sides of the nucleosome and always moving the nucleosome towards the longer linker results in centered mono-nucleosomes or evenly spaced nucleosomal arrays. The latter is monitored in the more classical and also more definitive spacing assay, i.e. in the context of other, neighboring nucleosomes (Varga-Weisz et al., 1997). If irregular nucleosomal arrays are used as starting material, a remodeler with spacing activity will equalize the linker length between neighboring nucleosomes. This is monitored by the generation of extensive regular "ladders" after limited MNase digestion ("MNase ladders").

Recently, a careful biochemical study analyzed the nucleosome spacing activity of various remodelers at various histone densities. All tested remodelers were known to have nucleosome spacing activity and all of them were found to set a constant spacing-independent of nucleosome densities. This contrasts the prediction of the length sensor model that spacing should be a function of nucleosome density. Therefore, remodelers with spacing activity must also have some activity that sets not just a regular but also a constant spacing. This stricter version of spacing activity was called clamping activity (Figure 1.8 C) (Lieleg et al., 2015).

Nucleosome assembly and eviction results in the appearance or disappearance of nucleosomes, respectively, which can be monitored by many assays, e.g., by nucleosome mobility shift assays, MNase ladders, or topology analysis of covalently closed circular DNA. The latter is based on nucleosomes introducing toroidal supercoils that are converted into plectonemic supercoils by topoisomerase (TopoI) treatment and detected in chloroquine gel electrophoresis (Morse, 1999).

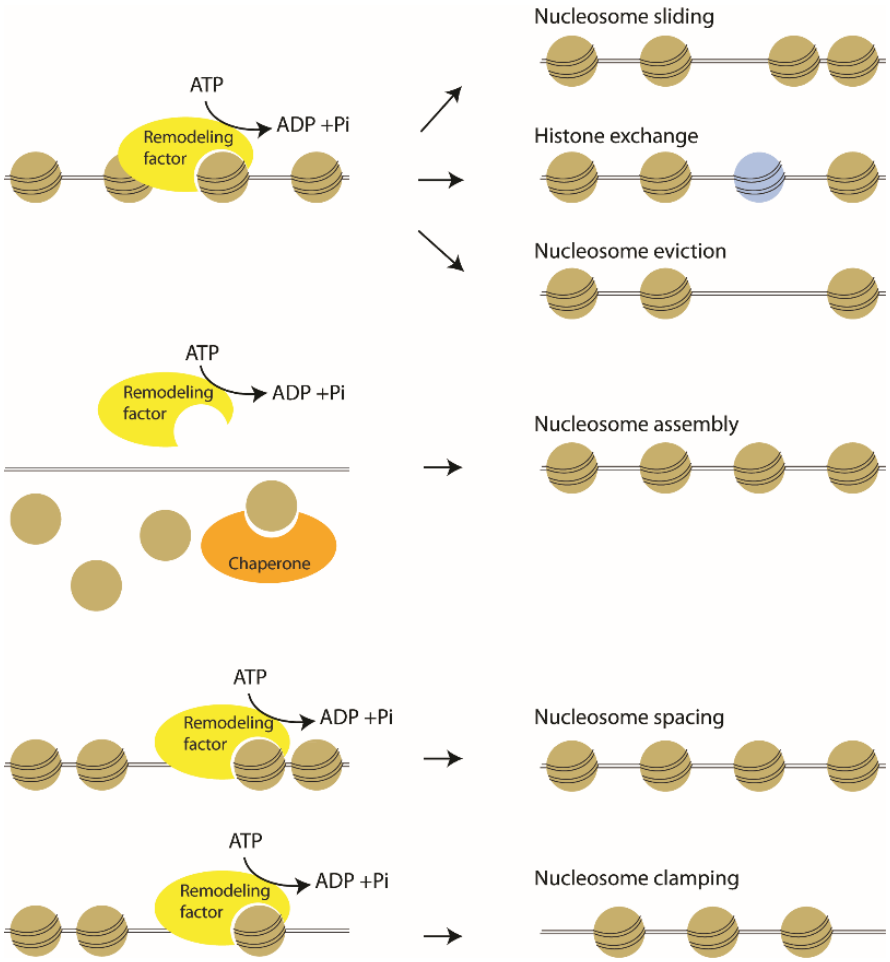

Figure 1.8 Basic nucleosome remodeling enzyme activities. Chromatin remodeling factors can translocate (= slide) nucleosomes along the DNA, exchange histone variants, or evict (= disassemble) nucleosomes. Together with histone chaperones, some remodelers can assembly nucleosome. Further, some remodelers have the ability to regularly space nucleosomes. An extended nucleosome spacing activity is nucleosome clamping, here remodelers adjust a constant spacing-independent of histone density. [This figure was inspired by (Becker and Workman, 2013) and extended for nucleosome clamping (Lieleg et al., 2015)]

1.4 Aim of this thesis

Nucleosome positioning is mainly determined by *trans*-factors, and this seems to involve sequence-specific DNA binding factors and chromatin remodelers. *In vivo* studies suggested distinct functions for some of these factors. For example, GRFs like Reb1 and Abf1 or remodelers like RSC are involved in organizing NDRs (van Bakel et al., 2013; Hartley and Madhani, 2009). Others, like ISWI and CHD type remodelers, seem involved in nucleosomal array formation and spacing (Gkikopoulos et al., 2011; Ocampo et al., 2016; Yen et al., 2012). The main aim of this thesis is to biochemically dissect the individual contributions of such factors to the generation of the stereotypical NDR-+1-array nucleosome organization.

Such dissection *in vivo* appeared problematic. On the one hand, factors involved in NDR formation are essential. Therefore, only conditional mutants can be studied. On the other hand, some nucleosome positioning mechanisms appear to be redundant, thus only combined deletions displays severe effects, which makes it difficult to identify the contribution of individual factors.

Therefore we chose an *in vitro* approach. *In vivo*-like nucleosome positioning can be recapitulated *in vitro* for *S. cerevisiae* at single loci or on a genome-wide scale with WCEs in an ATP-dependent manner (Ertel et al., 2010; Hertel et al., 2005; Korber and Horz, 2004; Krietenstein et al., 2012; Lieleg et al., 2015; Wippo et al., 2011). Such an *in vitro* reconstitution system allows the biochemical distinction if the contributions of individual factors are direct or indirect, necessary and/or sufficient, and specific or unspecific (Ertel et al., 2010; Wippo et al., 2011).

In particular, we followed a candidate approach using mutant WCEs, purified remodelers and DNA binding factors. First, we used WCEs from cells that lack the Isw1, Isw2, and Chd1 remodeler ATPases (Tsukiyama et al., 1999). *In vivo*, these cells can form NDRs and position +1 nucleosomes but show impaired alignment of nucleosomal arrays with physiological spacing to +1 nucleosomes (Gkikopoulos et al., 2011; Ocampo et al., 2016). Such a WCE was the perfect background to study specific contributions of the purified remodeling enzymes Chd1, ISW1a, ISW1b, ISW2, RSC, INO80, SWI/SNF, and SWR on array formation. Second, we studied the requirements for NDR formation and +1 nucleosome positioning using only purified factors, including the aforementioned remodelers and the GRFs Abf1 and Reb1. Ultimately, we aimed to combine identified factors according to their nucleosome positioning properties for establishing a sufficient minimal system for *in vitro* reconstitution of genome-wide NDR-+1-array formation with only purified factors.

2 Results

2.1 Refining the protocol for genome-wide reconstitution of physiological nucleosome positions

The major technique used in this study is a genome-wide *in vitro* approach to reconstitute physiological nucleosome positions using wild type whole cell extracts (Krietenstein et al., 2012; Zhang et al., 2011). This approach consists of two steps. First, the preparation of chromatin by salt gradient dialysis (SGD) and second, the ATP-dependent "re-positioning" reaction in which nucleosomes are relocated to physiological positions by *trans*-factors. These nucleosome positions are measured by MNase-(ChIP)-seq (4.2.12).

Previously, *in vitro* positioning reactions were performed using KCl based buffers (Krietenstein et al., 2012; Zhang et al., 2011). In contrast to previous studies, purified factors (e.g. chromatin remodelers) were added at various concentrations. These factors were purified according to established protocols (Smith and Peterson, 2003) with final elution into a NaCl based buffer. The addition of chromatin remodelers to our standard positioning reaction would be substantial enough to strongly alter the final salt concentrations if positioning reactions were performed in KCl based buffers. As salt concentration and type can affect chromatin *in vitro*, especially the nucleosomal repeat length (Blank and Becker, 1995; Korolev et al., 2010), we compared genome-wide *in vitro* nucleosome positioning experiments with KCl and NaCl based buffers. To keep the final buffer condition constant while accommodating various amounts of purified remodelers and factors, we redesigned the pipetting scheme and buffer conditions for the positioning reaction.

In accordance with previous studies, nucleosome positioning through salt gradient dialysis partially reconstituted the NDR, but no other features of the stereotypical NDR-array organization (Kaplan et al., 2009; Zhang et al., 2009, 2011). This effect was independent of the cation type (Figure 2.1 A graph 2 and 3 and Figure 2.1 B blue and green trace). This "intrinsic" nucleosome positioning data was used to sort genes according to their degree of physiological nucleosome positioning just by salt gradient dialysis. This degree was computed as the ratio of nucleosome dyad tags within the *in vivo* +1 nucleosome regions over those within the NDR (4.3.3.4). Thus, genes are sorted in gene-by-gene representations (heat maps, Figure 2.1 A) in descending order according to how physiological NDRs and +1 nucleosomes were intrinsically reconstituted, referred to as "+1-to-NDR-tag-ratio". This representation revealed that about 1/4 to 1/3 of genes showed a partially physiological reconstitution of NDR and +1 nucleosome independent of salt type. Positioning reactions with wild-type whole cell extract (wtWCE) were able to position nucleosomes to physiological levels for most genes independent of ion source (Figure 2.1 A/B,

(Zhang et al., 2011). Note, "Native" represents native chromatin that was extracted from cells before cross-linking and processing for MNase sequencing *in vitro* (Zhang et al., 2011) and served as positive control for *in vitro* reconstituted chromatin.

In summary, the type of cations neither effected intrinsic nor wtWCE driven nucleosome positioning. Thus we decided to use the NaCl based buffer that allows facile addition of a wide range of purified remodelers to the pipetting scheme without changing final buffer conditions.

In vivo, the measured occupancy of nucleosomes depend on the MNase digestion degrees (Weiner et al., 2010). In our experiments, the MNase digestion degree *in vitro* strongly depended on buffer conditions, especially on the concentrations of ATP and crude protein extracts. In experiments without ATP, a much lower MNase concentration was needed to digest chromatin to mono-nucleosomal DNA than in the presence of ATP. Our interpretation here is that ATP or inorganic phosphate, generated from ATP hydrolysis, can bind Ca^{2+}, and MNase activity is highly sensitive to the availability of Ca^{2+} ions. Experiments in the presence of WCEs required more MNase to digest chromatin to mono-nucleosomal DNA, presumably because some proteins in the extract can bind Ca^{2+} and/or extract proteins bind to chromatin, thereby limiting access for MNase. To ensure that our experiments were not biased by MNase digestion, we compared the nucleosome profiles of *in vitro* reconstituted chromatin without ATP and proteins and with ATP and WCEs, i.e. the most extreme cases with respect to MNase digestion effects, at different MNase digestion degrees for the new NaCl buffer conditions. We titrated MNase concentration to 70%, 100%, and 130% (= low, medium, high) of standard MNase concentration, that were previously determined as 0.000708 U/µl for SGD-ATP and 0.0708 U/µl for SGD+ATP+WCE chromatin (Krietenstein et al., 2012).

No substantial differences in the nucleosome positioning profiles around promoters were detected for the different MNase concentrations in SGD -ATP and SGD +ATP +WCE experiments in the new NaCl buffer conditions (Figure 2.2 C and D, respectively). Thus, our standard digestion protocol allows reliable detection of nucleosome positions, even if the effective MNase digestion degree in a given case may vary by up to +/- 30%.

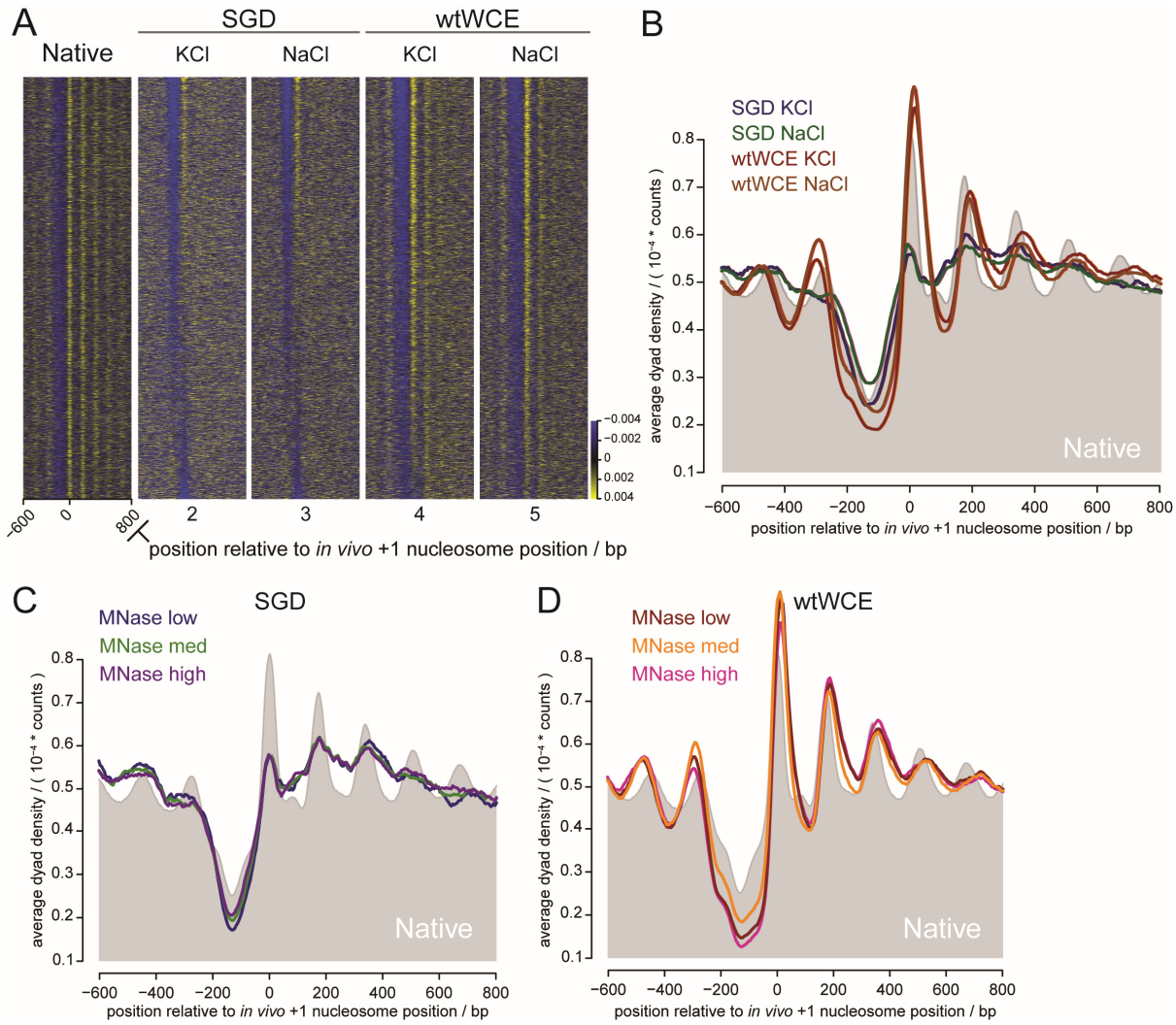

Figure 2.1 Genome-wide patterns of in vitro reconstituted nucleosomes are largely unaffected by newly established salt conditions and by a range of MNase digestion degrees. (A) Color-coded nucleosome dyad densities for 4,118 genes (row-by-row). Yellow, black, and blue represent high, medium, and low tag density, respectively. Genes are aligned to *in vivo*-called +1 nucleosome positions. The rows are sorted in descending order according to +1-to-NFR-tag ratio in graph 3. "Native" denotes chromatin isolated *ex vivo*, crosslinked and MNase digested *in vitro*. *In vitro* processing of *in vivo* chromatin represents the "gold" standard for *in vitro* prepared and processed samples. Salt gradient dialyzed chromatin (SGD) shows nucleosome positions obtained by pure histone-DNA interactions during salt gradient dialysis and after further incubation for 2 h in nucleosome positioning buffer. KCl and NaCl denote the salt ions used in positioning buffer (graphs 2 to 5), KCl was used in previous studies *(Krietenstein et al., 2012; Zhang et al., 2011)*, NaCl in this study. WtWCE indicates incubation with yeast whole cell extracts (WCE), generated from wild type BY4741 cells, in positioning reactions, either with KCl or NaCl based positioning buffer (graphs 4 and 5). (B) Composite nucleosome dyad distribution of data as in A aligned at *in vivo* +1 nucleosome positions. (C) SGD chromatin as in A (graph 3) digested at low, medium, and high MNase concentrations. Medium corresponds to standard concentration (0.0059 U/µl)*(Krietenstein et al., 2012)*, low and high to 70% and 130% respectively. (D) Chromatin positioned with wtWCE as in A (graph 5) digested at low, medium (0.59 U/µl), and high MNase concentrations as in C.

2.2 *In vitro* reconstitution of genome-wide nucleosome positioning using mutant whole cell extracts

2.2.1 The lack of three remodeler ATPases in *isw1 isw2 chd1* mutants uncouples NDR formation from the formation of +1 nucleosomes and of nucleosomal arrays *in vivo* and *in vitro*

In vivo, nucleosome positions are regulated by redundant mechanisms as single mutations mostly show no or minor effects and only combined mutations lead to impaired positioning. This makes

it difficult to dissect the contribution of individual factors. In addition, it is difficult to distinguish direct from indirect effects *in vivo*. As a yeast wtWCE is able to reconstitute physiological nucleosome positions *in vitro* (Zhang et al., 2011), we used this system to now test WCEs from mutants.

In vivo, the simultaneous deletion of genes coding for the *isw*1, *isw*2, and *chd*1 ATPases results in strongly compromised arrays over the gene bodies, but does not affect NDR formation and +1 and -1 nucleosome positions (Gkikopoulos et al., 2011). We prepared *isw1Δ isw2Δ chd1Δ* mutant WCEs of two independent strains with this genotype, YTT227 (Tsukiyama et al., 1999) and MP28 (Gkikopoulos et al., 2011), and determined their ability to reconstitute physiological nucleosome positions *in vitro*. Both mutant extracts could generate NDRs and position the -1 and +1 nucleosomes (only shown for YTT227: Figure 2.2 A graph 4 and Figure 2.2 B blue trace), similar to a wtWCE (Figure 2.2 A graph 3 and Figure 2.2 B green trace). Reflecting the *in vivo* phenotype of these mutants, the extracts failed to establish extensive nucleosomal arrays. Of note, in *in vitro* experiments using wtWCE the +1 nucleosome was somewhat shifted downstream compared to *in vivo* positions (Fig 2B, compare green trace (wtWCE) with grey background pattern (Native)) and this shift was even more pronounced in reconstitution experiments with an *isw1Δ isw2Δ chd1Δ* WCE (Fig 2B, compare green trace (wtWCE) with blue trace (*isw1Δ isw2Δ chd1Δ* WCE)). This suggests, that in our WCE preparation factor(s) involved in +1 nucleosome positioning are depleted. Another explanation would be that mechanisms, that we do not recapitulate *in vitro*, such as transcription, are involved in positioning the +1 nucleosome, and that these factors and/or mechanisms lack even more in the mutant WCE (see discussion).

Importantly, because this mutant WCE is unable to reconstitute a well-positioned +1 nucleosome and nucleosomal arrays, we could take advantage of it as the ideal platform to study the contribution of remodelers forming these organizational feature.

2.2.2 Add-back experiments reveal that ISW1a, but not ISW1b or CHD1, establishes physiological spacing

The inability to organize genic nucleosomal arrays upon depletion of *chd*1, *isw*1 and *isw*2 suggests that the remodeling complexes containing these ATPases, ISW1a, ISW1b, ISW2, and monomeric Chd1 are involved in regular spacing of nucleosomes (array formation) and aligning these arrays to genomic features (e.g., transcription start sites). We purified these remodelers and supplemented the *isw1Δ isw2Δ chd1Δ* WCE in reconstitution reactions (Figure 2.2 A graphs 4 vs. 5 to 9).

Neither Chd1 (Figure 2.2 A graph 6 and Figure 2.2 D red trace) nor ISW1b (Figure 2.2 A graph 8 and Figure 2.2 D orange trace) were able to reconstitute nucleosomal arrays when added to the

isw1Δ isw2Δ chd1Δ WCE. In contrast, addition of ISW1a restored the ability to reconstitute physiological nucleosome positions (Figure 2.2 A graph 7). On average, the +1 nucleosome was positioned close to its physiological position, as accurately as with the wtWCE (Figure 2.2 E red trace vs. Figure 2.2 B green trace), but the +1 nucleosome occupancy was decreased. Most strikingly, the spacing of the nucleosomal array was even more physiological than in reconstitutions with wtWCE.

Deletion of the gene encoding Chd1 has a very strong effect on nucleosome positioning *in vivo* (van Bakel et al., 2013; Gkikopoulos et al., 2011; Lee et al., 2012; Ocampo et al., 2016), and Chd1 exhibits nucleosome sliding (McKnight et al., 2011; Patel et al., 2011) as well as spacing (Lieleg et al., 2015; Torigoe et al., 2013) activity *in vitro*. In contrast, ISW1b has hardly any spacing activity *in vitro* (Vary et al., 2003). So the lack of an effect on array formation by ISW1b in our reconstitutions was somewhat expected, but very surprising for Chd1. We normalized the amounts of remodeler preparations taking their ATPase activity (4.2.5) as measure, as this is the shared activity of all remodelers. We confirmed that these remodelers, especially ISW1b and Chd1, had remodeling activity besides their ATPase activity in nucleosome sliding experiments with Chd1 (Figure 2.3 A) and in restriction enzyme accessibility experiments with ISW1b, ISW1a, and RSC (Figure 2.3 B). Thereby we demonstrated that purified Chd1 catalyzed nucleosome positioning reactions as described in the literature but failed to organize nucleosome positions on a genome-wide scale *in vitro*. Similarly, both ISW1b and ISW1a mobilized nucleosomes in our reconstitution conditions and were still active after a complete reconstitution reaction, thereby excluding that ATP-depletion or protein inactivation might negatively affect remodeler performance. However, only ISW1a generated genome-wide spacing. This is in agreement with the lack of ISW1b spacing activity in classical spacing assays (Vary et al., 2003). We conclude that both, Chd1 and ISW1b, were active in classical *in vitro* assays, but that their roles in establishing genome-wide nucleosome patterns as suggested by *in vivo* studies (van Bakel et al., 2013; Smolle et al., 2012) required mechanisms that were not reconstituted in our system. This could point to their activity being coupled to transcription (see discussion).

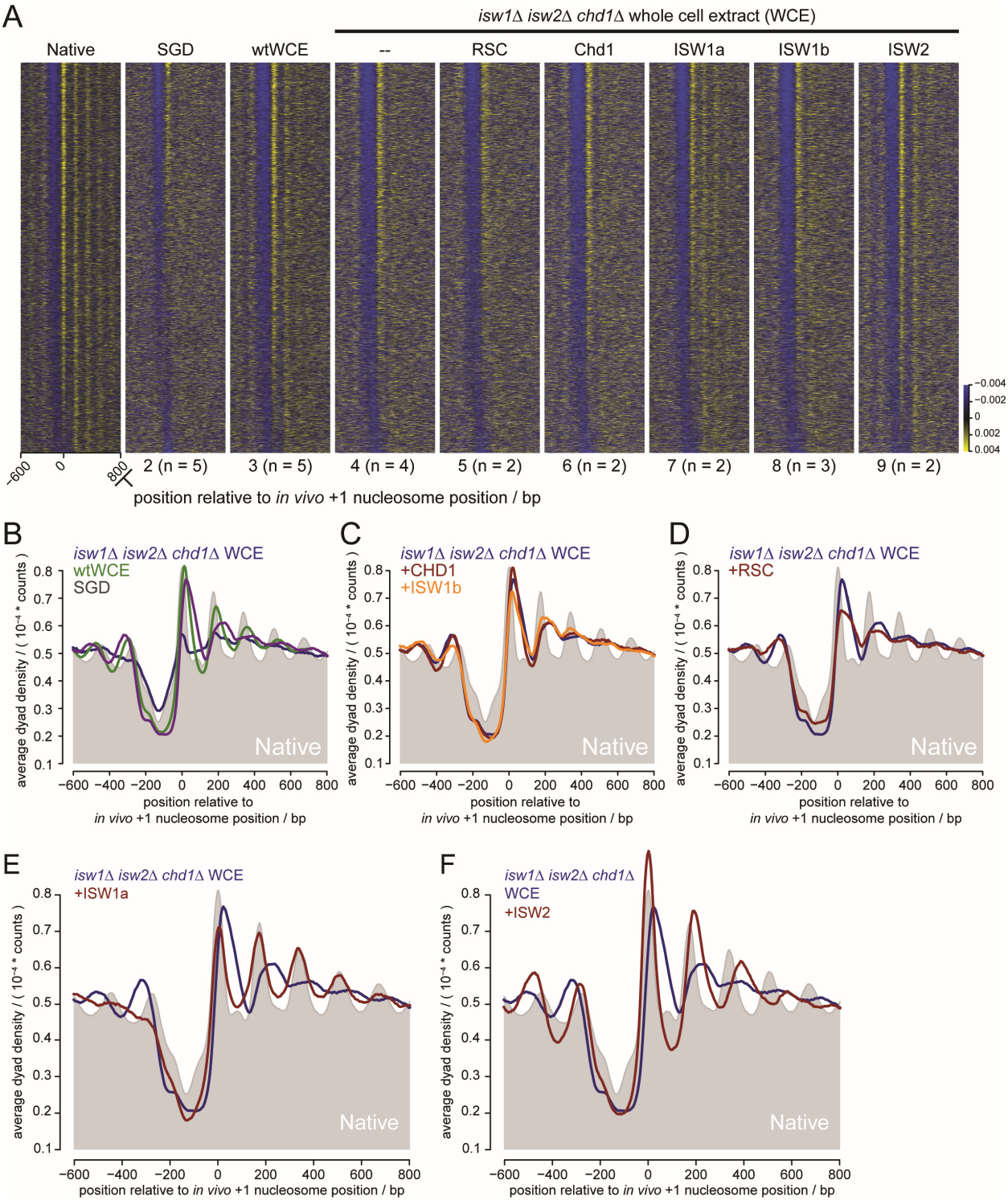

Figure 2.2 Purified remodelers reconstitute genome-wide NFR/+1/array nucleosomal organizations in remodeler-depleted extract. **(A)** Color-coded gene-by-gene representation (3926 genes plotted) of nucleosome dyad densities as in Figure 2.1 A. Native, SGD, and wtWCE are same data as in Figure 2.1 A. Graphs 4 to 10 represent experiments using an extract depleted for the remodeler ATPases Chd1, Isw1, and Isw2 *(Tsukiyama et al., 1999)*. In these experiments purified remodelers were added to the extract at a remodeler-to-nucleosome molar ratio of 1:10. Experiments were performed in multiple replicates and the mean was plotted (replicate number indicated by "n")**(B-F)** Composite representation of the data shown in **A**.

2.2.3 ISW2 accurately positions the +1 nucleosome and generates nucleosomal arrays but with non-physiological spacing

Lack of ISW2 in cells leads to only modest effects on nucleosomal array formation (Gkikopoulos et al., 2011; Ocampo et al., 2016), but entire nucleosomal arrays, i.e. the +1 positions, are shifted downstream for at least some genes (Whitehouse et al., 2007; Yen et al., 2012). In positioning experiments, where *isw1Δ isw2Δ chd1Δ* WCE was supplemented with purified ISW2, +1 nucleosomes were accurately positioned at *in vivo* positions with high average occupancy (Figure 2.2 F, red trace) at most genes throughout the genome (Figure 2 A panel 9). ISW2 also generated nucleosomal arrays, but with non-physiological too wide spacing. On average, this spacing was about 200 base pairs, which is similar to ISW2 spacing activity *in vitro* (200 bp) and in accordance with the described ISW2 linker requirement (Gangaraju and Bartholomew, 2007; Kagalwala et al., 2004; Tsukiyama et al., 1999).

2.2.4 ISW1a imposes proper spacing on nucleosomal arrays with non-physiological spacing generated by ISW2

ISW1b and Chd1 did not affect nucleosome positioning on their own, but we considered the possibility that they may alter the effects of other remodelers. However, neither of both alter appreciably the effect of ISW1a (Figure 2.3 C, 3 D) or of each other (Figure 2.3 C) or of ISW2 (data not shown) in our *in vitro*-system. Again, this supports the notion that these remodelers are part of a nucleosome positioning mechanism that is not recapitulated here. As ISW1a and ISW2 both positioned +1 nucleosomes and generated nucleosomal arrays. +1 nucleosome positioning was more accurate for ISW2 than for ISW1a compared to physiological +1 nucleosome position. The nucleosomal array generated by ISW2 had showed a too wide, non- physiological spacing. We wished to see which NDR-array features were generated by a combination of both. For this titration experiment we lowered the ISW2 concentration to 1:30 relative to our standard conditions. This ISW2 concentration was still sufficient to yield the full ISW2 positioning effect (Figure 2.3 F), i.e. accurate +1 nucleosome positioning with high occupancy and widely spaced arrays, but allowed us to titrate the relative ISW1a concentration in a wider range. Strikingly, ISW1a imposed the narrow, more physiological spacing on the nucleosomes aligned to +1 nucleosomes with wider spacing by ISW2 (Figure 2.3 F).

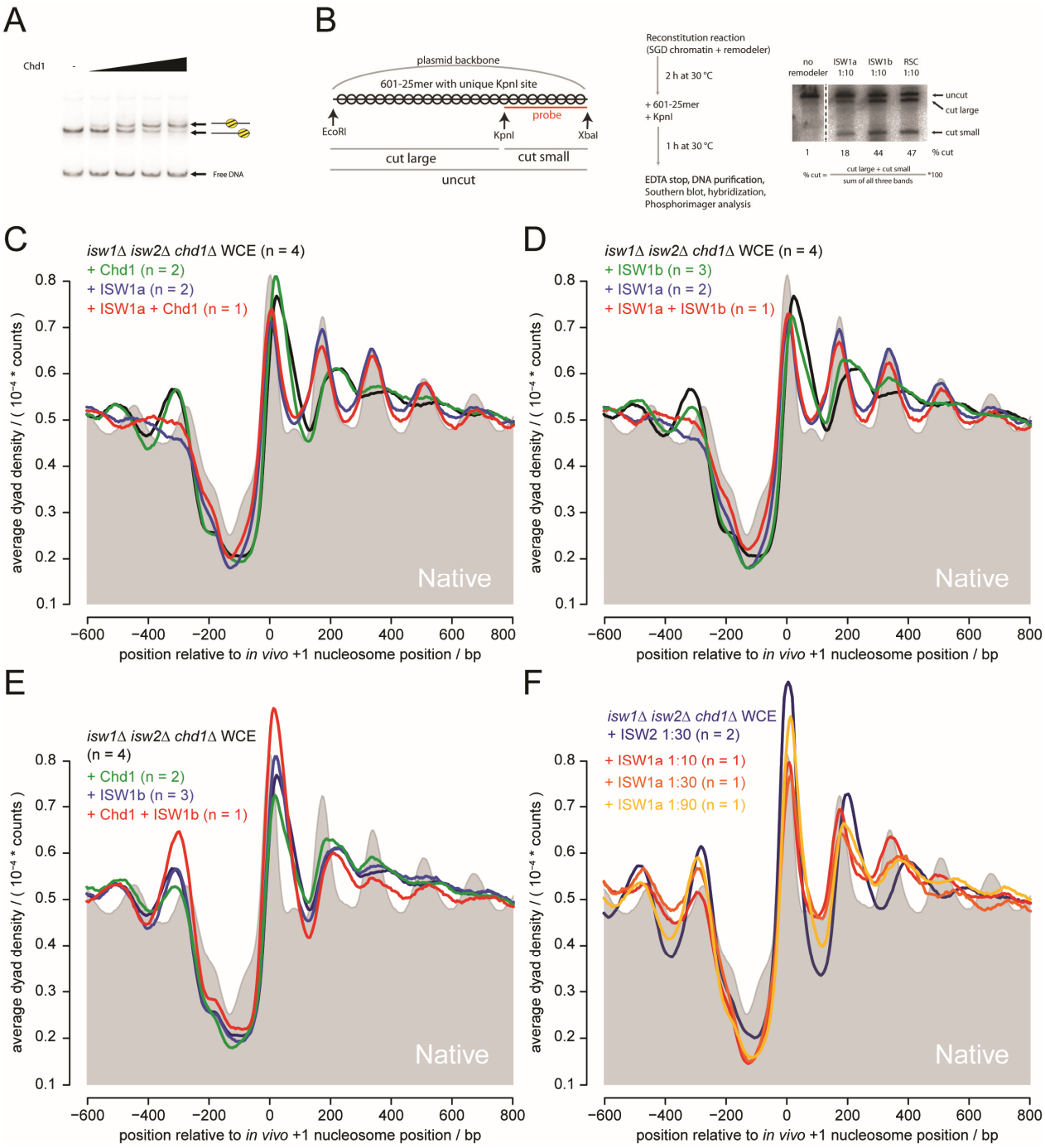

Figure 2.3 Tug-of-war between ISW2 and ISW1a leads to in vivo-like positioning and spacing of nucleosomes. **(A)** Nucleosome sliding assay for Chd1, performed by Shinya Watanabe. **(B)** DNA accessibility to unique KpnI restriction enzyme recognition site as indicator of remodeling activity. The KpnI site is protected by a 601-sequence positioned nucleosome within chromatinized plasmid unless the nucleosome is remodeled (scheme). After a 2 h positioning reaction, 601-array chromatin and KpnI were added and incubated for one additional hour. At the level of purified DNA the 601-array was cut out by EcoRI and XbaI. KpnI-accessibility generated by chromatin remodelers was detected by separating the cut large, cut small and uncut fragments and Southern blotting. Appearance of the "cut small" and "cut large" bands indicates remodeling activity. Results from the same membrane are shown but rearranged (stippled line) using Adobe Photoshop 12.0 x64. **(C-F)** Composite distributions of average nucleosome dyad densities for experiments with *isw1*, *isw2*, and *chd1* depleted extracts plus indicated purified remodelers at a remodeler-to-nucleosome molar ration of either 1:10 or as indicated was plotted (replicate number indicated b "n"). *(A) and (B) are reprinted with permission from Elsevier (Krietenstein et al., 2016).*

This dominant effect of ISW1a was dependent on the concentration of ISW1a relative to ISW2. The more ISW1a was added to the reaction with ISW2, the more the ISW2-specific spacing was changed towards the ISW1a-specific physiological spacing. Nonetheless, the concentration of

ISW1a (1:10) that was sufficient to properly position up to nucleosomes +3/+4 when added on its own to the *isw1Δ isw2Δ chd1Δ* WCE was not sufficient when ISW2 was added. This was not only true with regard to spacing, but also with regard to +1 nucleosome positioning. In contrast to experiments, where only ISW1a was added, the +1 nucleosome position was more accurate in presence of ISW2. This suggests antagonizing positioning activity of the two remodelers. This supports the idea that both, +1 nucleosome positioning and spacing, result from the combination of independent and specific remodeler activities.

2.3 Reconstitution of nucleosome positions by purified remodelers only

Testing remodelers in the background of WCEs allowed us to assess remodeler-specific contributions to the reconstitution of NDR-array features. To test if remodeler activity is also sufficient by itself, we studied the impact of remodelers using only purified factors without cell extract in our genome-wide nucleosome positioning assay.

2.3.1 RSC reads poly(dA:dT) elements and widens NDRs asymmetrically

In contrast to DNA sequence encoded nucleosome positioning a remodeler code hypothesis was proposed as general model for nucleosome positioning. The latter hypothesis is based on the observation that steady-state nucleosome positions on one and the same DNA sequence were different after incubation with different remodelers (Rippe et al., 2007). In the original framework of the remodeler code hypothesis, some nucleosomes are “good” and others are “poor” substrates of specific remodelers. The “good” substrates are translocated until they take a distinct position and become “poor” substrates, which are not further translocated. Such a mechanism could explain ATP-driven nucleosome positioning and would predict that (some) remodelers can position nucleosomes on their own. To test this, we performed nucleosome positioning experiments with purified remodelers alone on SGD reconstituted chromatin. None of the so far tested remodelers could move nucleosomes to their physiological positions in the absence of crude extracts (Figure 2.4 A), but all of them widened the intrinsically generated NDRs to some extent (NDRs appear wider and more “blue” in gene-by-gene analysis). We quantified the average NDR length of SGD chromatin and after remodeling by purified factors (Figure 2.4 C). Only RSC and INO80 (see below) generated an NDR of about physiological extent.

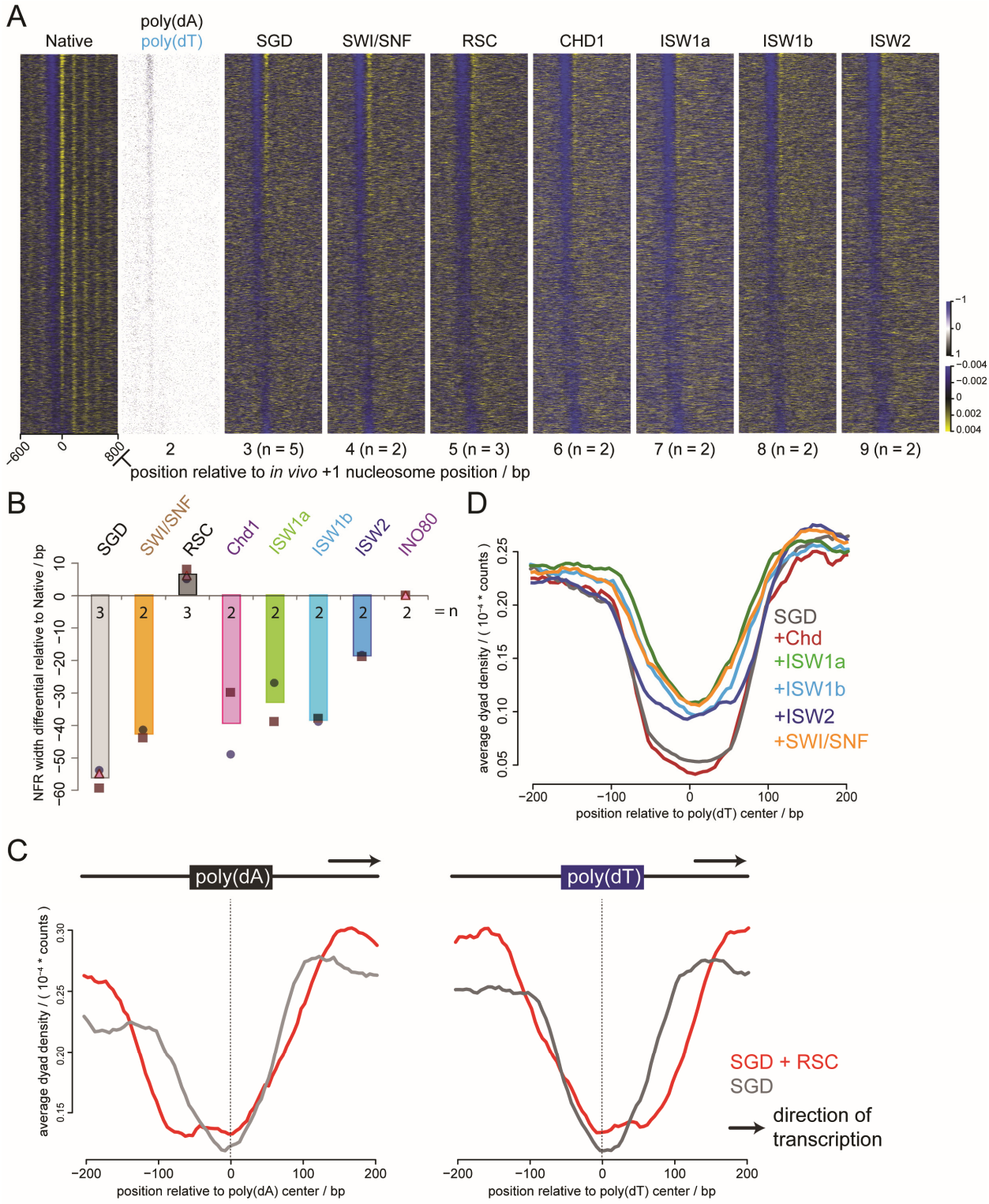

Figure 2.4 poly(dT)/(dA) elements signal RSC to generate physiological NDRs. (A) Color-coded gene-by-gene representation (3926 genes plotted) of nucleosome dyad densities as in Figure 2.1 A. Native and SGD show same data as in Figure 2.1 A. Graph 2 displays distribution of poly(dT) and poly(dA) tracks > 5 bp in blue and black, respectively. Graphs 4 - 9 display nucleosome dyad densities after incubation with indicated purified remodelers. The mean of n (as indicated) was plotted. (B) Average NFR width difference between Native chromatin and SGD chromatin without or with indicated remodelers. Bars show averages of n replicates (as indicated), symbols show values of individual datasets. (C) Composite nucleosome dyad distribution of data as in A, graphs 3 and 5, but only for promoters with unique poly(dA) or poly(dT) elements, respectively, on the sense strand. (D) as right side of C, but for remaining data sets of A not plotted in C. Remodeler-to-nucleosome molar ratios were 1:10, except for RSC which is the mean of three experiments with remodeler-to-nucleosome ratios of 1:10, 1:20, and 1:40 yielding similar results. *(A) is reprinted with permission from Elsevier (Krietenstein et al., 2016).*

In vivo, nucleosome occupancy in NDRs increases upon depletion of RSC activity (Hartley and Madhani, 2009). Further, RSC was specifically required to reconstitute NDRs at four promoters *in vitro* (Wippo et al, 2011) and selectively removes nucleosomes at promoters *in vitro* (Lorch et al., 2011). Thus, RSC was a likely candidate for NDR formation and our genome-wide reconstitution confirms this activity in a purified system. Even more, we could distinguish now that NDR formation by RSC does not involve positioning of the flanking -1 and +1 nucleosomes, i.e. RSC-mediated NDR formation is biochemically distinct from +1 nucleosome positioning.

Next, we asked how RSC-specifically recognizes promoters to create NDRs. The Rsc3/30 subunits of the RSC complex are suggested to recognize a CGCGCGG DNA motif (Badis et al., 2008). Centering our nucleosome positioning reconstitution data after RSC remodeling on such motifs did not show especially pronounce NDR formation (data not shown), and tag density remained largely unchanged after remodeling by RSC. This suggested that RSC targeting for NDR formation did not primarily depend on recruitment via Rsc3/30 but involved an alternative mechanism.

NDR formation by RSC *in vitro* scaled with intrinsic NDR formation by SGD, i.e. intrinsically well reconstituted NDRs appeared to be strongly affected by RSC (Figure 2.4 A, top third of genes in gene-by-gene analysis). This suggested a link between intrinsic NDR formation by SGD and recognition by RSC. Poly(dA:dT) tracts are suggested to destabilize nucleosomes *in vitro*, and such destabilization is proposed to create intrinsic NDRs, especially at promoter regions that are enriched for poly(dA:dT) (Kaplan et al., 2009; Segal and Widom, 2009; Sekinger et al., 2005; Struhl and Segal, 2013; Zhang et al., 2009). RSC might sample nucleosomes and evict unstable nucleosomes more efficiently, thus enhancing intrinsically DNA-encoded NDRs. Recently, it was shown that RSC nucleosome eviction activity *in vitro* is stimulated by poly(dA:dT) elements and it is suggested that RSC recognizes these elements also *in vivo* (Kubik et al., 2015; Lorch and Kornberg, 2015; Lorch et al., 2014). As another hint in this direction, poly(dA) and poly(dT) elements are distributed asymmetrically in NDRs *in vivo*, which would not be expected of an intrinsic biophysical mechanism - as poly(dA) and poly(dT) elements in a double helix are biophysical equivalent with regards to nucleosome stability - but rather suggests that such elements may be read by another factor (de Boer and Hughes, 2014; Wu and Li, 2010) (Figure 2.4 A graph 2). We wondered if RSC is this factor. RSC translocates in 3' to 5' direction along DNA (Saha et al., 2005) and may thereby distinguish between poly(dA) and poly(dT) elements in a directional way for nucleosome remodeling. According to this novel hypothesis, directional remodeling relative to such sequence elements would be observed. In contrast, if nucleosome instability were the signal for RSC, remodeling should be independent of feature orientation. To distinguish between these hypotheses, we selected poly(dA) and poly(dT) elements within promotor regions

upstream of TSSs that are unique, i.e. not accompanied by poly(dT) or poly(dA), respectively, on the same strand. As expected, symmetric NDRs are formed around these elements by SGD equally for poly(dT) and poly(dA) elements (Figure 2.4 B, grey traces), as both have the same destabilizing effect. However, NDRs are widened asymmetrically upon RSC remodeling. In the case of poly(dA) elements, NFR widening occurred asymmetrically in the upstream direction, vice versa for poly(dT) elements (which are poly(dA) elements on the complementary strand). These experiments make intrinsic nucleosome instability as cause for RSC-dependent NDR formation less likely and strongly suggest that RSC reads poly(dA) elements in a RSC-specific way, like a signal. Importantly, all other remodelers did not respond to these elements in a directional manner, even though they more or less effected NDR widening (Figure 2.4 D).

In summary, we show directly in a purified system that RSC can cause NDR formation, as previously suggested(Hartley and Madhani, 2009; Kubik et al., 2015; Lorch et al., 2011; Wippo et al., 2011). Our approach allowed to identify two new aspects of this NDR formation mechanism by RSC. First, RSC NDR formation is biochemically distinct from positioning the NDR flanking -1 and +1 nucleosomes. Second, poly(dA:dT) elements function as a signal for RSC to displace nucleosomes in a directional manner.

2.3.2 INO80 on its own places nucleosomes to physiological positions

Since RSC and all other so far tested remodelers caused NDR formation but not +1 nucleosome positioning, we purified INO80, the only remaining major remodeling complex with sliding activity. We performed reconstitution experiments with SGD chromatin incubated solely with INO80 at various concentrations. Remarkably, INO80 on its own was robustly able to position the physiological +1 and -1 nucleosomes at most of all genes, independent of a strong SGD intrinsic NDR, and also some +2 nucleosomes (Figure 2.5 A, B). This effect was even more pronounced in the context of crude extracts (Figure 2.5 A graph 2). Here, INO80 generated very strong +1 nucleosomes at accurate positions and nucleosomal arrays albeit with non- physiological too wide spacing, similar to ISW2 (Figure 2.5 A graph vs. Figure 2.2 A graph 9).

Next, we asked how INO80 “knows” where to place the +1 nucleosomes in a 12 Mbp genome. Since +1 nucleosome organization appeared throughout the genome (Figure 2.5 A graph 4), independent of NDR formation or +1 nucleosome positioning by SGD, we searched for motifs beyond the poly(dA:dT) elements around *in vivo* +1 nucleosome regions by MEME analysis. No clear motifs were detected (data not shown).

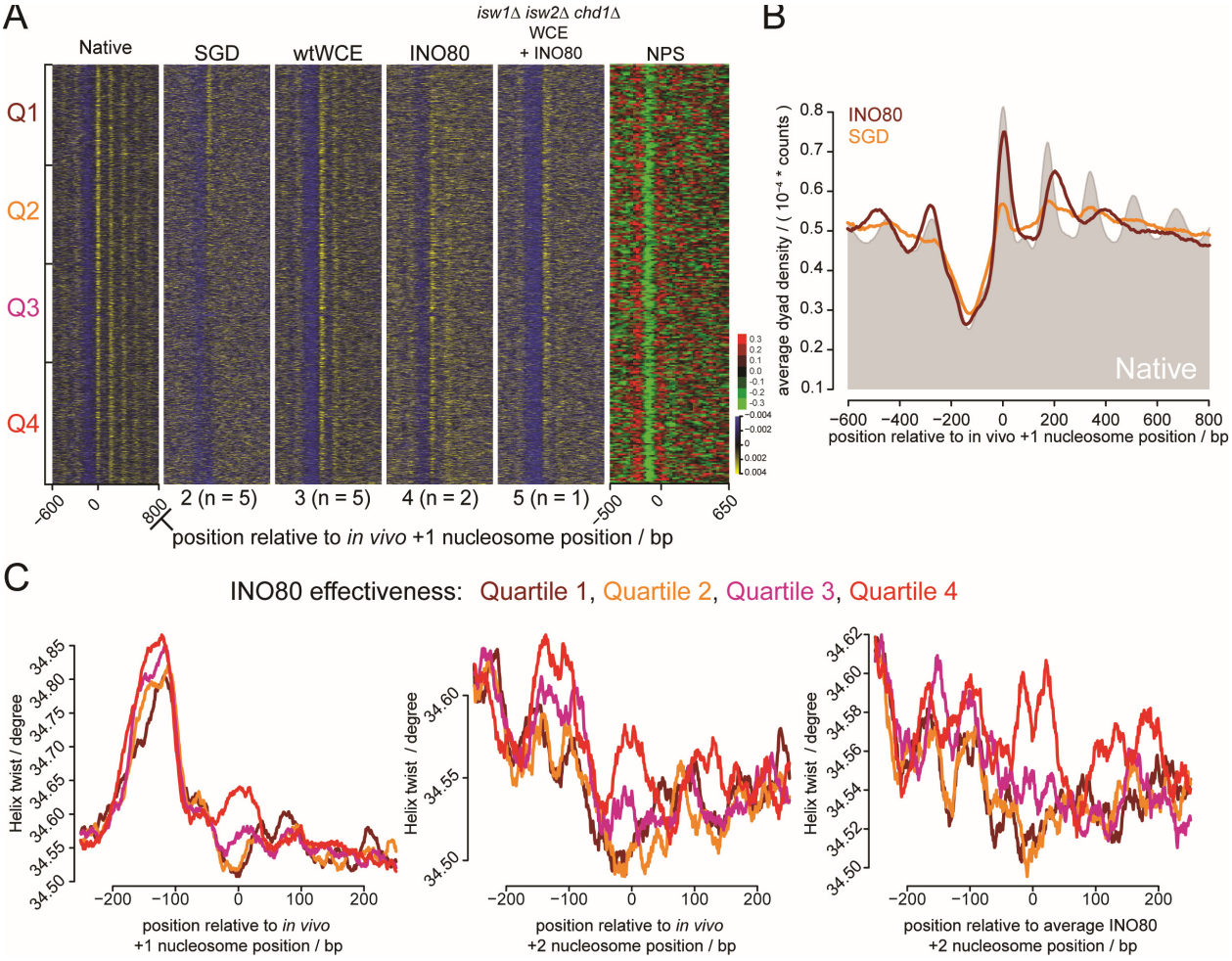

Figure 2.5 INO80 alone positions the majority of* +1 nucleo*somes, speculatively in dependence of DNA shape features. (A) Color-coded nucleosome dyad densities for 3928 genes (row-by-row) sorted by INO80-"effectiveness" (ratio of graphs 2 vs. 4) and subdivided into quartiles Q1-Q4. Yellow, black, and blue represent high, medium, and low tag density, respectively. Genes are aligned to *in vivo*-called +1 nucleosome positions. Native, SGD, and wtWCE as in Figure 2.1 A. INO80 represents nucleosome dyad density set by adding only purified INO80 to SGD chromatin. *isw1Δ isw2Δ chd1Δ* WCE + INO80 represents nucleosome dyad density generated by INO80 together with *isw1Δ isw2Δ chd1Δ* WCE. (B) Composite nucleosome dyad distribution of data as in A, graphs 2 and 4. (C) Average predicted DNA helical twist (Chiu et al., 2016; Zhou et al., 2013) of DNA sequences around indicated features (x-axis) for genes in Q1-Q4. *In vivo* +1 and +2 nucleosome positions were called from *in vivo* MNase-seq data (Zhang et al., 2011). The average INO80 +2 nucleosome corresponds to the *in vivo* called +1 nucleosome position shifted downstream by 200 bp for each gene, i.e. by the average distance between +1 and +2 nucleosome positions (first and second maxima downstream of NDR) for INO80 data in B. Remodeler-to-nucleosome molar ratios were 1:10.

As second approach, we sorted the genes according to "INO80-effectiveness" regarding physiological +1 nucleosome positioning (Figure 2.5 A). This is the ratio of tag density at *in vivo* +1 nucleosome regions of experiments with INO80 treated SGD chromatin over SGD only chromatin (4.3.2.2). We sorted all genes in ascending order according to this INO80-effectiveness and divided the genes into four quartiles, Q1-Q4. Q1 contains genes with intrinsically physiologically positioned nucleosomes that are scattered by INO80 remodeling. Q2 and Q3 represent intermediate states. Q4 represents genes with intrinsically non- physiologically positioned nucleosomes that are moved to *in vivo* positions by INO80 remodeling. Using this sorting scheme, we looked at the distribution of nucleosome positioning sequences (NPS) that are based on 10 bp periodicity of AA dinucleotides (Ioshikhes et al., 2006). Such NPSs are enriched

at +1 nucleosome positions throughout all 4 quartiles (Figure 2.5 A) and therefore are insufficient to explain or predict physiological +1 nucleosome positioning by INO80. Next, we used sequence based prediction of DNA shape (Chiu et al., 2016; Zhou et al., 2013) at *in vivo* +1 nucleosome positions for all four quartiles (Figure 2.5 C left graph). This predicted a relative average DNA over-twist for +1 nucleosome regions, which are strongest affected by INO80 +1 nucleosome positioning (Q4). In contrast, nucleosome positions that had intrinsically properly positioned nucleosomes were predicted to be relatively under-twisted on average (Q1). This trend also scaled through the intermediate quartiles Q2 and Q3. To test if this correlation is confounded by any unidentified feature in the neighboring NDR, like a motif or availability of free DNA, we sorted the genes according to "INO80-effectiveness" at *in vivo* +2 and average INO80 +2 (+1 nucleosome positions shifted 200 bp downstream) nucleosome positions (Figure 2.5 C panel 2 and 3). The same trend holds true for Q1-Q4 at these nucleosome positions. Over-twisting of DNA might disfavor nucleosome assembly. INO80 may slightly untwist DNA, thereby making the NPS more effective in Q4 or less effective in Q1. This hypothesis is highly speculative and solely based on correlation, but it is the first attempt to explain these novel remodeler activity, observed for INO80.

In summary, INO80 by itself is able to position most of all +1 nucleosomes throughout the genome. This ability to precisely position +1 nucleosomes is intrinsic to INO80 since no other factors than chromatin are present in this positioning reactions. These finding shows for the first time, that +1 nucleosome positioning is independent on SGD intrinsic chromatin organization. Also, INO80 generates a nucleosomal array with non-physiological spacing. Further, no DNA sequence motives could be identified that could predict this novel INO80 activity. INO80-effectiveness scaled with DNA over-twisting, where nucleosomes that were positioned by INO80 were placed onto DNA with a predicted over-twist. Speculatively, INO80 untwists DNA, which regulates other effectors like NPSs.

2.4 Reconstitution using a GRF barrier, Reb1 and Abf1

Since most remodelers, besides INO80 and RSC, were not able to reconstitute any features of nucleosomal NDR-array formation on their own but in presence of a crude extract, we asked if there are factors in the crude extract that may guide remodelers to their place of action. Abf1, Rap1, and Reb1 are the GRFs that are essential in yeast (Bussemaker et al., 2001; Chasman et al., 1990; Pilpel et al., 2001). It is shown, that upon depletion of the GRFs Rap1, Abf1 and Reb1 NDRs become occupied by nucleosomes (Hartley and Madhani, 2009; Yu and Morse, 1999). The general

usage of GRFs in NDR formation seems to be conserved, even though different proteins have evolved to fulfill this function (Tsankov et al., 2011, 2010). Thus it is likely that these factors may contribute to NDR-array organization. Further, GRF binding sites can be swapped and protein domains substituted without loss of function suggesting that GRFs have similar functions (Gonçalves et al., 1996; Lieb et al., 2001). Reb1 and Abf1 are associated with genic features that have canonical nucleosome organization (genes and replication origins), Rap1 is enriched at ribosomal protein genes, which have almost no nucleosomal organization. Therefore, we purified recombinant Reb1 and Abf1 and performed genome wide nucleosome positioning assays.

2.4.1 Abf1 functions as a barrier and nucleates NDR-array formation

Both, the depletion of RSC (sth1-td) or Afb1 (Abf1-ts) lead to increased nucleosome occupancy at NDRs. This suggests that both are involved in a similar pathway keeping NDRs nucleosome free. We performed Abf1-ChIP-exo (Rhee and Pugh, 2011) to determine *in vivo* Abf1 binding sites at base pair resolution (Figure 2.6 A graph 1) and used Abf1 tag enrichment for gene sorting in gene-by-gene analysis (Figure 2.6 A). The top 25% genes were defined as Abf1 bound, the bottom 25% as Abf1 unbound. To test if remodelers interact with Abf1, we performed *in vitro* nucleosome positioning reactions with purified remodelers in presence and absence of purified Abf1. Incubation of SGD chromatin with Abf1 did not change nucleosome positions (compare Figure 2.6 A graph 3 and 7). As well, the addition of RSC, ISW2 and, ISW1a alone did not organize nucleosomes (Figure 2.6 A graphs 4 to 6). Note, the RSC effect observed in 2.3.1 is not obvious because of *in vivo* Abf1-binding-site-sorting. Second, ISW2 typical +1 nucleosome positioning is specific to Abf1 bound genes (Figure 2.6 A graph 9 and 6D) and was not observed in absence of Abf1 (Figure 2.6 D panel 1and 2) or at Abf1 unbound genes (Figure 2.6 D panel 2). Again, the nucleosomal array with non-physiological spacing is also observed at Abf1 bound genes (Figure 2.6 D). Third, ISW1a generates +1 nucleosome positioning at Abf1 bound genes with lower occupancy compared to ISW2, even at a higher concentrations (Figure 2.6 A graph 10 and 2.6 C panel 1). Also a nucleosomal array is generated, even though to a lesser extent as observed in presence of crude extract. This observation was specific for Abf1 bound genes only in presence of Abf1 (compare Figure 2.6 C panel 1 and 2). This suggests that ISW1a required not only a GRF to nucleate array formation but also positioned +1 nucleosomes.

Since our experiments with purified factors demonstrated that the observed nucleosome positioning effects are indeed specific to the tested factors, we wondered if the reconstitution of a physiological NDR-array organization is possible with only purified factors. We combined Abf1,

RSC, the NDR forming factor, ISW2, the +1 nucleosome position factors, ISW1a, the physiological spacing factor, ISW1b, and Chd1, that were inefficient in our assay. Indeed, this combination was sufficient to generate a NDR-array pattern with physiological NDR and +1 nucleosome occupancy. The nucleosomal array was established to almost physiological levels at Abf1 bound genes (Figure 2.6 E).

In summary, GRFs were not only involved in NDR establishment, but also in organizing the whole nucleosomal NDR-array architecture around promotors. Further, this architecture could be established in a minimal system with ISW2, ISW1a and RSC in combination with a barrier factor. The observation that +1 nucleosome position was the consequence of antagonizing remodeler functions, suggests that this minimal system has also the properties to regulate transcription.

2.4.2 Reb1 functions as a barrier and nucleates NDR-array formation

The integration of a Reb1 binding site and an AAAAAA stretch causes nucleosome depletion in a normally nucleosomal occupied region (Hartley and Madhani, 2009). This depletion depends on Reb1 and RSC, since the depletion of Reb1 (Reb1-td) or RSC (sth1-td) restores wt nucleosomal occupancy. Incubation of chromatin with Reb1 is not sufficient to position nucleosomes (data not shown), as with remodelers RSC and ISW2 alone (Figure 2.7 A graph 4 and 5), even though ISW2 displayed strong nucleosome positioning effect in context of a crude extract (section 2.2.2 and 2.2.3).

Similar to experiments with Abf1, these remodelers selectively organize nucleosomes at Reb1 bound genes (Figure 2.7 A graph 6 and 7). RSC generates NDRs and ISW2 positions the +1 nucleosomes (compare Figure 2.7 B and C). Also, ISW2 generated a modest nucleosomal arrays, again, non-physiological, too wide spacing. Further, the remodeling factors ISW1b and Chd1 were without effects in experiments with Reb1 (data not shown).

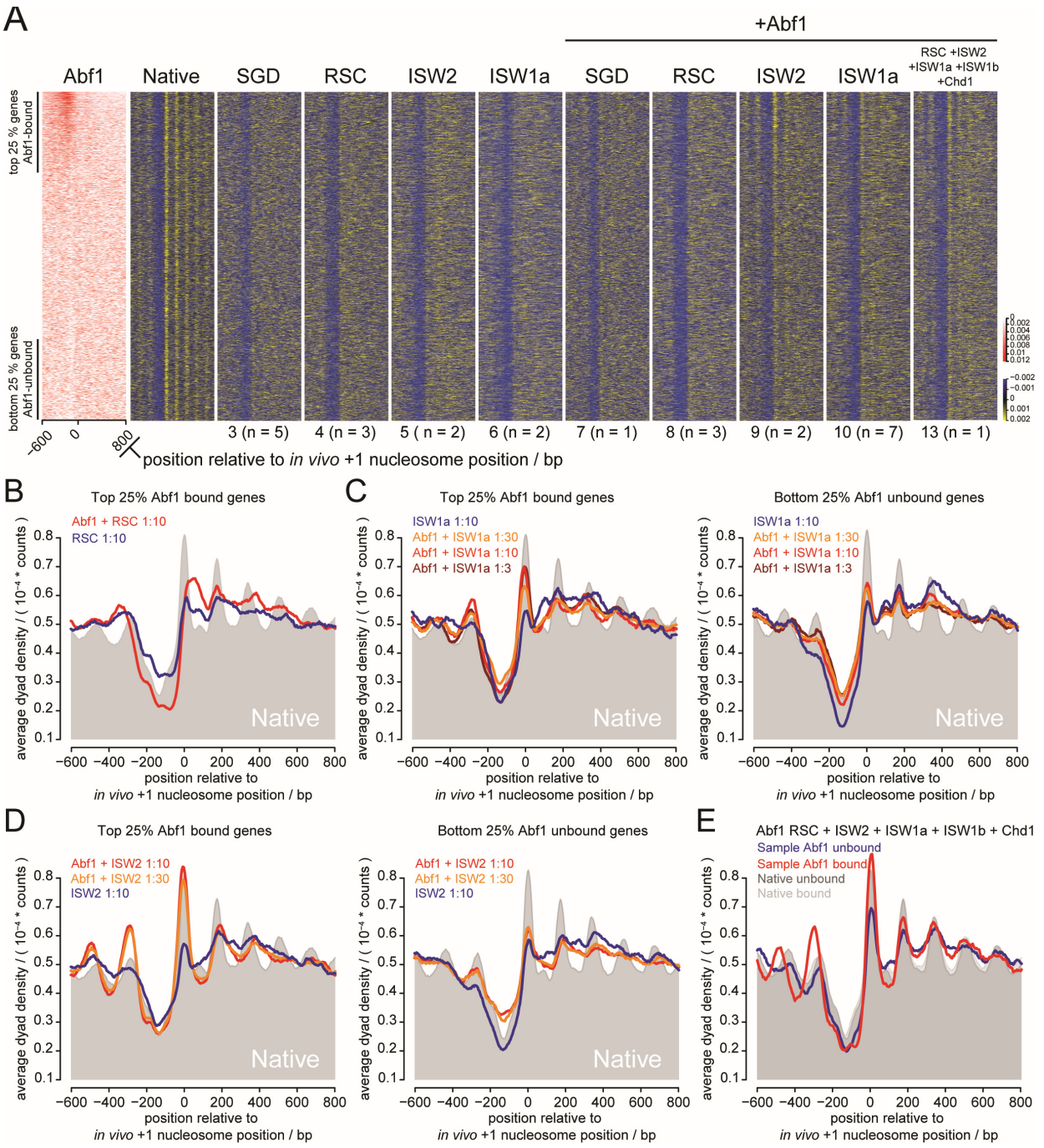

Figure 2.6 Abf1 functions as a barrier and nucleates NDR-array formation. (A) Color-coded gene-by-gene representation (3931 genes plotted) of nucleosome dyad densities as in Figure 2.1 A. Genes were sorted in descending order according to in vivo Abf1-ChIP-exo tag density (graph 1). The top 25% genes represent the Abf1 bound genes, the bottom 25% represent the Abf1 unbound genes. Native and SGD, experiments as in Figure 2.1. Graphs 3-6, SGD incubated with purified remodelers, as indicated, without Abf1. Graphs 7-10, SGD incubated with purified remodelers, as indicated, alongside with Abf1. (B-E) Composite distributions of nucleosome dyad densities for SGD incubated with remodelers and Abf1 and for the gene subgroups as indicated. Remodeler-to-nucleosome molar ratios were 1:10 unless indicated otherwise.

RSC-specific remodeling is selectively increased at Reb1 bound genes in presence of Reb1 (compare Figure 2.7 A graph 4 and 6, also 7B). NDRs become less nucleosome occupied, but no +1 nucleosomes were positioned. It appeared that RSC piles up nucleosomes downstream of promoters (Figure 2.7 B). Thus, we thought that RSC antagonizes ISW2 +1 nucleosome

positioning, as observed when RSC was added to *isw1Δ isw2Δ chd1Δ* WCE. To test this, we performed experiments with RSC at 1:30 and titrated ISW2. RSC at a concentration of 1:30 widens the NDR and does not position the +1 nucleosomes (Figure 2.7 E, blue trace). Addition of ISW2 increases the precision of the +1 nucleosome with increasing concentration (Figure 2.7 E, orange to red traces). At a concentration of ISW2 1:30, the +1 nucleosome is established, but not to the same extend as in experiments with ISW2 alone. Further the +1 nucleosome is shifted downstream compared to the *in vivo* +1 nucleosome position (compare Figure 2.6 E red trace with grey native pattern), suggesting that RSC remodeling antagonizes +1 nucleosome positioning. This effect could also be the reason that +1 nucleosome positioning in wtWCE and mutant WCEs is shifted downstream by RSC being over active or overrepresented in crude extract preparations.

In summary, Reb1 as well as Abf1 instruct NDR formation and +1 nucleosome positioning. This NDR-+1 organization nucleates NDR-array formation to physiological levels.

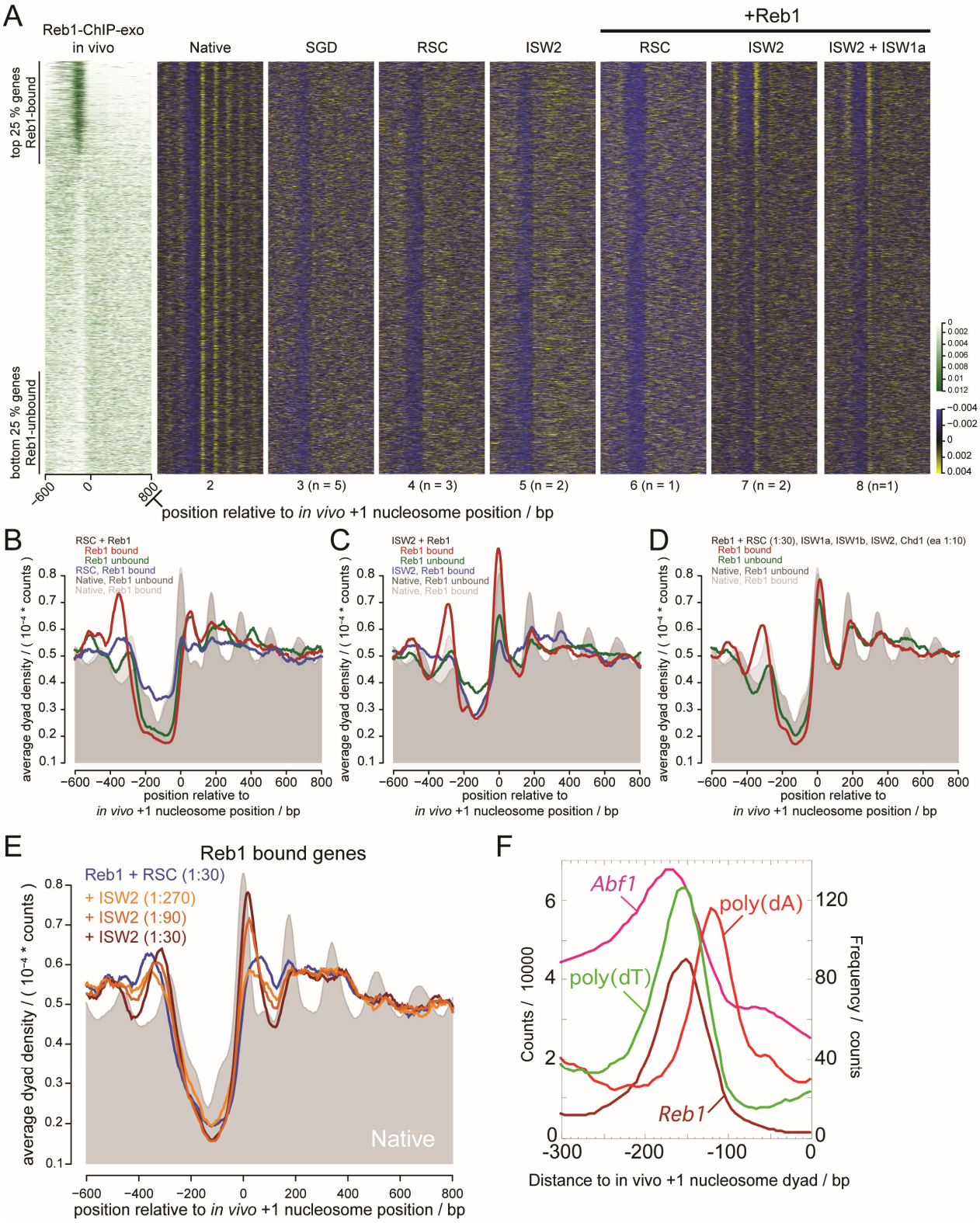

Figure 2.7 Reb1 functions as a barrier and nucleates NDR-array formation. **(A)** As figure 6A but sorted in descending order according to *in vivo* Reb1-ChIP-exo tag density *(Rhee and Pugh, 2011)* (3931 genes plotted). **(B-E)** as figures 6B-D, but for Reb1 bound or unbound genes as indicated. **(F)** Composite distributions of poly(dA)/(dT) elements and Reb1- and Abf1-ChIP-exo tag density. Remodeler-to-nucleosome molar ratios were 1:10 unless indicated otherwise.

2.5 Dissection of INO80-specific nucleosome positioning with recombinant INO80

2.5.1 Endogenous vs. recombinant INO80

The generation of *in vivo*-like +1 nucleosome positioning by INO80 on its own (2.3.2) amounts to a novel function for INO80 discovered by us here. To exclude any contaminating factors that may have co-purified via TAP purification and may be (co-)responsible for this novel activity we tested recombinant INO80 in our *in vitro* nucleosome positioning experiments. Moreover, using recombinant expressed protein complex allowed to explore different mutant variants of INO80, for example, a complex lacking the otherwise essential Rvb1/2 ATPase activities.

Both, endogenous and recombinant, INO80 showed INO80-specific nucleosome positioning (Figure 2.8 A panel 3 and 4). Nucleosome positioning followed the same trend when sorted by *in vivo* NFR length (as in Figure 2.5 A), computed from experiments with endogenous INO80. Over all, recombinant and endogenous INO80 displayed a similar activity. In some experiments, recombinant INO80 displayed higher activity in the sense that the peaks were higher and the widely spaced nucleosomal array extended further into the gene body in some experiments (Figure 2.8 C *H. sapiens* histones). However, this may also be due to different INO80 concentrations as the endogenous preparations were quantified by Shinya Watanabe according to ATPase activity and normalization to a Peterson lab SWI/SNF standard, and recombinant INO80 was quantified by Sebastian Eustermann according to protein mass. Normalization via ATPase activity is the best way to compare between different remodeler types as ATP hydrolysis is the common denominator of their otherwise disparate remodeling activities. However, as this part of the study focused only on INO80 and compared various mutant versions, including mutations in the Ino80 ATPase and the AAA+ ATPases Rvb1/2, a normalization via ATPase activity was not appropriate here and total protein mass was used for normalization. Whether recombinant INO80 really has higher specific remodeling activity than endogenous INO80 was for the present purpose irrelevant and remains to be determined.

Importantly, overexpression of recombinant yeast INO80 in insect cells allows the purification of a highly active complex with the same remodeler-specific nucleosome positioning properties as the endogenous INO80. Therefore, recombinant INO80 is a suitable tool to study the mechanism of the INO80-specific nucleosome positioning activity.

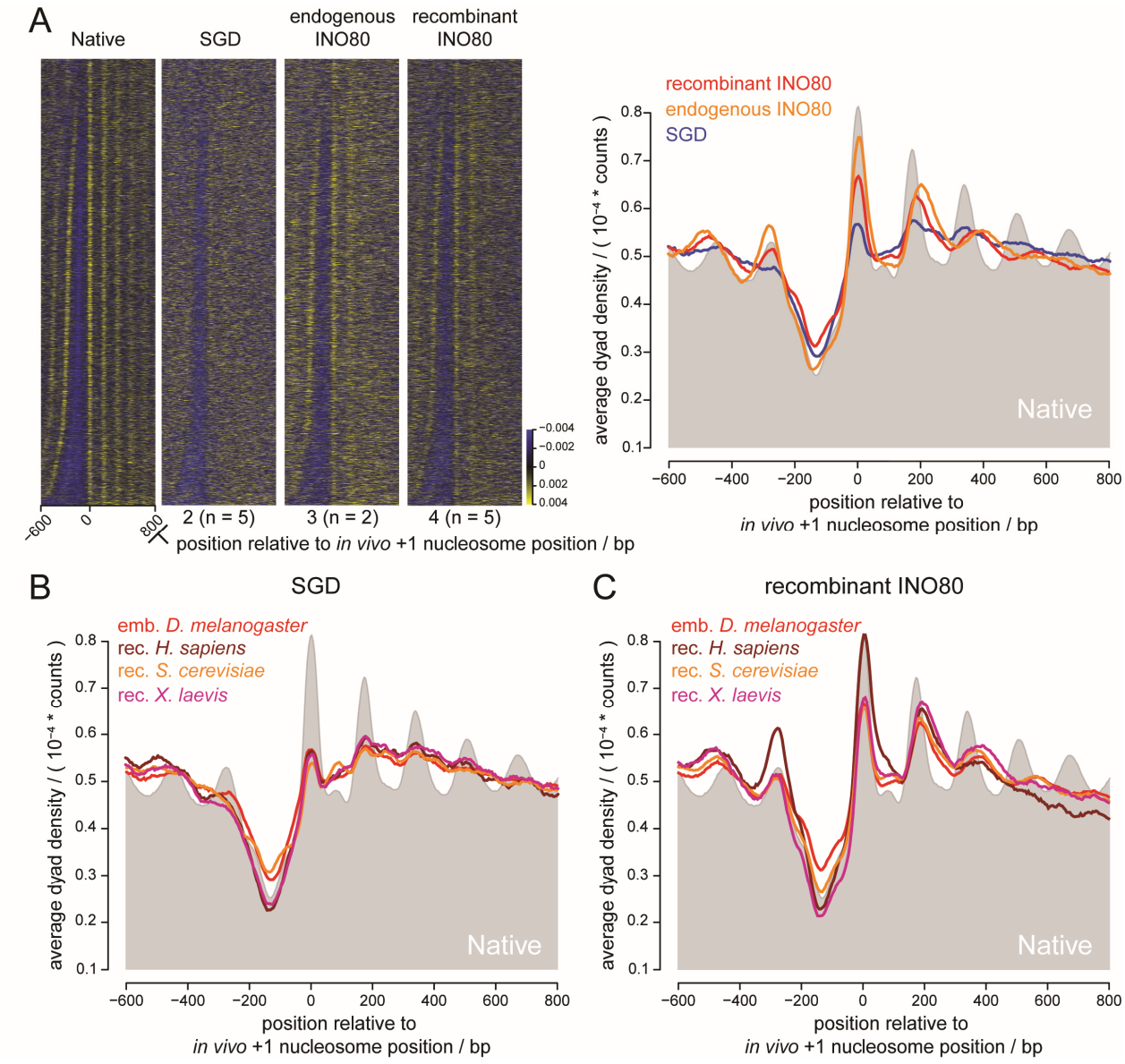

Figure 2.8 INO80-specific nucleosome positioning is equally achieved with endogenous vs. recombinant INO80 and independent of histone source, PTMs, and variants. (A) Color-coded nucleosome dyad densities for genes 3931 (row-by-row) sorted *in vivo* NFR length (distance between *in vivo* -1 and +1 nucleosomes). Yellow, black, and blue represent high, medium, and low tag density, respectively. Genes are aligned to *in vivo*-called +1 nucleosome positions. Native, SGD, and endogenous INO80 as in Figure 2.5 A. Recombinant INO80 represents nucleosome dyad density set by adding only recombinant INO80 to SGD chromatin. (B) Composite representation of nucleosome positions after SGD with different recombinant histone octamers (*H. sapiens*, *S. cerevisiae*, and *X. laevis*) compared to "standard" embryonic drosophila histone octamers. (C) As B but with positions set by recombinant INO80. Remodeler-to-nucleosome molar ratios were 1:10.

2.5.2 Nucleosome positioning by INO80 is not affected by histone modifications, histone variants, or species-specific core histones

Throughout the previous experiments we used histone octamers purified from *Drosophila melanogaster* embryos. These histone octamers contain histone PTMs and variants that are present in *Drosophila* embryos (Imhof and Bonaldi, 2005). To test whether histone variants, histone modifications, or species-specific core histones have an impact on NDR-+1-array formation, we tested recombinant expressed core histones from *S. cerevisiae*, *H. sapiens*, and *X. laevis* in

genome-wide reconstitution experiments with recombinant INO80. Chromatin reconstituted by SGD with any of these recombinant histones displayed the same intrinsic nucleosome positioning (Figure 2.8 A and B). This demonstrated that histone octamers from different species and without modifications or variants have the same DNA preference during SGD. Also the INO80-specific nucleosome positioning was independent of histone source and modifications and variants and displayed typical +1 nucleosome positioning and widely spaced array formation (Figure 2.8 A and C). To test if the recombinant histones allowed *in vitro* positioning also by other factors and not only by INO80, we performed nucleosome positioning reactions with wtWCE. This resulted in physiological NDR-+1-array formation as observed with embryonic fly histones (data not shown).

Collectively, transcription-independent nucleosome positioning by recombinant INO80 and wtWCE remodelers and is independent of histone source, PTMs and histone variants. This argues for a conserved core mechanism.

2.5.3 Histone tails are required for INO80-dependent genome-wide nucleosome positioning

Since genome-wide nucleosome positioning was independent of histone modifications and variants, we wondered if histone tails were required. INO80 shows increased ATPase and nucleosome remodeling activity when histone tails are deleted (Udugama et al., 2011). We obtained histones with and without tails and used them for chromatin reconstitution. Both displayed the basically the same nucleosome positioning preferences in SGD (Figure 2.9). Therefore, determination of intrinsic nucleosome positioning by SGD is largely independent of histone tails. Next, we monitored nucleosome positioning of such chromatin as altered by INO80. In contrast to experiments with full-length histones, we did not observe INO80-specific nucleosome positioning for chromatin without histone tails (Figure 2.9 A). The same was true in a perfectly internally controlled experiment (Figure 2.9 B). We used a library consisting of 1588 independent clones covering the entire yeast genome (Jones et al., 2008). This entirely defined library allowed the preparation of separate plasmid pools covering two separate halves of the genome. Both halves were reconstituted separately by SGD with either wild type or tailless recombinant *X. laevis* histones, combined and incubated with recombinant INO80. As both library pools contained separate and non-overlapping halves of the yeast genome, the resulting sequencing tags after MNase-seq could be bioinformatically attributed to the chromatin with either full length or tailless histones. This experiment directly demonstrated that INO80 was active in the very same reaction tube where nucleosomes without histone tails were not moved to *in vivo*-like positions.

In summary this suggests that histone tails are necessary for *in vivo*-like nucleosome positioning by INO80, and demonstrates that this nucleosome positioning activity is biochemically distinct from general nucleosome remodeling and ATP hydrolysis.

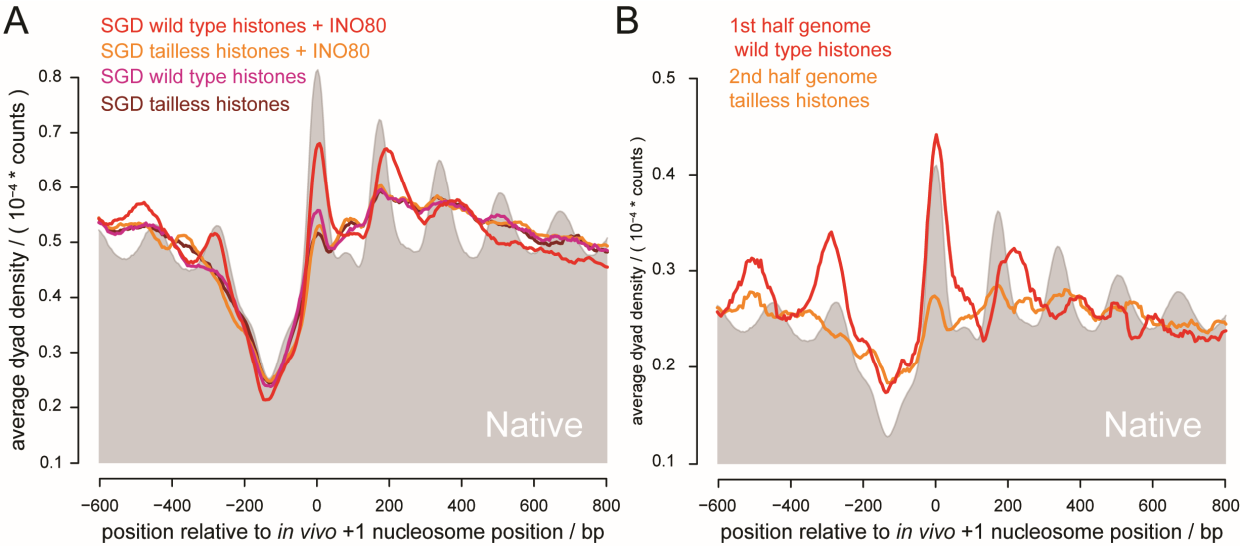

Figure 2.9 Histone tails are required for INO80-dependent nucleosome positioning. (A) Composite representation of nucleosome positions after SGD with *X. laevis* wild type (pink) and tailless (brown) histones and nucleosome positions set by INO80 for the respective chromatins (red and orange). (B) A custom library that covers the entire yeast genome with 1588 individual clones *(Jones et al., 2008)* allowed the preparation and assembly of two individual halves of the genome (first half: Chromosome I – chromosome X position 1-104253, second half: Chromosome X position 106749 – chromosome XVI). The first half of the genome was assembled with wild type *X. laevis* histones, the second half with tailless *X. laevis* histones. Composite nucleosome positions set by INO80 for the separate halves of the genome are shown. Remodeler-to-nucleosome molar ratios were 1:10.

2.5.4 Rvb1/2 ATPase activities are not required for genome-wide nucleosome positioning

INO80 contains a ring structure consisting of Rvb1 and Rvb2 AAA+ ATPases (Shen et al., 2000). Such ring structures are shown to undergo large conformational changes upon ATP hydrolysis (Lopez-Perrote et al., 2012; Petukhov et al., 2012) and could therefore regulate INO80 activity, especially with view of our speculations regarding untwisting DNA by INO80 (2.3.2). To test if these Rvb1/2 ATPases were required for nucleosome positioning *in vitro*, we purified INO80 with catalytically dead Rvb1 and Rvb2 subunits. This mutant version was able to slide nucleosomes with similar rates as the wt complex (Sebastian Eustermann, data not shown). Also in genome-wide nucleosome positioning experiments, this mutant remodeler was able to position nucleosomes much as the wtINO80 (Figure 2.10 A graph 3 and 4). This demonstrates that ATPase activity of the Rvb1/Rvb2 module is not required for INO80-specific nucleosome positioning.

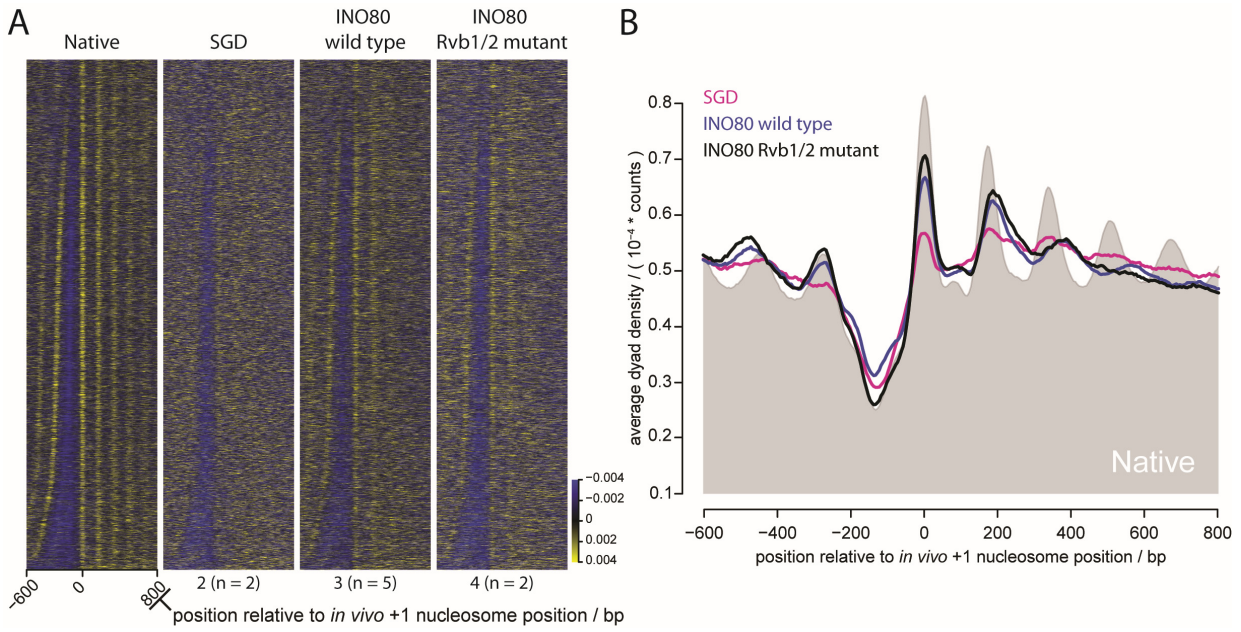

Figure 2.10 INO80-specific nucleosome positioning is independent of Rvb1/Rvb2 activity. (A) Color-coded nucleosome dyad densities for genes 3931 (row-by-row) sorted by *in vivo* NFR length (as Figure 2.5 A). Yellow, black, and blue represent high, medium, and low tag density, respectively. Native, SGD and wild type INO80 (recombinant) are as in Figure 2.8 A. INO80 Rvb1/2 mutant represents nucleosome positions set by an INO80 mutant that contain catalytically inactive variants of Rvb1 and Rvb2 (walker point mutation). (B) Composite representation of data in A. Remodeler-to-nucleosome molar ratios were 1:10.

2.5.5 Reb1 guided nucleosome positioning by INO80

We found that GRFs are not only involved in NDR formation, but also in +1 nucleosome positioning. To test if INO80 cooperates with Reb1, we titrated Reb1 into positioning reactions with INO80 (Figure 2.11 A 5-7). We observed enhanced INO80-specific nucleosome organization at Reb1 bound genes with increasing amounts of Reb1. This was not observed when either Reb1 or INO80 were absent (Figure 2.11 A graph 3 and 4, respectively). This demonstrates a direct cooperation between Reb1 and INO80 that results in enhanced +1 nucleosome positioning at Reb1 bound genes.

2.5.6 INO80 has nucleosome clamping activity

Besides +1 nucleosome positioning, INO80 generated a partial nucleosomal array with non-physiologically wide spacing. INO80 has a linker length requirement of 70 bp *in vitro* and set a linker length with 30 bp that could explain the observed spacing in our genome-wide experiments (Udugama et al., 2011). However, full assembly degrees of our whole-genome plasmid library correspond to one nucleosome per 212 bp (Krietenstein et al., 2012). Therefore, the observed spacing could be explained by a length sensing mechanism (2.3.1), i.e. result from the lower average nucleosome density than *in vivo* (one nucleosome per 165 bp (Jiang and Pugh, 2009a)).

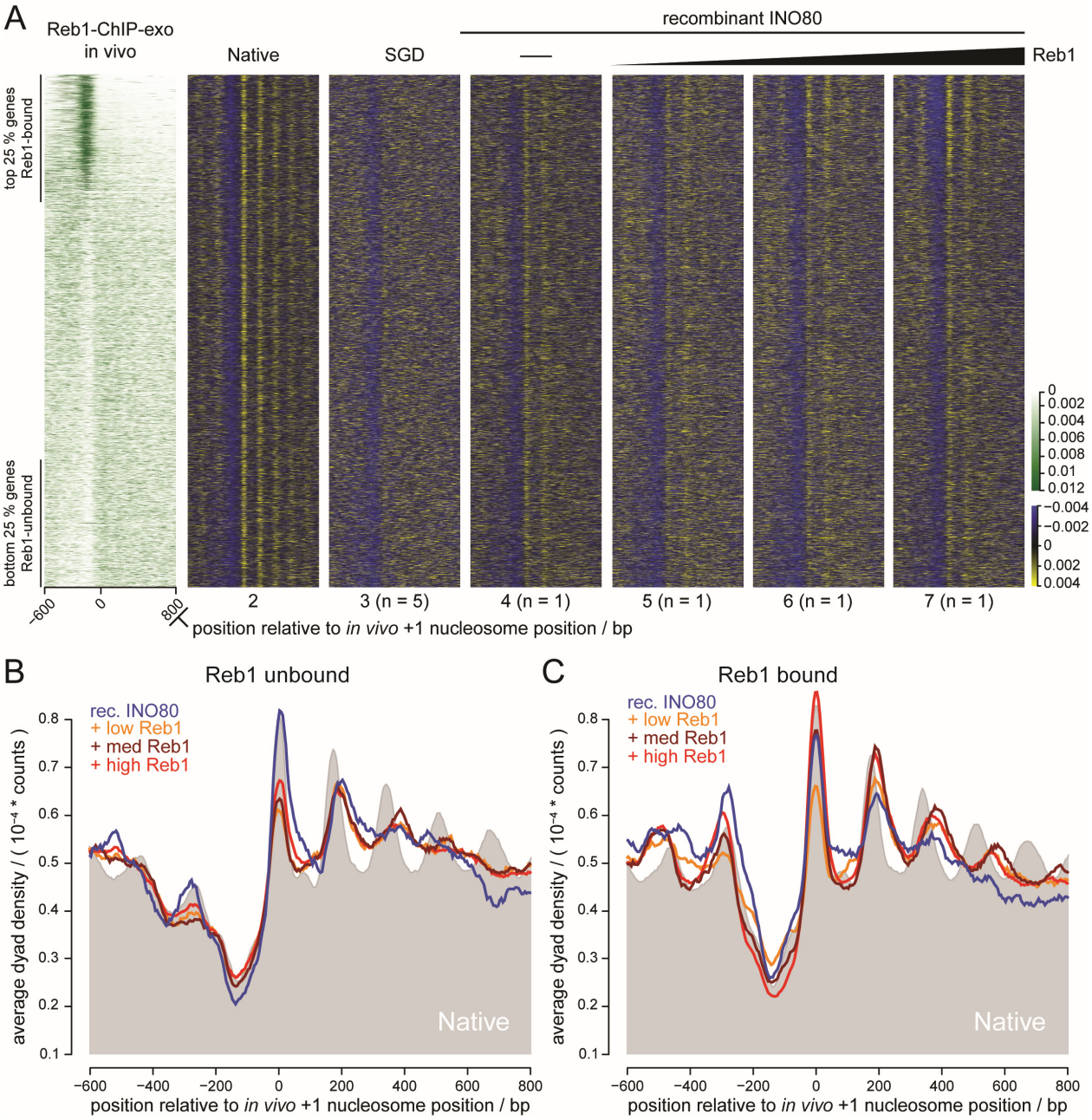

Figure 2.11 INO80-specific remodeling activity is guided to Reb1 bound genes by Reb1, in a Reb1 dose-dependent manner. (A) Color-encoded gene-by-gene representation (3931 genes plotted) of nucleosome dyad densities sorted as in Figure 2.7 A. Native and SGD experiments as in Figure 2.7 A. Nucleosome positions set by INO80 in presence of no Reb1 (graph 4) or increasing concentrations of Reb1 (2.2, 6.6 or 20 µM, graph 5-7). (B-C) Composite distribution of nucleosome positions set by INO80 with no and increasing amount of Reb1 from A for Reb1 unbound (B) and Reb1 bound (C) genes. Remodeler-to-nucleosome molar ratios were 1:10 and recombinant H. sapiens histones were used.

To test if the spacing generated by INO80 was specific for INO80 or nucleosome density-dependent we performed nucleosome dilution experiments. We adjusted the histone:DNA mass ratios in SGD 0.9 and 0.45 relative to our standard assembly degree, i.e. prepared full and half assembly chromatin, respectively. Overall, intrinsic nucleosome positioning was independent of nucleosome density (Figure 2.12). Upon remodeling by INO80, the resulting nucleosome positions were also independent of histone density. +1 nucleosomes were accurately positioned and +2

nucleosomes were aligned with the INO80-specific ~200 bp spacing at both the full and half assembly degrees (Figure 2.12). This showed that INO80 positions and spaces nucleosomes independently of nucleosome density and therefore has clamping activity (Lieleg et al., 2015).

The difference in peak height for the +1 and +2 positions was higher at lower nucleosome density, i.e. the +1 nucleosome peak showed a relatively higher nucleosome dyad density. This argues that INO80 preferentially positions the +1 and then the +2 nucleosome if nucleosomes are limiting. Such a positioning activity would argue for an active packaging mechanism (Zhang et al., 2011). However, at the half assembly degree, DNA is more accessible to MNase and the measured nucleosome occupancy (peak height) may therefore be affected by more or less different MNase digestion degrees. Over-digestion of chromatin emphasizes array nucleosomes and not the +1 nucleosome (Weiner et al., 2010, Dr. Corinna Lieleg (*S. cerevisiae*) and Maria Walker (*S. pombe*) unpublished). Therefore, we would expect that chromatin over-digestion would emphasize the +2 nucleosome occupancy over +1 nucleosome occupancy. This was exactly the opposite of the observed effect. To control for such a MNase effect, we performed again experiments with the two separate pools of yeast genomic plasmid libraries (2.5.3). We assembled the first half of the genome with a DNA:histone mass ratio of 0.75 and the second half with a ratio of 0.25 and pooled both SGD preparations before remodeling by INO80. Consequently, both SGD chromatin preparations with different assembly degree were MNase digested in one tube and nucleosome position determinations should be equally affected by MNase digestion degree. Also here, +1 nucleosomes were preferentially positioned at the lower nucleosome density, suggesting active packing by INO80 (Figure 2.12 C).

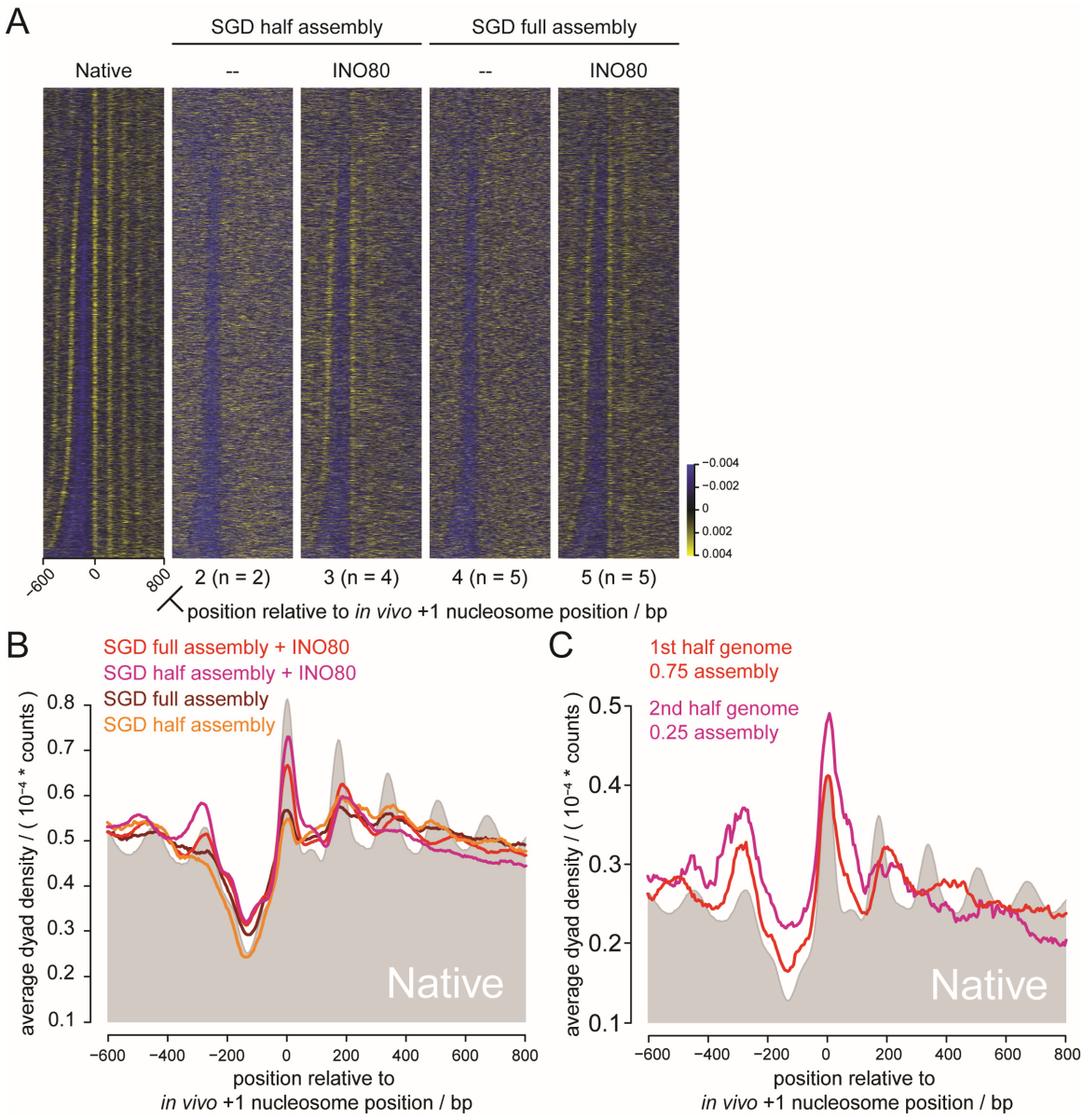

Figure 2.12 INO80-specific spacing is independent of nucleosome density, indicating clamping activity. (A) Color-encoded gene-by-gene representation of nucleosome dyad densities sorted as in Figure 2.7 A. Native, SGD (full assembly) and SGD *(full assembly*) +INO80 are experiments as in Figure 2.8 A. SGD half assembly corresponds SGD with half the amount of histone octamers as for full assembled chromatin. SGD half assembly + INO80 corresponds to nucleosome positions set by INO80 on half assembled chromatin. (B) Composite representation of data in A. (C) Similar to Figure 2.9 B, to separate halves of the yeast genome were assembled differentially with different amounts of histone octamers. 75% of the amount of histone octamers used for full assembly degrees *(Krietenstein et al., 2012)* were used to assemble the first half of the yeast genome, 25% for the second half of the genome. Nucleosome positions for both halves were set by INO80 and separated bioinformatically. This controlled for nucleosome density-dependent MNase digestion effects. Remodeler-to-nucleosome molar ratios were 1:10.

3 Discussion

The key conclusions of this study are based on the here established first reconstitution of genome-scale physiological NDR-+1-array formation *in vitro* with only purified factors. This achievement allowed to demarcate the direct, specific and necessary/sufficient contributions of individual remodelers and barrier factors (GRFs).

3.1 A four stage model of NDR-+1-array formation

In this study we showed that the combination of purified histones, chromatin remodelers, GRFs, and DNA was sufficient to reconstitute the basic pattern of physiological nucleosome organization at the 5' ends of genes. It is in agreement with the literature that GRFs and chromatin remodelers are important for *in vivo* NDR-+1-array organization (Badis et al., 2008; van Bakel et al., 2013; Ganguli et al., 2014; Gkikopoulos et al., 2011; Hartley and Madhani, 2009; Ocampo et al., 2016; Parnell et al., 2008; Pointner et al., 2012). We found clear evidence *in vitro* that chromatin remodelers catalyze specific nucleosome positioning reactions and that the *in vivo* observed nucleosomal organization results from the dynamic competition or composite of these reactions. This idea was derived previously from *in vivo* studies (Ganguli et al., 2014; Ocampo et al., 2016; Parnell et al., 2015), but it was difficult to dissect individual remodeler contributions to nucleosome positioning by such mutant studies (Ocampo et al., 2016). Further, nucleosome positioning *in vivo* is also strongly affected by DNA templated processes, like transcription (Weiner et al., 2010), which our *in vitro* reconstitution of genome-wide nucleosome positioning allowed to eliminate.

Collectively, our results lead us to suggest a four-stage mechanism for the generation of nucleosomal NDR-+1-array organization.

3.1.1 Stage 1: NDR formation

The formation of many NDRs depends *in vivo* on the GRFs Reb1 and Abf1 (Hartley and Madhani, 2009) as well as on the remodeler RSC (van Bakel et al., 2013; Hartley and Madhani, 2009; Kubik et al., 2015; Parnell et al., 2015). Further, poly(dA:dT) elements contributed to GRF guided NDR organization (Hartley and Madhani, 2009; Raisner et al., 2005), as well as form NDRs by an intrinsic biophysical mechanism. Indeed, such elements are enriched within NDRs in *S. cerevisiae* (Segal and Widom, 2009). Nonetheless, they are not in other species, like *S. pombe* (Lantermann et al., 2010). In SGD, these elements have a low propensity to be incorporated into nucleosomes,

therefore they were suggested to have intrinsic nucleosome repelling properties that contribute to NDR formation *in vivo* (Kaplan et al., 2009; Raveh-Sadka et al., 2012; Segal and Widom, 2009). GRF binding sites and poly(dA:dT) elements are enriched in NDRs throughout evolution, suggesting a conserved mechanism that links these elements to NDR formation (Tsankov et al., 2011, 2010). The flexible use of different factor as GRFs, e.g., unrelated Abf1 and Reb1 in *S. cerevisiae* (Hartley and Madhani, 2009), but yet another unrelated GRF, Sap1, in S. pombe (Lantermann et al., 2010; Tsankov et al., 2011), as well as the enrichment of poly(dA:dT) elements in promoter NDRs (*S. cer*evisiae (Lee et al., 2007)) or not (S. pombe (Lantermann et al., 2010)) suggests that there is some evolutionary freedom in usage of poly(dA:dT) elements and GRFs to generate NDRs, presumably because all of them are engaged in the same mechanism. We demonstrated that this mechanism ultimately relies on specific remodeling activities.

Intrinsically generated (SGD) NDRs slightly widened upon incubation with any remodeler, but only upon incubation with RSC and INO80 the NDRs were reconstituted to physiological levels (Figure 2.4.C). Interestingly, these two remodelers showed two distinct mechanisms of NDR formation. RSC widened NDRs to approximately physiological widths by evicting or translocating nucleosomes, but without accurate positioning of the +1 nucleosome (Figure 2.4 A). INO80 instead positioned the -/+1 nucleosomes, thus defining the proper NDR boarders (Figure 2.5 A). So there is a mechanistic distinction between generating NDRs by just clearing out nucleosomes or by setting a certain distance between -1/+1 nucleosomes.

For both RSC and INO80 NDR formation was enhanced by GRFs, Abf1 and Reb1 (Figures 2.6 A, 2.7 A). For RSC, this is in agreement with literature reports that *in vivo* NDR formation depends on RSC, Abf1, and Reb1 (Hartley and Madhani, 2009) and suggests that there are direct interactions between RSC and GRFs.

Further, our analyses showed a correlation between RSC-dependent NDR formation and poly(dA:dT) elements that is not seen with other remodelers (Figure 2.4 A). We considered two different mechanisms how poly(dA:dT) elements may affect NDR formation by RSC. The first is that poly(dA:dT) elements intrinsically destabilize nucleosomes (Kaplan et al., 2009; Segal and Widom, 2009; Sekinger et al., 2005; Struhl and Segal, 2013; Zhang et al., 2009). Such destabilized nucleosomes would be more efficiently removed by RSC resulting in NDRs over poly(dA:dT) elements. Alternatively, poly(dA:dT) elements could activate RSC, thus signal RSC to evict nucleosomes (Kubik et al., 2015; Lorch et al., 2014). In contrast to *in vivo* experiments, we could monitor RSC remodeling in absence of all GRFs and other factors that potentially recruit and modulate RSC activity. Therefore, the observed RSC-specific nucleosome positioning is affected

only by chromatin, DNA sequence and histones. This allowed us to distinguish between these two mechanisms. We selected all unique poly(dT) and poly(dA) elements (on the sense strand) at promoters that have no other poly(dA) or poly(dT) element in their proximity. A prediction of the mechanism that nucleosome remodeling is based on nucleosomal stability would be that NDRs form similarly at poly(dA) and poly(dT) elements, since they have identical biophysical properties due to the double stranded nature of DNA. A prediction of the RSC activation/signaling mechanism would be that the orientation of poly(dA) and poly(dT) might matter for RSC remodeling. One hint in this direction is the previous finding that RSC translocates specifically along one DNA strand in 3' to 5' direction (Saha et al., 2005). Indeed, we observed not symmetrical but directional nucleosome removal in response to poly(dA) and poly(dT) elements. NDRs around poly(dA) elements were widened towards upstream and NDRs around poly(dT) elements towards downstream (Figure 2.4 B). This demonstrates that RSC remodeling is affected by the orientation of such elements, supporting the idea that these elements function as a signal. This may explain why these elements are asymmetrically distributed in NDRs *in vivo* with poly(dT) upstream of poly(dA), on average. Further, the average location of poly(dT) elements is ~30 bp from the +1 nucleosome, similar to the average locations of Reb1 and Abf1 binding sites (Figure 2.7 F). This suggests that GRF binding sites and poly(dT) elements may both be interchangeable in guiding NDR formation by RSC, either by recruitment of RSC, in the case of GRFs, or by RSC recognizing these elements.

3.1.2 Stage 2: +1 nucleosome positioning

In vivo, no mutations are known that are compatible with viability and severely affect +1 nucleosome positions, presumably because proper +1 positioning is essential for gene regulation and redundant +1 nucleosome positioning mechanisms are in place. Mutants that are singly deleted for *isw2*, *ino80, or isw1* are viable and display only minor effects on nucleosomal organization, supporting the redundancy aspect (Gkikopoulos et al., 2011; Ocampo et al., 2016; Papamichos-Chronakis et al., 2011; Whitehouse et al., 2007; Yen et al., 2012). Our experiments suggest that at least two alternative mechanisms to position +1 nucleosomes exist: first, by INO80, a remodeler that positions +1 nucleosomes on its own (Figure 2.5 A and B), and second, by remodeler guidance via GRFs, here Abf1 (Figure 2.6 A, C, and D) and Reb1 (Figure 2.7 A and C).

3.1.2.1 Stage 2 option 1: +1 nucleo*some positioning by INO80.*

INO80 on its own positioned +1 nucleosomes at most genes (Figure 6 A). To our knowledge, INO80 is the first remodeler that has intrinsic property to position nucleosomes at physiological positions. *In vivo,* INO80 subunits co-localize with +1 nucleosomes and ino80delta mutants show at least some small shifts of +1 nucleosome positions (Yen et al., 2012). Further, INO80 is suggested to be involved in H2A.Z exchange, a +1 nucleosome enriched H2A variant (Papamichos-Chronakis et al., 2011; Watanabe et al., 2013). This fits to our finding that INO80 is involved in physiological +1 nucleosome positioning. We even found first hints about how INO80 may select physiological nucleosome positions. The nucleosome structure (section 1.1.1, Luger et al., 1997) demonstrates that incorporation of DNA into the nucleosome requires non-uniform bending that highly distorts DNA. Therefore, DNA parameters that affect bending, like shape parameters, may play a role in nucleosome formation and could be distinguished by INO80. Indeed, DNA shape prediction for +1 nucleosome regions revealed: those regions of nucleosomes that were effectively positioned by INO80 to their *in vivo* locations displayed a predicted DNA over-twist (Figure 2.5 D, Q4). On the contrary, sequences of nucleosomes that were accurately positioned already by SGD and then displaced by INO80 had a lower DNA twist (Figure 2.6 D, Q1). In contrast to this distinction, classical NPSs (Ioshikhes et al., 2006) were similarly abundant in both cases. This led us to speculate that NPSs may be ineffective because of nucleosome repelling shape properties, like intrinsic over-twist. INO80 may counteract this by slightly untwisting DNA such that intrinsically over-twisted regions become conducive for nucleosome positioning, (Figure 2.6 D, Q4). At the other extreme, untwisting of properly-twisted DNA may even lead to a delocalization of intrinsically positioned nucleosomes (Figure 2.6 D, Q1). This is highly speculative, but it establishes a first framework to explain this novel nucleosome positioning property, first described for INO80.

3.1.2.2 Stage 2 option 2 and 3: GRF guided +1 nucleo*some positioning.*

GRFs, like Abf1 and Reb1, could guide INO80 (Figure 2.9 A and C), ISW2 (Figure 2.6 A and D and Figure 2.7 A and C), and ISW1a (Figure 2.6 A and C) to position +1 nucleosomes. Potentially, GRFs help to define the position of the +1 nucleosome by serving as a barrier or alignment point utilized by ISW2 and/or ISW1a (Li et al., 2015). Upon deletion of *isw2* entire nucleosomal arrays moved upstream in some cases, positioning the +1 nucleosome at a less repressive location (van Bakel et al., 2013; Whitehouse et al., 2007; Yen et al., 2012) and consistent with ISW2 moving nucleosomes in a directional way against a barrier. Compared to ISW2, the potential of ISW1a to position the +1 nucleosome at GRF sites was lower (compare Figure 2.6 C and D). For both

remodelers, +1 nucleosome positioning was specific to GRF bound genes. However, this +1 positioning extended to most genes in presence of *isw1Δ isw2Δ chd1Δ* mutant WCE, presumably because the WCE contains many more barrier factors, maybe also due to INO80. This demonstrates that the effects on +1 nucleosome positioning observed for the minimal sets of factors, GRF plus remodeler, were the rule and not the exception for global nucleosome positioning. While GRFs were shown to contribute to nucleosomal organization *in vivo*, most evidently to NDR formation (Hartley and Madhani, 2009; Tsankov et al., 2011; Yu and Morse, 1999), our experiments show their direct role and with which remodelers they cooperate.

3.1.3 Stage 3 and 4: Array formation and physiological spacing

Interestingly, the remodelers INO80 and ISW2 that had the strongest effects on +1 nucleosome positioning also generated and aligned a nucleosomal array downstream of the +1 nucleosome, but with non-physiological spacing (Figure 3.1: Stage 3 options 1 and 2). This may be because both remodelers have linker length requirements *in vitro* that are longer than the average *in vivo* linker length (Fazzio et al., 2005; Udugama et al., 2011). It remains curious why there should be remodelers with spacing activity that generate too wide spacing. Nonetheless, proper physiological spacing was achieved by ISW1a. Potentially, ISW1a recognized the too long linkers and used them to adjust physiological spacing (Figure 3.1: Stage 4). ISW1a may be able to do so due to a short "protein ruler" domain (Yamada et al., 2011). A decisive role for ISW1a in setting physiological spacing is in accordance with *in vivo* finding (Ocampo et al., 2016).

3.1.4 Dynamic competition and NDR-array formation

Some of the mechanisms that implement the four stages of nucleosome positioning are antagonistic to each other. This suggests a dynamic competition between different remodelers. For example, RSC generated NDRs, but in extreme cases beyond *in vivo* +1 nucleosome positions (Figure 2.6B and 2.7B). Also the +1 nucleosome positions generated by the *isw1Δ isw2Δ chd1Δ* mutant WCE appear to be shifted downstream, suggesting that some activity generated wider NDRs and antagonizes +1 nucleosome positioning, probably RSC endogenous to this WCE. Accordingly, this effect was enhanced when RSC was added to the mutant WCE (Figure 2.2 C). In contrast, this downstream shift of +1 nucleosome positioning could be counteracted by addition of INO80, ISW2, or ISW1a (Figure 2.2 D-F and Figure 2.5 A). In titration experiments, we showed that RSC remodeling antagonizes +1 nucleosome positioning by ISW2 (Figure 2.7 E). This argues for a dynamic competition between these remodelers that can modulate +1 nucleosome positioning

and potentially affect transcription. A competition of remodeling activities was also observed between ISW2 and ISW1a when titrated against each other in the background of *isw1Δ isw2Δ chd1Δ* mutant WCE (Figure 2.3 D). Here, intermediates between ISW2-generated non-physiological and ISW1a-generated physiological spacing of nucleosomal arrays were observed.

3.1.5 Transcription-independent nucleosome positioning *in vivo*

Transcription was not reconstituted by us *in vitro*. Thus, our experiments suggest that transcription is not required for formation of basic NDR-+1-array patterns. There is even *in vivo* evidence that chromatin is organized before transcription commences from a zebra fish study (Haberle et al., 2014). Here, activation of embryonic transcription after mid-blastula transition was monitored by CAGE-sequencing. This allowed distinguishing between maternally deposited and endogenously transcribed RNAs, especially as some RNAs appeared to have different TSSs depending on the time window of their synthesis. In this experimental system it was found that nucleosomal organization was established at promoters and around TSSs before the respective TSSs were used and genes transcribed. This demonstrates that transcription independent nucleosome positioning mechanisms exist *in vivo* and are not artificial or only present *in vitro*. However, we still expect that transcription initiation and elongation modulates nucleosome positioning (Hughes et al., 2012; Ocampo et al., 2016; Struhl and Segal, 2013; Weiner et al., 2010). Two of the remodelers we tested, ISW1b and Chd1, did not contribute to genome-wide nucleosomal organization in our *in vitro* system, even though both were active and even though Chd1 is a major regulator of nucleosomal array regularity *in vivo* (Gkikopoulos et al., 2011; Ocampo et al., 2016) and ISW1b is involved in decreasing histone turnover and preventing cryptic transcription over gene bodies *in vivo* (Smolle et al., 2012). We consider that Chd1 and ISW1b may be recruited by elongating RNA polymerase and mainly exert their effects in the context of transcription which was not part of our system. This elongation coupled function could also explain why the aligned arrays reconstituted by us were much less extensive than *in vivo*. Presumably, Chd1 and ISW1b are brought deeper into genes via transcription thus extending genic arrays (Lee et al., 2012; Park et al., 2014; Simic et al., 2003; Smolle et al., 2012).

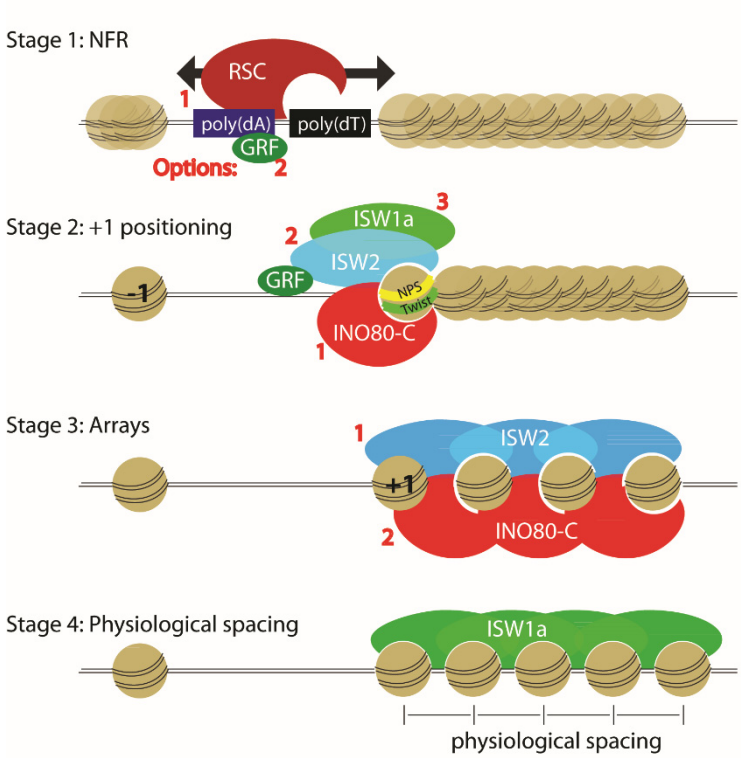

Figure 3.1 Schematics of the four stage model towards NDR-array formation. The red numbers indicate different options at respective stages and may be different for individual genes. Nucleosomes are depicted in brown, transparency defines fuzziness of positioning. (Stage 1) Directional nucleosome displacement by RSC leads to NDR formation. This could be guided by poly(dA)/(dT) elements (option 1) and/or by GRFs (option 2). (Stage2) +1 nucleosome positioning by INO80, either by reading unique DNA sequences (NPS in yellow) and shape (helical twist green) or via recruitment by GRFs (option 1), or by ISW2 (option 2) or ISW1a (option 3) which require guidance by GRFs. (Stage 3) Both, ISW2 (option 1) or INO80 (option 2) generate nucleosomal arrays with non-physiological spacing aligned to the +1 nucleosome. (Stage 4) ISW1a introduces physiological spacing. At present, we make no assumption regarding the temporal order of events.

In summary, we could identify four stages of genome-wide nucleosomal NDR-+1-array formation (Figure 3.1). Chromatin remodelers catalyze specific nucleosome positioning reactions that are partially in competition with each other (Figure 3.1). The combination of individual chromatin remodeler activities resulted in the *in vivo* observed nucleosomal organization. GRFs could specifically guide remodeling activity at promoters, demonstrating how global nucleosomal organization mechanisms could be modulated and orchestrated at specific promoters, for example via expression levels of GRFs. We reconstituted physiological NDR-array formation with purified factors only, specifically for GRF bound genes (Figure 2.6 E and 2.7F). This demonstrates that NDR-+1-array formation can be brought about without transcription by the here identified factors, GRFs and remodelers, only.

3.2 Dissection of INO80-specific nucleosome positioning

3.2.1 *In vitro* nucleosome positioning with recombinant INO80

Use of recombinant instead of endogenous proteins checks if PTMs or co-purifying contaminants are responsible for observed activities. Expression of recombinant proteins in host cells might alter or abolish PTMs compared to native protein. PTMs of enzymes are a common mechanism to regulate their activity. For example, this can include substrate specificity, catalytic activity, localization within cellular compartments, or interaction with other molecules, like RNAs or proteins (Biggar and Li, 2014; Verdin and Ott, 2015). The ATPase subunit Ino80 itself builds the scaffold to assemble the INO80 (Tosi et al., 2013). Proteomic studies revealed that INO80 has multiple phosphorylation sites at the N- and C-terminus that are phosphorylated upon DNA damage or via the TOR signaling pathway (Albuquerque et al., 2008; Chen et al., 2010; Soulard et al., 2010; Swaney et al., 2013). Even though none of these studies confirmed regulatory functions of these PTM sites, INO80 activity could potentially be regulated by them.

However, neither yeast-specific PTMs nor contaminants, like DNA binding proteins that could target INO80 to promoters, were responsible for novel nucleosome positioning activity of INO80 as nucleosome positioning by recombinant INO80 mirrors that by endogenous INO80 (Figure 2.8), also when genes were sorted by “INO80-effectiveness”.

3.2.2 INO80-specific nucleosome positioning is not affected by histone variants and histone PTMs

In most reconstitution experiments endogenous histone octamers from *D. melanogaster* embryos were used. These histones contained all histone variants and PTMs present in such embryos. INO80 is supposedly involved in exchanging the histone variant H2A.Z for H2A (Papamichos-Chronakis et al., 2011), even though this is currently under debate (Carl Wu, personal communication). This exchange activity depends on the acetylation of H3K56 (Watanabe et al., 2013). Thus, it could be that nucleosome positioning by INO80 might be affected by histone variants and histone PTMs.

The *D. melanogaster* homologue of H2A.Z is called H2A.V. This variant is the only H2A variant in *D. melanogaster* and functions as a hybrid of the variants H2A.Z and H2A.X, which are conserved within most eukaryotes. Thus, it is not surprising that H2A.V differs from H2A.Z in yeast and other species, most strikingly at the C-terminus, where H2A.V is extended and carries a SQ[E/D]Φ motif, which is characteristic for the H2A.X variants (reviewed in Baldi and Becker,

2013). Therefore, endogenous fly histones did not allow to conclude if histone variants, especially H2A.V, or histone PTMs affected INO80-specific nucleosome positioning.

To have a fully defined, recombinant system, we tested nucleosome positioning by recombinant INO80 with recombinant core histones from *S. cerevisiae*, *X. laevis,* and *H. sapiens* (Figure 2.8 B and C). In all these cases, nucleosome positions reconstituted first by SGD and then re-positioned by INO80 were basically the same positions as with endogenous *D. melanogaster* histones, e.g., +1 nucleosome positioning follows the same "rules" when sorted by "INO80-effectivness".

Therefore, we conclude that intrinsic nucleosome by SGD as well INO80-specific nucleosome positioning is independent of histone variants, histone PTMs, and the source of histones. Importantly, these experiments demonstrate that yeast-specific nucleosome positions can be reconstituted in a completely recombinant system, all factors used in this experiments were never in contact with a yeast cell.

3.2.3 Histone tails couple nucleosome positioning and nucleosome remodeling by INO80

The activity of chromatin remodelers can be modulated by histone tails *in vitro* (Clapier et al., 2001a, 2001b; Dang et al., 2006; Hamiche et al., 2001) and *in vivo* (Fazzio et al., 2005), presumably via allosteric regulation (Hwang et al., 2014). In contrast, INO80 remodeling *in vitro* does not depend on any histone tails (Udugama et al., 2011). Here, the deletion of individual histone tails result in increased ATPase activity and remodeling, especially the H2A-tail seems to inhibit INO80 activity.

Our experiments demonstrated that tailless histones take the same intrinsic positions as histones with tails in SGD (Figure 2.9 A and B). However, INO80-specific nucleosome positioning was not observed upon incubation with INO80 for recombinant tailless histones but for only histones with tails (Figure 2.9 A). This demonstrates that nucleosome positioning is biochemically distinct from nucleosome remodeling, as assays by sliding and ATP hydrolysis. We conclude that histone tails are required to couple these activities.

3.2.4 Rvb1/2 ATPase activity is not required for +1 nucleosome positioning by INO80

The INO80 contains a ring structure consisting of Rvb1 and Rvb2 AAA+ ATPases (Shen et al., 2000). This ring structure is also found in the remodeling complex SWI/SNF (Krogan et al., 2003;

Mizuguchi et al., 2004). These ATPases are essential *in vivo* and are incorporated in many complexes involved in transcription, DNA damage repair and RNA maturation (Jha and Dutta, 2009). The Rvb1/2 module assembles at the N-terminus of Ino80 and forms the "head" of INO80 (Tosi et al., 2013). Proximity-crosslinking experiments suggest an interaction between the nucleosome and the Rvb1/2 module within an INO80-nucleosome complex (Tosi et al., 2013). Rvb1/2 dodecamers can undergo large conformational changes (Lopez-Perrote et al., 2012; Petukhov et al., 2012) that may alter INO80 conformation thus maybe altering INO80-specific nucleosome positioning activity.

Experiments with purified INO80 that contained catalytically inactive Rvb1/2 ATPases still showed INO80-specific nucleosome positioning as seen with wild type INO80. This demonstrates that the activity of the Rvb1/2 ATPases is not required for nucleosome positioning, leaving the function of Rvb1/2 to be addressed in future studies.

3.2.5 INO80 activity is targeted to promotors by Reb1

Genome-wide mapping of INO80 subunits revealed that INO80 not only co-localizes with the +1 nucleosome but also to Reb1 binding sites via its Nph10/Ies5 subunits, presumably via direct interaction with Reb1 (Yen et al., 2013). ChIP-exo experiments, dissecting the binding profiles of PIC components, revealed that many factors are positioned at fixed distances to the +1 nucleosome (Rhee and Pugh, 2012). Thus, it is difficult to draw conclusions about direct interactions between factors based only on localization correlation data, especially if many factors correlate with each other at the same place. To test if INO80 responded to Reb1, we performed nucleosome positioning reactions with recombinant INO80 and Reb1. These experiments demonstrated that INO80-specific nucleosome positioning activity was specifically high at Reb1 bound genes in a Reb1 dose-dependent manner. This underscores that INO80 potentially regulates +1 nucleosome positioning guided by GRFs, presumably affecting transcription.

3.2.6 INO80-Specific nucleosome positioning is independent of histone density

INO80 generates a specific nucleosomal organization at the 5'-ends of genes. This includes +1 nucleosome aligned arrays with non-physiological, too wide spacing. So called "full" assembly degrees achieved in our experiments correspond on average to one nucleosome per 190 bp (Krietenstein et al., 2012). INO80 is shown to have a linker length requirement of 40 bp (Udugama et al., 2011). Therefore, the INO80 generated spacing *in vitro* (185 bp) could be explained by a

length sensing or molecular ruler model (1.3.2). In case of the length sensing model spacing should scale reciprocally with nucleosome density, in case of the molecular ruler model, the spacing should remain constant regardless of nucleosome density (Lieleg et al., 2015). We tested this, much in the style of the "clamping assay" developed by Corinna Lieleg by observing INO80-specific spacing at different nucleosome densities (Figure 2.12). As the spacing remained rather constant, we conclude that INO80 has not only nucleosome spacing, but also nucleosome clamping activity. Reduced nucleosome density has to reduce nucleosome occupancy, but this was more the case for the +2 than the +1 nucleosome. This supports the idea of an active packaging mechanism by INO80

In summary, our experiments showed that INO80-specific nucleosome positioning is independent of yeast-specific PTMs of INO80 or co-purifying factors, and independent of histone variants, histone PTMs, and nucleosome density. Nonetheless, it requires histone tails, which seem to link ATPase-dependent remodeling with the nucleosome positioning activity. The INO80 intrinsic nucleosome positioning activity can be further enhanced by GRFs. Future experiments with recombinant INO80 mutant complexes and mutant/truncated histones will address which histone tails as well as which INO80 are required for INO80-specific nucleosome positioning.

4 Methods

4.1 Molecular biology methods

4.1.1 Plasmid library expansion

The YCp50 plasmid library is described elsewhere (Zhang et al., 2011), and expanded as described (Krietenstein et al., 2012). This YCp50 plasmid library was used for most experiments and referred to as plasmid library throughout this work. The pGP564 library, that were used for experiments shown in figures 2.9 B and 2.12 C, was described in (Jones et al., 2008) and purchased from OpenBiosystems (#YSC4613). 1588 individual cones were plated on LB-Amp using RoToR HDA Station (Singer) and incubated at 37 °C over night. Clones from plates 1-8 and 9-16, covering the first and second half of the yeast genome respectively, were washed separately and used to inoculate 1 L LB-amp. After 3 h incubation at 37 °C, plasmids were prepared using a QIAGEN Plasmid Giga Kit (cat. # 12191).

4.2 Biochemical methods

4.2.1 Whole cell extracts from *S. cerevisiae*

Whole cell extracts were prepared from logarithmically growing cells as described in the literature (Krietenstein et al., 2012; Wippo et al., 2011; Zhang et al., 2011). Here, strain BY4741 was used for wild type WCE, and strains YTT227 (Tsukiyama et al., 1999) or BM28 (Gkikopoulos et al., 2011) for the *isw1Δ isw2Δ chd1Δ* mutant WCE. In brief, cell were grown in log phase to an OD_{600} of 2-4 in YPDA medium. Grown cells were harvested in 1 L buckets by centrifugation for 15 min at 4 °C and 6000 x g average (Heraeus Cryofuge 6000i, 4000 rpm), washed with 200 ml ice cold ddH_2O, transferred into a 250-ml conical centrifuge tube, and collected by centrifugation for 15 min at 4 °C, 6000 x g average (Heraeus Cryofuge 6000i, 4000 rpm). The cells were resuspended in 40 ml extraction buffer (200 mM HEPES-KOH, pH 7.5,10 mM $MgSO_4$, 20% (v/v) glycerol, 1 mM EDTA, 390 mM $(NH_4)_2SO_4$, 1mM freshly added DTT), transferred to a 50 ml reaction tube, collected by centrifugation for 10 min at 4 °C and 2047 x g average (Eppendorf 5810R, rotor A-4-62, 4000 rpm), resuspended in 20 ml extraction buffer plus 1x Complete™ (Roche Applied Science) and collected by centrifugation (as above). The final pellet weight was determined. The pellet was transferred with a spatula into a 10 ml syringe with a cut-off nozzle and pushed into a 50 ml reaction tube filled and cooled with liquid nitrogen. The remaining nitrogen was discarded and the "frozen spaghetti" were stored at -80°C. For extract preparation, the frozen cells were grinded with a nitrogen cooled electronic mortar (Retsch RM100, setting 5.5) for approx. 8-10 min. While grinding, 0.4 ml extraction buffer per gram wet weight (determined above) were added drop-wise. The fine powder was transferred into a small beaker and thawed under constant

stirring. After thawing, the paste was transferred to precooled SW55Ti Ultra-Clear™ tubes (Beckman) and centrifuged for 2 h at 4 °C and 82,500 x g average (Beckman Coulter Optima LK-80k ultracentrifuge, SW55Ti rotor, 29,500 rpm). The clear interphase was removed carefully with a needle and transferred to precooled Microfuge®Polyallomer TLA55 (Beckman or equivalent) tubes. The volume of extract was determined by comparing to water filed reaction tubes. Fine ground ammonium sulfate was added (337 mg per ml cell lysate) in three small portion steps (e.g., 50% + 25% + 25%). Each time, the sample was carefully mixed with a fresh inoculation loop and incubated rotation at 4°C for 20-30 min. After the powder was completely dissolved, the tubes were rotated for an additional 30 min and centrifuged for 20 min, 4 °C, at 26,000 rpm (30,300 x g average in TLA55 rotor). The supernatant was carefully removed and discarded. The precipitate was resuspended in 0.2–0.5 ml of dialysis buffer (20 mM HEPES–KOH, pH 7.5, 80 mM KCl, 10 or 20% (v/v) glycerol, 1 mM EGTA and freshly added 5 mM DTT, 0.1 mM phenylmethylsulfonyl fluoride (PMSF), and 1 mM sodium metabisulfite) and dialyzed (MWCO 3.5 kDa) twice for 1.5 h against 500 ml dialysis buffer. The protein content was determined by Nanodrop (Thermo Scientific) reading at 280 nm against dialysis buffer. The cell extract was diluted to 50 mg/ml with dialysis buffer and stored in one-time-use aliquots at -80°C. Of note, a Nanodrop read of 50 mg/ml protein was approximal equivalent to a protein concertation of 20 mg/ml as determined by Bradford assays. 10 µl extract were used for shifting reactions.

4.2.2 Histone octamer purification from *Drosophila melanogaster* embryos

Drosophila melanogaster histones were prepared from 12 h embryos as described in detail in (Faulhaber and Bernardi, 1967; Krietenstein et al., 2012; Simon and Felsenfeld, 1979). In brief, 50 g of 0-12 h *D. melanogaster* embryos plates were collected over the course of 3 d and stored at 4°C (Kunert and Brehm, 2008). For harvest, embryos were washed through a three sieve embryo collection apparatus, transferred into 3% sodium hypochlorite, and incubated for 3 min under constant stirring. After incubation the embryos were washed with 0.7% (w/v) NaCl, 0.04% (v/v) Triton X-100, and once with tap water for further 5 min. The so dechorionated embryos were stored at -80°C. For histone octamer purification, the embryos were resuspended in lysis buffer (15 mM HEPES–KOH, pH 7.5, 10 mM KCl, 5 mM $MgCl_2$, 0.1 mM EDTA, 0.5 mM EGTA, 17.5% (w/v) sucrose, 1 mM DTT, 0.2 mM PMSF, 1 mM sodium metabisulfite), homogenized 6x with Yamato LSC LH-21 homogenizator at 1000 rpm, and filter through Miracloth (Calbiochem-Novabiochem Corporation, La Jolla, CA). The nuclei were collected by centrifugation (6573 x g average, 15 min, 4°C), the nuclei pellet was carefully resuspended in 50 ml suc-buffer (15 mM HEPES–KOH, pH 7.5, 10 mM KCl, 5 mM $MgCl_2$, 0.05 mM EDTA, 0.25 mM EGTA, 1.2% (w/v)

sucrose, 1 mM DTT, 0.1 mM PMSF) without disturbing the lipid layer on the bottom of the pellet, centrifuged again (6573 x g average, 15 min, 4°C), resuspendend in final 30 ml suc-buffer per 50 g embryos, and dounced 20 times with a glass dounce homogenizer (Dounce Tissue Grinder, Wheaton/Fisher Scientific GmbH) fitted with a B pestle. For MNase fragmentation of chromatin, the sample was prewarmed to 26°C in a water bath for 5 min and 90 µl 1 M $CaCl_2$, 1x Complete™ (Roche Applied Science) and 30 µl 0.1 M PMSF were added. After addition of 125 µl of 0.59 U/ml MNase, the sample was incubated for 10 min at 26 °C. The digestion was stopped by adding 600 µl 0.5 M EDTA. Note: The MNase concentration and incubation time was titrated to yield mostly mono-nucleosomal fragments. The digested nuclei were centrifuged (6573 x g average, 15 min, 4°C), the pellet was resuspended in 6 ml TE (10 mM Tris-HCl, 1 mM EDTA) pH 7.6, 1 mM DTT, 0.2 mM PMSF (added freshly) for hypotonic lysis of nuclei and rotated for 30–45 min. The lysed nuclei were centrifuged for 30 min at 15,322 x g (Sorvall RC 6 plus, SS-34 rotor, 14,000 rpm), adjusted to 0.63 M KCl by adding 2 M KCl, 0.1 M potassium phosphate, pH 7.2, and centrifuge for 15 min at 15,322 x g average (SS-34 rotor or equivalent). Subsequently, the supernatant sample was consecutively filtered through 0.45 and 0.22 µm syringe filters and loaded on a hydroxylapatite column buffered in 0.63 M KCl, 0.1 M potassium phosphate, pH 7.2, 1 mM DTT using an ÄKTA purifier system (GE). The column was washed with 2 column volumes 0.63 M KCl, 0.1 M potassium phosphate, pH 7.2. The histone octamers were eluted with 2 M KCl, 0.1 M potassium phosphate, pH 7.2. The elution fractions were analyzed by 18% SDS-PAGE and fractions with highest amounts of pure histones were pooled and concentrated by ultrafiltration (10 kDa MWCO) to a volume of about 0.15–0.5 ml. An equal volume of 87% glycerol was added and Complete™ (Roche Applied Science) was adjusted to 1x. The histone octamers were stored at -20°C in a no "no-frost" freezer to avoid though-freeze cycles. The histone octamer concentrations were compared to BSA standards and older histone pools for quantitation. Further, the protein content was measured by Bradford assay and Nanodrop measurements. These quantifications were used as a starting point for chromatin assembly degree measurements. Of note, the histone batch of *D. melanogaster* histone octamers used in this thesis is exactly the one extensively titrated in Krietenstein et al., 2012.

4.2.3 Recombinant *H. sapiens* histones

Recombinant *H. sapiens* histones were purified and supplied by Kevin Schall (Hopfner laboratory) according to published protocols (Klinker et al., 2014b). Protein quality and quantity was compared to *D. melanogaster* histones by SDS-PAGE as described in (Krietenstein et al., 2012). Proper chromatin assembly degrees were confirmed by MNase digestion.

4.2.4 Recombinant *X. laevis*, wild type and tailless, and *S. cerevisiae* histone octamers

Recombinant *X. laevis*, wild type and tailless, and *S. cerevisiae* histone octamers were purchased from the Protein Expression and Purification Facility (PEPF, Colorado State University). Protein quality and quantity was compared to *D. melanogaster* histones by SDS-PAGE as described in (Krietenstein et al., 2012). Proper chromatin assembly degrees were confirmed by MNase digestion.

4.2.5 TAP-purification of endogenous chromatin-remodeling complexes.

ISW1a (TAP-Ioc3), ISW1b (TAP-Ioc2), CHD1 (TAP-Chd1), RSC (TAP-Rsc2), INO80 (TAP-Ino80) were purified via tandem affinity purification (TAP) as described (Smith and Peterson, 2003) by Shinya Watanabe (Peterson laboratory). ISW2 (FLAG-Isw2) was purified according to the manufacturer's protocol (Sigma), except that E-buffer (20 mM HEPES pH7.5, 350 mM NaCl, 10% glycerol, 0.1% Tween) was used during the entire purification. The ATPase activity of each remodeling complex was determined as described (Smith and Peterson, 2005), and the concentration of each remodeling complex was estimated relative to a standard SWI/SNF. If not otherwise indicated, remodelers were used at a concentration of 1:10, that is 9.2 nM remodeler per 92 nM nucleosomes.

4.2.6 Purification of recombinant INO80 complexes.

Recombinant INO80 complex was purified by Dr. Eustermann (Hopfner laboratory). Here, two baculovirus expression cassettes of all 15 INO80 subunits (Snf2 Ino80 main ATPase, AAA+ ATPases Rvb1 and Rvb2, actin-related-proteins Arp4, Arp5 and Arp8, Act1 (actin), TBP-associated factor 14 (Taf14), nonhistone protein 10 (Nhp10), and Ino80 subunits 1–6 (Ies1–Ies6)) were engineered using MultiBac technology (Fitzgerald et al. 2006). Integrity of respective bacmid preparations was verified by PCR and viruses were generated using SF9 cells (Bieniossek et al. 2008). Recombinant INO80 complex was expressed in High Five insect cells and purified with a double FLAG-tag at the C-terminus of Ino80's main ATPase (Shen et al. (2000). Briefly, cells were lysed in H-0.5 buffer (25 mM HEPES pH 8.0, 500 mM KCl, 10% glycerol, 1 mM MgCl2 and 1 mM DTT) and INO80 complex was eluted from Anti-FLAG M2 affinity gel with FLAG peptide (Sigma Aldrich). Subsequently, the complex was purified to homogeneity by MonoQ ion exchange and Superose 6 size exclusion chromatography (GE Healthcare) with H-0.2 buffer (25 mM HEPES pH 8.0, 200 mM KCl, 10% glycerol, 1 mM MgCl2 and 1 mM DTT). INO80 integrity, stoichiometry, and activity was verified by SDS PAGE, native PAGE, mass spectrometry, electron microscopy, and nucleosome sliding assays.

4.2.7 Purification of recombinant GRFs.

The protocol for GRF purification is published in Krietenstein et al., 2016, as follows: Reb1 and Abf1 coding sequences were amplified by PCR (primers Reb1for CCATGGCTTCAGGTC, Reb1rev CTCGAGTTAATTTTCTGTTTTC, Abf1 for CGAGGATCCCATGGACAAATTAGTCG, Abf1rev CGTCTCGAGCTATTGACCTCTTAATTC) from BY4741 genomic DNA pProEx HTa A (Invitrogen) via NcoI/AvaI for Reb1 or via BamHI/HindIII for Abf1, which adds a His_6-TEV tag to the N-terminus. Correct expression plasmid sequences were confirmed by Sanger sequencing. Plasmids were transformed into BL21cd+ cells (Stratagene). 50 ml LB were inoculated with a single clone and growen overnight. One liter LB medium with 600 mg/l ampicillin was inoculated with 20 ml of the over-night culture and cells were grown at 37 °C (Infors shaker, 120 rpm, 50 mm offset) to an OD_{600} of 0.4-0.6 (Ultrospec 2000, Pharmacia) and then induced by addition of IPTG (1 mM final concentration), further incubated for 1-4 h, collected by centrifugation (Cryofuge 6000i, Heraeus), resuspended in 40 ml lysis buffer (50 mM NaH_2PO_4, 300 mM NaCl, 10 mM imidazole, pH 8.0) transferred to a 50 ml tube, collected by centrifugation, and stored at -80° C. Pellets were resuspended in 10 ml lysis buffer per gram cell pellet followed by lysozyme (1 mg/ml final concentration) treatment for 30 min on ice and subsequent sonication (Branson sonifier 250D, 6 cycles of 10 s burst and 10 s break at 50% peak power on ice). Cell extracts were cleared by centrifugation (20 min, 20,000 g, SW34 rotor, Sorvall) and two filtration steps (45 and 20 µm, VWR).

Abf1 was purified by immobilized metal ion affinity chromatography (IMAC) using a 1 ml HisTrap HP column (GE, 17-5247-01) and an ÄKTA purifier system (GE). After loading the extract derived from 1 l cell culture, the column was washed with three column volumes of wash buffer (as lysis buffer but with 20 mM imidazole) and the protein eluted with elution buffer (as lysis buffer but with 250 mM imidazole). Abf1 containing fractions were determined by Coomassie SDS-PAGE, pooled and dialyzed over night against 1 l buffer C (20 mM Tris-HCl, pH 8.0, 0.25 M KCl, 1 mM EDTA, 10% glycerol), and applied to a HiTrap Heparin HP column (GE, 17-0406-01) pre-equilibrated with buffer C. After washing with three column volumes of buffer C, Abf1 was eluted with a gradient of KCl concentration from 0.25 to 1 M in buffer C. Abf1 eluted at approximately 0.5 M KCl as detected by Coomassie SDS-PAGE. Fractions containing Abf1 were pooled, dialyzed against E-buffer, snap frozen in liquid nitrogen and stored at -80°C. Final Abf1 concentration was 0.1 mg/ml as determined by Bradford assay with BSA as standard (Biorad, 500-0002).

Reb1 was purified via IMAC using about 1 ml Ni-NTA Agarose (Qiagen, 30210) in a self-packed gravity flow column (Biorad, 737-4711). After loading the extract derived from 1 l cell culture, the column was washed with 5 ml wash buffer and Reb1 was eluted with 2 ml elution buffer. Reb1 containing fractions were detected by Coomassie SDS-PAGE, pooled, and loaded onto an E-buffer equilibrated 24 ml Superdex 200 10/300 column (GE, cat #17-5175-01). Fractions containing purest Reb1 (Coomassie SDS-PAGE) were pooled, snap frozen in liquid nitrogen and stored at -80°C. The final Reb1 pool had a concentration of 1.32 mg/ml as determined by Bradford as for Abf1.

4.2.8 Salt gradient dialysis (SGD)

Salt gradient dialysis was performed as described in Krietenstein et al., 2012. In brief, plasmid library DNA and purified histone octamers were pooled in a final volume of 100 µl 1x high salt buffer (10 mM Tris–HCl, pH 7.6, 2 M NaCl, 1 mM EDTA) and BSA (20 µg) without IGEPAL CA630 at room temperature. The final solution was transferred to a floating dialysis chamber (MWCO 3.5 kDa cutoff) on 300 ml 1x high salt buffer with IGEPAL CA630 (0.05% v/v) and 300 µl β-mercaptoethanol. For overnight gradient dialysis, 3 L of low salt buffer (10 mM Tris–HCl, pH 7.6, 50 mM NaCl, 1 mM EDTA, 0.05% (w/v) IGEPAL CA630) were gradiantly added with a speed of 3.33 ml/min using a peristaltic pump. On the next day, the sample was dialyzed against 1 L fresh low salt buffer with 300 µl β-mercaptoethanol for 1 h at RT. Finally, the sample was transferred to a low-binding 1.5 ml reaction tube, centrifuged (4°C, 10 min, 10,000 rpm) and stored at 4°C. To high concentrations of histone octamers per DNA – too high assembly degrees – lead to aggregation and precipitation of chromatin. As an initial quality control, the DNA concentration was determined with an NanoDrop 1000 ® against low salt buffer. Good quality chromatin resulted in DNA concentrations of 100-50 ng/µl and was used for nucleosome reconstitution experiments.

4.2.9 Reconstitution reactions.

Reconstitution reactions were performed described in Krietenstein et al., 2012 with minor variation as written in Krietenstein et al., 2016: Reconstitution reactions were performed at 30 °C, usually in 100 µl and with the following final buffer conditions: 1 mM Tris-HCl, pH 7.6, 2 mM HEPES-KOH, pH 7.5, 19.6 mM HEPES-NaOH, pH 7.5, 13% glycerol, 2.7 mM DTT, 3 mM $MgCl_2$, 0.6 mM EGTA, 0.1 mM EDTA, 85.5 mM NaCl, 8 mM KCl, 0.005 % Tween, 0.1 mM $Na_2O_5S_2$, 10 mM $(NH_4)_2SO_4$, 3 mM ATP, 30 mM creatine phosphate (Sigma), 20 ng/µl creatine kinase (Roche Applied Science). For more details of individual reconstitution reactions see Supplementary Table 1. Purified factors and whole cell extracts (ug extract protein as determined by Bradford assay with

BSA as standard (Biorad, 500-0002)) were added to SGD chromatin (usually corresponding to 1 µg DNA reconstituted by SGD) as indicated in Supplementary Table 1 and the reaction was incubated for 2 h at 30 °C. The nucleosome concentration per reconstitution reaction was estimated to be 92 nM according to 1 µg DNA assembled by SGD at the full assembly degree (Krietenstein et al., 2012). Remodelers were usually used at a molar ratio per nucleosome of 1:10 unless indicated otherwise.

4.2.9.1 MNase treatment.

MNase treatment was performed as described in (Krietenstein et al., 2016). For MNase-anti-H3-ChIP-seq, reconstitution reactions were stopped by cross-linking with 0.05 % formaldehyde (Sigma-Aldrich, F8775-500ML) for 15 min at 30 °C followed by quenching with glycine (125 mM final concentration) at 30 °C for 5 min and treatment with 200 mU apyrase (NEB, M0398L) for 30 min. For MNase-seq, reconstitution reactions were stopped only by apyrase treatment at 30 °C for 30 min. All stopped reconstitution reactions were supplemented with CaCl2 (1.5 mM final concentration). Digestions with various MNase (Sigma Aldrich, N3755-500UN) concentrations (Supplementary Table 1) were at 30 °C for 5 min and stopped with EDTA (10 mM final concentration). MNase digestion efficiency was titrated to result in mainly mono-nucleosomal and some di-nucleosomal, in accord with published recommendations (Weiner et al., 2010).

4.2.10 Restriction enzyme accessibility assay.

KpnI accessibility assays were performed similar to (Lieleg et al., 2015) by spiking SGD chromatinized 601-25mer designer array into an aliquot of a reconstitution reaction, but bands were detected by Southern blotting and hybridization with a probe spanning the “cut small” fragment. Note that this probe will equally hybridize to the “cut large” and “uncut” fragment. The 601-25mer array was still part of the circular plasmid (2,659 bp backbone plus 4,937 bp 601-25mer array) during the KpnI digest and excised by XbaI and EcoRI after DNA purification.

4.2.11 Nucleosome sliding assay.

Nucleosome-sliding assays were performed as previously described (Watanabe et al., 2015). Mononucleosomes were reconstituted onto a 245bp ^{32}P-labeled DNA fragment containing the 601 nucleosome-positioning sequence at the fragment end. Mononucleosomes (1 nM) were incubated with Chd1 at 0, 0.125, 0.25, 0.375, 0.5 nM and 2 mM ATP in 70 mM NaCl, 10 mM Tris-HCl, pH 8.0, 5 mM $MgCl_2$, 0.1 mg/ml BSA and 1 mM DTT for 5 min at 30ºC. The reactions were quenched with 5% glycerol and 1 mg/ml salmon sperm DNA, incubated for 5 min at 30ºC, and resolved on 5% Native-PAGE in 0.5 X TBE.

4.2.12 Preparation of sequencing libraries.

The Illumina sequencing libraries were prepared as written in Krietenstein et al., 2016: MNase-anti-H3-ChIP-seq libraries were prepared as previously described (Krietenstein et al., 2016; Wal and Pugh, 2012), with the following specifications. (1) One microgram of anti-H3-antibody (Abcam, ab1791) was used per sample, (2) blunting/polishing reaction was performed at 20 °C with 1 U Klenow enzyme (NEB, M0210L), 3 U T4 DNA polymerase (NEB, M0203L), and 10 U T4-PNK (NEB, M0210L) in 50 µl 1x ligation buffer (NEB, B0202S) for 30 min, (3) nick repair step was omitted, (4) 2.5 µM NEB -NextSeq adapter were used in the ligation step, (5) the entire IP reaction was reverse-cross-linked and amplified by PCR, using NEB NextSeq primer with adopted annealing temperature (65 °C), and (6) dsDNA concentration was measured by Qubit® (LifeTechnologies) after 12 PCR cycles to estimate if DNA was amplified sufficiently for deep sequencing. Finally, end-repaired, A-tailed, adapter ligated, and indexed mono-nucleosomal DNA was isolated via gel electrophoresis and purified as described below for MNase-seq experiments.

For MNase-seq experiments, MNase digested samples were heated to 55 °C, supplemented with SDS (0.5% final concentration), glycogen (0.25 mg/ml final concentration), and 200 µg ProteinaseK (BioLine or Roche) and incubated overnight. $NaClO_4$ was added to a final concentration of 1 M and the volume adjusted to 250 µl with ddH_2O. In case of samples without WCEs, *E. coli* tRNA (Sigma) was added as carrier (2.1 µg/ml final concentration). DNA was phenol/chloroform purified, EtOH precipitated, resuspended in 100 µl TE buffer (10 mM Tris-HCl, pH 8.0, 1 mM EDTA), treated with 1 µg RNaseA (Roche, 10109169001) for 3 h at 37 °C, 2-propanol precipitated, resuspended in 32 µl ddH_2O and prepared for sequencing essentially according to the NEBNext® ChIP-Seq Library Prep Reagent Set for Illumina® protocol. Briefly, the purified DNA was end-repaired with Klenow (1 U, M0210L, NEB), T4 DNA polymerase (3 U, M0203L, NEB), and T4-PNK (10 U, M0210L, NEB), in 50 µl 1x ligation buffer (B0202S NEB) at 20 °C for 30 min. DNA was purified with 50 µl AMPureXP beads (Beckman Coulter) and 75 µl NaCl-PEG solution (20 % PEG-4000, 1.25 M NaCl), washed and eluted according to manufacturer's instructions. The DNA was resuspended in 50 µl A-tailing reaction (5 U Klenow Fragment (3' to 5' exo-), M0210L, NEB, 1x NEBuffer 2, B7002S, NEB), incubated for 30 min at 37 °C, rebound to the AMPureXP beads by addition of 125 µl NaCl-PEG solution, washed, eluted in 20 µl ddH_20 and transferred without beads to a fresh tube. NEBNext Adaptor (0.05 µM final concentration, E7335L and E750L, NEB) was ligated to A-tailed DNA with T4-Ligase (12 U, M0202L, NEB) in 30 µl 1x T4 Ligase reaction Buffer (B0202S, NEB) at 16 °C overnight**,** then cleaved by addition of USER™ Enzyme (3 U, M5505L, NEB) for 15 min at 37 °C. DNA was purified using 30 µl AMPureXP beads according to manufacturer's instructions. DNA was

resuspended in 30 µl ddH_2O and amplified by PCR (NEBNext Index 1-16, 18-23, 25 or 27 Primer for Illumina (0.5 µM, E7335L and E750L, NEB) and NEBNext Universal PCR Primer for Illumina (0.5 µM, E7335L and E750L, NEB), Phusion® High-Fidelity DNA Polymerase (1 U, M0530L, NEB), and Deoxynucleotide (dNTP) Solution Mix (2.5 mM, N0047S, NEB) in a final volume of 50 µl Phusion® HF Buffer (1x M0530L, NEB) with the following protocol: 98 °C for 30 s, 12 cycles (98 °C for 10 s, 65 °C for 30 s, 72 °C for 30 s) and paused. The dsDNA content of 1 µl PCR reaction was measured by Qubit® dsDNA HS Assay Kit (Q32851, Invitrogen). If DNA concentration was higher than 3 ng/µl, the reaction was incubated for final elongation for 5 min at 72 °C. In rare cases of lower DNA concentrations, two additional amplification cycles were added and DNA concentration controlled again by Qubit until resulting DNA concentration was >3 ng/µl. Adaptor-ligated mono-nucleosomal DNA was purified by 1.5 % agarose gel electrophoresis. The DNA was extracted from agarose with Freeze N Squeeze DNA Gel Extraction Spin Columns (732-6166, Bio-Rad) and purified by 2-propanol precipitation. The pellet was resuspended in 12 µl 0.1x TE and measured with Qubit® dsDNA HS Assay Kit (Q32851, Invitrogen). Concentrations were calculated assuming a DNA fragment length of 272 bp (147 bp mono-nucleosomal DNA and 122 bp sequencing adapter) and diluted to 10 nM. For sequencing, 10 nM solutions were pooled according to match sequencing lane requirements. Either the final pools or single samples were analyzed and quantified by BioAnalyzer (Agilent) or qPCR (using standard Illumina protocol).

4.2.13 ChIP-exo.

ChIP-exo of Abf1-TAP bound *in vivo* was performed by the Pugh laboratory in duplicates as described (Rhee and Pugh, 2011).

4.2.14 DNA sequencing.

Nucleosomal libraries were sequenced on either an Illumina Genome Analyzer IIx (LMU, single-end mode, 36 cycles), a HiSeq 1500 (LMU, single-end mode, 50 cycles), an Illumina HiSeq 2000 (PSU, single read mode, 40 cycles), or an Illumina NextSeq 500 (PSU, paired-end mode, 40 cycles, but only using Read1 for analysis after ascertaining that essentially the same patterns were observed using both reads). Sequences were mapped against the *S cerevisiae* genome obtained from Saccharomyces Genome Database (www.yeastgenome.org/download-data/sequence: S288C_reference_genome_R55-1-1_10-Nov-2006) using Bowtie (Langmead et al., 2009).

4.3 Bioinformatic methods

The bioinformatic methods used in this thesis are were developed by the Pugh laboratory and are essentially as described in Krietenstein et al. 2016. The published paragraphs were adopted from this publication and complemented wherever methods vary from published protocols.

4.3.1 Reference datasets, genomic coordinates and row sorting for heat maps

Reference data sets, genomic coordinates, like poly(dA)/(dT) elements and *in vivo* nucleosome positions, and row sorting for heat maps were computed by Megha Wal (Pugh Lab).

4.3.1.1 Reference datasets

Table 1 source and usage of reference data sets

Name	Usage	source
***In vivo* nucleosome positions α-H4-MNase-ChIP-seq**	Determination of *in vivo* nucleosome positions as alignment points for composite and heat map analysis	(Zhang et al., 2011)
Native nucleosome positions (MNase-seq)	Reference data set ("gold standard") for nucleosome positions of *in vitro* chromatin	(Zhang et al., 2011)
Reb1-ChIP-exo	*In vivo* Reb1 binding, row sorting	(Rhee and Pugh, 2011)
S288C reference genome	Sequencing read mapping, computation of poly(dA)/d(T) element distribution and DNA shape analysis	S288C_reference_genome_R55-1-1_10-Nov-2006 (Saccharomyces Genome Database)
NPS score		(Ioshikhes et al., 2006)

4.3.1.2 In vivo nucleosome position coordinates

In vivo and native MNase-sequencing data was retrieved (Zhang et al., 2011). Sequencing tag were shifted by 73 bp in 3' direction to obtain nucleosomal dyads. Nucleosome dyads were called from the *in vivo* data set with GenTrack software (Albert et al., 2008) and +1 nucleosomes were assigned according to their location in a +1 zone as defined in (Jiang and Pugh, 2009a) . Ribosomal proteins genes were excluded from the analysis since they organize their nucleosomes by a unique mechanism that was not reconstituted here (Reja et al., 2015). Such genes represent only 3% of all genes.

4.3.1.3 Unique poly(dT) and poly(dA) elements

Poly(dA:dT), poly(dT), and poly(dA) were defined by Megha Wal (Pugh laboratory) to be at least 6 nucleotides: 5'-TTTTTT-3' and 5'-AAAAAA-3'. Unique poly(dT) tracts were selected to be <200 bp upstream of the corresponding TSS and on the sense strand. Unique poly(dA) tracts were selected to be <200 bp upstream or <80 bp downstream of the corresponding TSS and on the sense strand. Only those TSS that had either poly(dT) or poly(dA) but not both on the sense strand were

selected. The limits of these intervals were set based on the observed average poly(dA:dT) distribution around all TSSs.

4.3.2 Row sorting for heat maps

4.3.2.1 +1/NFR tag ratios

+1/NFR tag ratios for SGD sample were based on a merge of four SGD datasets and calculated by Megha Wal (Pugh laboratory) using the following limits. For +1: number of tag 5' ends located ±30 bp from *in vivo* defined +1 nucleosome dyads; for NFR: number of tag 5' ends located within a calculated *in vivo* NFR midpoint zone (108-188 bp upstream of the +1 dyad). In a very small fraction of genes (rows), the sum of tags for the +1 and/or NFR regions as defined above had zero values. If both values were zero, then the row was removed. If only one of them was zero, then this sum was set to 1. This does not introduce a significant error as both zero and one are very small tag numbers, but it spares the respective gene from dropping out of the analysis.

4.3.2.2 INO80 effectiveness

Occupancy levels, computed by Megha Wal (Pugh laboratory), within ±30 bp from *in vivo*-defined +1 nucleosome dyads were summed up, and the ratios between the corresponding sums for experiments of SGD + INO80 (one experiment) and for SGD (four independent replicates were merged) were determined and used for row sorting. A similar pattern was obtained for another independent replicate of INO80. Sorting for the +2 and +3 nucleosome regions. +2 nucleosomes were assigned according to their location in a +2 zone as defined in[74]. +3 nucleosome dyads were defined as 165 bp from +2 nucleosome dyads.

4.3.2.3 In vivo Abf1 and Reb1 binding (row sorting)

In vivo Abf1 (this study) and Reb1 (Rhee and Pugh, 2011) binding, computed by Megha Wal (Pugh laboratory), were determined by genes bound by Abf1 or Reb1 *in vivo* were required to show Abf1 or Reb1 binding by *in vivo* ChIP-exo measurement, respectively, and to have a cognate recognition site. Rows/genes within heat maps were sorted based on Abf1 or Reb1 *in vivo* occupancy located <400 bp upstream of TSSs, which is where Abf1 and Reb1 are normally enriched.

In vivo NFR length

The nucleosomes positions were called as described in (Tirosh, 2012) and the distances between in vivo +1 nucleosome (4.3.1.2) and the next upstream nucleosome was calculated and used for *in vivo* NFR length sorting.

4.3.3 Data processing

4.3.3.1 in vitro MNase-seq data sets

Data processing was essentially done as described in (Zhang et al., 2011). Sequencing tags were shifted by 73 bp to obtain nucleosomal dyads. To plot nucleosome dyad densities at genomic features, the nucleosome dyad tag distribution within a window of +/-1 kbp around a respective feature, either +1 nucleosome position, poly(dT), or poly(dA) elements, was retrieved. Genes with a low or no tag density over the 2001 bp windows displayed very noisy nucleosome positioning profiles. This is presumably due to a low or only partial representation of these genes in our genomic plasmid library. Therefore, the bottom 5% genes with the lowest sequencing read density were removed form analysis. For the remaining genes, the sum over given windows was set to 1 and the values were centered by subtracting the mean. This normalizes for differential representation of genomic loci within our plasmid library. Nucleosome dyad distributions were binned in 5 bp intervals and smoothed with a 9-bin moving average.

For composite plots, the mean of nucleosome dyad tag densities for all genes in the analysis of one sample was computed. The resulting average nucleosome dyad distributions of all replicates was averaged and plotted with respective plot window sizes.

For heat maps, genes were sorted according to respective sorting, e.g., INO80 effectiveness. The mean nucleosome dyad tag distribution of every replicate for each single bin was computed. The heat maps were generated using R and grid function for nucleosome tag within a window of -600 to 800 bp around the alignment point. Note, the maximum color intensity within heat maps was set to the 90 percentile of nucleosome dyad tag values of all experiments plotted within one Figure.

4.3.3.2 In vivo Abf1 and Reb1 binding (heat maps)

Heat maps for Abf1 and Reb1 were essentially plotted as MNase-seq data (4.3.3.1) with minor variations. First, the replicates were merged prior processing. Second, since ChIP-exo determines factor binding at single base pair resolution, the first bp of a sequencing read was used for computation. Third, the 99 percentile of tag values was used to define the maximum value within one heat map.

4.3.3.3 Poly(dA)/(dT) elements (heat maps)

The center of unique poly(dA)/d(T) elements was computed. The value 1 was assigned to poly(dA) elements and the value -1 was assigned to poly(dT) elements and plotted with respect to +1 nucleosomes.

4.3.3.4 NDR width computation

NFR widths were computed by Megha Wal and determined as follows. First, from composite plots aligned separately by the *in vivo* -1 and +1 nucleosome location (smoothed using a bin size of 5 and a step size of 9), the X-axis values having a Y-axis local maximum around -1 (± 15 bp from -1 peak center), and +1 (± 15 bp from +1 peak center) was determined, respectively. Second, the X-axis value having a local Y-axis minimum within the NFR region (105-145 bp downstream of -1 dyad for the -1 aligned plot or upstream of +1 dyad for the +1 aligned plot) was determined as the NFR minimum. The X-axis values midway between the NFR minimum and the -1 or +1 maxima, respectively, defined the upstream and downstream borders of the NFR, respectively. The distance between these borders represented the NFR width, and the difference between this and the native NFR width was reported. Calculation for Extended Data Figure 6 was analogous but for a Y-axis local maximum around -1 (± 20 bp from -1 peak center), +1 (± 65 bp from +1 peak center) and a local Y-axis minimum within the NFR region (70-155 bp downstream of -1 dyad for the -1 aligned plot or upstream of +1 dyad for the +1 aligned plot).

4.3.3.5 NPS score

NPS correlation data was retrieved from a prior publication (Ioshikhes et al., 2006) and plotted relative to +1 nucleosome dyads. NPS information for 56 genes was missing.

4.3.3.6 DNA shape prediction

Genes were sorted by INO80 effectiveness for +1, +2 and +3 nucleosome positions and split in quartiles. The DNA shape was predicted for each quartile as described (Zhou et al., 2013) with DNAshapeR (Chiu et al., 2016). The mean DNA shape for each quartile was subjected to a 20 bp smoothing average and plotted.

5 Abbreviations

A	adenine
aa	amino acid
Abf	ARS-binding factors
amp	ampicillin
ARS	autonomously replicating sequence
ATP	adenosine triphosphate
bp	base pare
C. elegans	*Caenorhabditis elegans*
CenH3	Centromeric histone H3
Chd	Chromodomain-helicase-DNA-binding
ChIP	Chromatin Immunoprecipitation
Cse	Chromosome segregation
C-terminus	Carboxyl-terminus
D. melanogaster	*Drosophila melanogaster*
Da	Dalton
DNA	deoxyribonucleic acid
E. coli	*Escherichia coli*
EM	Electron microscopy
G	Guanine
GRF	General regulatory factor
H. sapiens	*Homo sapiens*
H1	Histone H1
H2A	Histone H2A
H2A.v	Histone H2A.v
H2A.X	Histone H2A.X
H2A.Z	Histone H2A.Z
H2B	Histone H2B
H3	Histone H3
H4	Histone H4
Ino	Inositol requiring
Isw	Imitation switch

LB	lysogeny broth
MNase	Micrococcal nuclease
NDR	nucleosome depleted region
NLR	nucleosomal repeat length
NRL	nucleosome free region
NPS	nucleosome positioning sequence
N-terminus	Amino-terminus
PCR	polymerase chain reaction
PIC	preinitiation complex
PTM	post-translational modification
RE	restriction enzyme
Reb	RNA polymerase I Enhancer Binding protein
RNA	ribonucleic acid
Rsc	remodels structure of chromatin
Rvb	RuVB-like
S. cerevisiae	*Saccharomyces cerevisiae*
S. pombe	*Schizosaccharomyces pombe*
SDS-PAGE	SDS-polyacrylamide gel electrophoresis
SHL	superhelix location
Swi/Snf	switching defective/sucrose non-fermentig
T	thymine
TF	transcription factor
TOR	target of rapamycin
tRNA	transfer RNA
TSS	transcription start site
U	Unit
UASp	upstream activation sequence
WCE	whole cell extract
wt	wild type
X. laevis	*Xenopus laevis*

6 Acknowledgments

First, I would like to thank PD Dr. Philipp Korber for the opportunity to work with him on these phenomenal projects. Not only he gave me excellent consult, but also enough freedom to develop myself. Philipp is a very thoughtful scientist and person, I hope I could soak up some of his attitude and critical thinking. Thanks for the good time with great science and lots of fun! I will miss our long discussions about science and life.

Next, I would like to thank Prof. Dr. Peter B. Becker, who followed this project with great interest and constructive criticism. Moreover, I strongly profited from the creative and friendly environment that he has created in his department and beyond, as well as from his strong support. Thank you very much!

I also would like to thank my thesis advisory committee, Prof. Dr. Axel Imhof, Dr. Tobias Straub, and Dr. Felix Müller-Planitz, for their valuable feedback and ample advice.

I am grateful to all of my collaborators: Prof. B. Franklin Pugh, PhD, Prof. Craig Peterson, PhD, Megha Wal, PhD, Shinya Watanabe, PhD, and Bongso Park for the great collaboration that is summarized in the first half of this thesis. Especially, Frank Pugh and Megha Wal for their hospitality at PennState University. Prof. Dr. Karl-Peter Hopfner, Dr. Sebastian Eustermann, and Kevin Schall for the collaborative work on recombinant INO80. Prof. Dr. Ulrich Gerland, Dr. Johannes Söding, Mark Herold, Dr. Brendan Osberg, and Dr. Johannes Nübler for different perspectives on my projects. Prof. Dr. Slobodan Barbaric and Dr. Sanja Musladin for a collaboration that lasts back to the era of Prof. Dr. Wolfram Hörz. Importantly, I would like to thank Dr. Stefan Krebs and Dr. Helmut Blum for DNA sequencing and their advice on deep-sequencing.

Next, I would like to thank all present and past members of the Becker department, with special thanks to members of the "North Lab": Dr. Christian Wippo, Dr. Julia Pointner, Sebastian Sommer, Dr. Corinna Lieleg, Maria Walker and Elisa Oberbeckmann from the Korber Group. Lisa-Maria Zink, Dr. Sebastian Pünzeler, Silke Mildner, Dr. Antonia Jack, Dr. Clemens Bönisch, and Prof. Dr. Sandra Hake for brainstorming ideas and creating a fun work atmosphere!

Last but not least, I would like to thank PD Dr. Philipp Korber and Dr. Christl Gaubitz for critical reading and commenting this thesis.

7 Curriculum Vitae

Removed in this public version.

8 Bibliography

Albert, I., Mavrich, T.N., Tomsho, L.P., Qi, J., Zanton, S.J., Schuster, S.C., and Pugh, B.F. (2007). Translational and rotational settings of H2A.Z nucleosomes across the Saccharomyces cerevisiae genome. Nature *446*, 572–576.

Albert, I., Wachi, S., Jiang, C., and Pugh, B.F. (2008). GeneTrack--a genomic data processing and visualization framework. Bioinformatics *24*, 1305–1306.

Albuquerque, C.P., Smolka, M.B., Payne, S.H., Bafna, V., Eng, J., and Zhou, H. (2008). A multidimensional chromatography technology for in-depth phosphoproteome analysis. Mol. Cell. Proteomics *7*, 1389–1396.

Almer, A., and Hörz, W. (1986). Nuclease hypersensitive regions with adjacent positioned nucleosomes mark the gene boundaries of the PHO5/PHO3 locus in yeast. EMBO J. *5*, 2681–2687.

Almer, A., Rudolph, H., Hinnen, A., and Hörz, W. (1986). Removal of positioned nucleosomes from the yeast PHO5 promoter upon PHO5 induction releases additional upstream activating DNA elements. EMBO J. *5*, 2689–2696.

Amor, D.J., Kalitsis, P., Sumer, H., and Andy Choo, K.H. (2004). Building the centromere: from foundation proteins to 3D organization. Trends Cell Biol. *14*, 359–368.

Arents, G., Burlingame, R.W., Wang, B.-C., Love, W.E., and Moudrianakis, E.N. (1991). The nucleosomal core histone octamer at 3.1 A resolution: a tripartite protein assembly and a left-handed superhelix. Proc. Natl. Acad. Sci. *88*, 10148–10152.

Badis, G., Chan, E.T., van Bakel, H., Pena-Castillo, L., Tillo, D., Tsui, K., Carlson, C.D., Gossett, A.J., Hasinoff, M.J., Warren, C.L., et al. (2008). A Library of Yeast Transcription Factor Motifs Reveals a Widespread Function for Rsc3 in Targeting Nucleosome Exclusion at Promoters. Mol. Cell *32*, 878–887.

Bai, L., Ondracka, A., and Cross, F.R. (2011). Multiple Sequence-Specific Factors Generate the Nucleosome-Depleted Region on CLN2 Promoter. Mol. Cell *42*, 465–476.

van Bakel, H., Tsui, K., Gebbia, M., Mnaimneh, S., Hughes, T.R., and Nislow, C. (2013). A Compendium of Nucleosome and Transcript Profiles Reveals Determinants of Chromatin Architecture and Transcription. PLoS Genet. *9*, e1003479.

Baldi, S., and Becker, P.B. (2013). The variant histone H2A.V of Drosophila—three roles, two guises. Chromosoma *122*, 245–258.

Bannister, A.J., and Kouzarides, T. (2011). Regulation of chromatin by histone modifications. Cell Res. *21*, 381–395.

Bartholomew, B. (2014). Regulating the Chromatin Landscape: Structural and Mechanistic Perspectives. Annu. Rev. Biochem. *83*, 671–696.

Basehoar, A.D., Zanton, S.J., and Pugh, B.F. (2004). Identification and distinct regulation of yeast TATA box-containing genes. Cell *116*, 699–709.

Becker, P.B., and Workman, J.L. (2013). Nucleosome Remodeling and Epigenetics. Cold Spring Harb. Perspect. Biol. *5*, a017905–a017905.

Becker, P.B., and Wu, C. (1992). Cell-free system for assembly of transcriptionally repressed chromatin from Drosophila embryos. Mol. Cell. Biol. *12*, 2241–2249.

Bell, O., Tiwari, V.K., Thomä, N.H., and Schübeler, D. (2011). Determinants and dynamics of genome accessibility. Nat Rev Genet *12*, 554–564.

Berbenetz, N.M., Nislow, C., and Brown, G.W. (2010). Diversity of Eukaryotic DNA Replication Origins Revealed by Genome-Wide Analysis of Chromatin Structure. PLoS Genet *6*, e1001092.

Biggar, K.K., and Li, S.S.-C. (2014). Non-histone protein methylation as a regulator of cellular signalling and function. Nat. Rev. Mol. Cell Biol. *16*, 5–17.

Blank, T.A., and Becker, P.B. (1995). Electrostatic Mechanism of Nucleosome Spacing. J. Mol. Biol. *252*, 305–313.

de Boer, C.G., and Hughes, T.R. (2014). Poly-dA:dT Tracts Form an In Vivo Nucleosomal Turnstile. PLoS ONE *9*, e110479.

Brogaard, K., Xi, L., Wang, J.-P., and Widom, J. (2012). A map of nucleosome positions in yeast at base-pair resolution. Nature.

Bussemaker, H.J., Li, H., and Siggia, E.D. (2001). Regulatory element detection using correlation with expression. Nat. Genet. *27*, 167–174.

Cairns, B.R. (2009). The logic of chromatin architecture and remodelling at promoters. Nature *461*, 193–198.

Celona, B., Weiner, A., Di Felice, F., Mancuso, F.M., Cesarini, E., Rossi, R.L., Gregory, L., Baban, D., Rossetti, G., Grianti, P., et al. (2011). Substantial Histone Reduction Modulates Genomewide Nucleosomal Occupancy and Global Transcriptional Output. PLoS Biol. *9*, e1001086.

Chasman, D.I., Lue, N.F., Buchman, A.R., LaPointe, J.W., Lorch, Y., and Kornberg, R.D. (1990). A yeast protein that influences the chromatin structure of UASG and functions as a powerful auxiliary gene activator. Genes Dev. *4*, 503–514.

Chen, S. -h., Albuquerque, C.P., Liang, J., Suhandynata, R.T., and Zhou, H. (2010). A Proteome-wide Analysis of Kinase-Substrate Network in the DNA Damage Response. J. Biol. Chem. *285*, 12803–12812.

Chiu, T.-P., Comoglio, F., Zhou, T., Yang, L., Paro, R., and Rohs, R. (2016). DNAshapeR: an R/Bioconductor package for DNA shape prediction and feature encoding. Bioinformatics *32*, 1211–1213.

Clapier, C.R., and Cairns, B.R. (2009). The Biology of Chromatin Remodeling Complexes. Annu. Rev. Biochem. *78*, 273–304.

Clapier, C.R., Nightingale, K.P., and Becker, P.B. (2001a). A critical epitope for substrate recognition by the nucleosome remodeling ATPase ISWI. Nucleic Acids Res.

Clapier, C.R., Langst, G., Corona, D.F.V., Becker, P.B., and Nightingale, K.P. (2001b). Critical Role for the Histone H4 N Terminus in Nucleosome Remodeling by ISWI. Mol. Cell. Biol. *21*, 875–883.

Cole, H.A., Howard, B.H., and Clark, D.J. (2011a). The centromeric nucleosome of budding yeast is perfectly positioned and covers the entire centromere. Proc. Natl. Acad. Sci. U. S. A. *108*, 12687–12692.

Cole, H.A., Howard, B.H., and Clark, D.J. (2011b). Activation-induced disruption of nucleosome position clusters on the coding regions of Gcn4-dependent genes extends into neighbouring genes. Nucleic Acids Res. *39*, 9521–9535.

Cole, H.A., Nagarajavel, V., and Clark, D.J. (2012). Perfect and imperfect nucleosome positioning in yeast. Chromatin Time Space *1819*, 639–643.

Dang, W., Kagalwala, M.N., and Bartholomew, B. (2006). Regulation of ISW2 by Concerted Action of Histone H4 Tail and Extranucleosomal DNA. Mol. Cell. Biol. *26*, 7388–7396.

Dion, M.F., Kaplan, T., Kim, M., Buratowski, S., Friedman, N., and Rando, O.J. (2007). Dynamics of Replication-Independent Histone Turnover in Budding Yeast. Science *315*, 1405–1408.

Dorigo, B., Schalch, T., Kulangara, A., Duda, S., Schroeder, R.R., and Richmond, T.J. (2004). Nucleosome Arrays Reveal the Two-Start Organization of the Chromatin Fiber. Science *306*, 1571–1573.

Drane, P., Ouararhni, K., Depaux, A., Shuaib, M., and Hamiche, A. (2010). The death-associated protein DAXX is a novel histone chaperone involved in the replication-independent deposition of H3.3. Genes Dev. *24*, 1253–1265.

Drew, H.R., and Travers, A.A. (1985). DNA bending and its relation to nucleosome positioning. J. Mol. Biol. *186*, 773–790.

Eaton, M.L., Galani, K., Kang, S., Bell, S.P., and MacAlpine, D.M. (2010). Conserved nucleosome positioning defines replication origins. Genes Dev. *24*, 748–753.

Elgin, S.C.R. (1981). DNAase I-hypersensitive sites of chromatin. Cell *27*, 413–415.

Ertel, F., Dirac-Svejstrup, A.B., Hertel, C.B., Blaschke, D., Svejstrup, J.Q., and Korber, P. (2010). In Vitro Reconstitution of PHO5 Promoter Chromatin Remodeling Points to a Role for Activator-Nucleosome Competition In Vivo. Mol. Cell. Biol. *30*, 4060–4076.

Fan, J.Y., Rangasamy, D., Luger, K., and Tremethick, D.J. (2004). H2A. Z alters the nucleosome surface to promote HP1α-mediated chromatin fiber folding. Mol. Cell *16*, 655–661.

Fascher, K.-D., Schmitz, J., and Hörz, W. (1993). Structural and Functional Requirements for the Chromatin Transition at the PHO5 Promoter in Saccharomyces cerevisiae upon PHO5 Activation. J. Mol. Biol. *231*, 658–667.

Faulhaber, I., and Bernardi, G. (1967). Chromatography of calf-thymus nucleoprotein on hydroxyapatite columns. Biochim. Biophys. Acta BBA - Protein Struct. *140*, 561–564.

Fazzio, T.G., Gelbart, M.E., and Tsukiyama, T. (2005). Two Distinct Mechanisms of Chromatin Interaction by the Isw2 Chromatin Remodeling Complex In Vivo. Mol. Cell. Biol. *25*, 9165–9174.

Finch, J.T., and Klug, A. (1976). Solenoidal model for superstructure in chromatin. Proc. Natl. Acad. Sci. U. S. A. *73*, 1897–1901.

Flaus, A. (2006). Identification of multiple distinct Snf2 subfamilies with conserved structural motifs. Nucleic Acids Res. *34*, 2887–2905.

Flaus, A., and Owen-Hughes, T. (2011). Mechanisms for ATP-dependent chromatin remodelling: The means to the end. FEBS J. *278*, 3579–3595.

Francis, N.J., Kingston, R.E., and Woodcock, C.L. (2004). Chromatin Compaction by a Polycomb Group Protein Complex. Science *306*, 1574–1577.

Fyodorov, D.V., and Kadonaga, J.T. (2002). Dynamics of ATP-dependent chromatin assembly by ACF. Nature *418*, 896–900.

Gangaraju, V.K., and Bartholomew, B. (2007). Dependency of ISW1a Chromatin Remodeling on Extranucleosomal DNA. Mol. Cell. Biol. *27*, 3217–3225.

Ganguli, D., Chereji, R.V., Iben, J.R., Cole, H.A., and Clark, D.J. (2014). RSC-dependent constructive and destructive interference between opposing arrays of phased nucleosomes in yeast. Genome Res. *24*, 1637–1649.

Givens, R.M., Lai, W.K.M., Rizzo, J.M., Bard, J.E., Mieczkowski, P.A., Leatherwood, J., Huberman, J.A., and Buck, M.J. (2012). Chromatin architectures at fission yeast transcriptional promoters and replication origins. Nucleic Acids Res. *40*, 7176–7189.

Gkikopoulos, T., Schofield, P., Singh, V., Pinskaya, M., Mellor, J., Smolle, M., Workman, J.L., Barton, G.J., and Owen-Hughes, T. (2011). A Role for Snf2-Related Nucleosome-Spacing Enzymes in Genome-Wide Nucleosome Organization. Science *333*, 1758–1760.

Goldberg, A.D., Banaszynski, L.A., Noh, K.-M., Lewis, P.W., Elsaesser, S.J., Stadler, S., Dewell, S., Law, M., Guo, X., Li, X., et al. (2010). Distinct Factors Control Histone Variant H3.3 Localization at Specific Genomic Regions. Cell *140*, 678–691.

Gonçalves, P.M., Maurer, K., Van Nieuw Amerongen, G., Bergkamp-Steffens, K., Mager, W.H., and Planta, R.J. (1996). C-terminal domains of general regulatory factors Abf1p and Rap1p in Saccharomyces cerevisiae display functional similarity. Mol. Microbiol. *19*, 535–543.

Gossett, A.J., and Lieb, J.D. (2012). In Vivo Effects of Histone H3 Depletion on Nucleosome Occupancy and Position in Saccharomyces cerevisiae. PLoS Genet. *8*, e1002771.

Gracey, L.E., Chen, Z.-Y., Maniar, J.M., Valouev, A., Sidow, A., Kay, M.A., and Fire, A.Z. (2010). An in vitro-identified high-affinity nucleosome-positioning signal is capable of transiently positioning a nucleosome in vivo. Epigenetics Chromatin *3*, 13–13.

Grigoryev, S.A., and Woodcock, C.L. (2012). Chromatin organization — The 30nm fiber. Exp. Cell Res. *318*, 1448–1455.

Guillemette, B., Bataille, A.R., Gévry, N., Adam, M., Blanchette, M., Robert, F., and Gaudreau, L. (2005). Variant Histone H2A.Z Is Globally Localized to the Promoters of Inactive Yeast Genes and Regulates Nucleosome Positioning. PLoS Biol *3*, e384.

Haberle, V., Li, N., Hadzhiev, Y., Plessy, C., Previti, C., Nepal, C., Gehrig, J., Dong, X., Akalin, A., Suzuki, A.M., et al. (2014). Two independent transcription initiation codes overlap on vertebrate core promoters. Nature *507*, 381–385.

Hahn, S., and Young, E.T. (2011). Transcriptional Regulation in Saccharomyces cerevisiae: Transcription Factor Regulation and Function, Mechanisms of Initiation, and Roles of Activators and Coactivators. Genetics *189*, 705–736.

Hake, S.B., and Allis, C.D. (2006). Histone H3 variants and their potential role in indexing mammalian genomes: The “H3 barcode hypothesis.” Proc. Natl. Acad. Sci. U. S. A. *103*, 6428–6435.

Hamiche, A., Kan, J.-G., Denn, C., Xiao, H., and Wu, C. (2001). Histone tails modulate nucleosome mobility and regulate ATP-dependent nucleosome sliding by NURF. Proc. Natl. Acad. Sci.

Hartley, P.D., and Madhani, H.D. (2009). Mechanisms that Specify Promoter Nucleosome Location and Identity. Cell *137*, 445–458.

Henikoff, S., and Ahmad, K. (2005). Assembly of variant histones into chromatin. Annu Rev Cell Dev Biol *21*, 133–153.

Hennig, B.P., Bendrin, K., Zhou, Y., and Fischer, T. (2012). Chd1 chromatin remodelers maintain nucleosome organization and repress cryptic transcription. EMBO Rep. *13*, 997–1003.

Hertel, C.B., Langst, G., Horz, W., and Korber, P. (2005). Nucleosome Stability at the Yeast PHO5 and PHO8 Promoters Correlates with Differential Cofactor Requirements for Chromatin Opening. Mol. Cell. Biol. *25*, 10755–10767.

Hewish, D.R., and Burgoyne, L.A. (1973). Chromatin sub-structure. The digestion of chromatin DNA at regularly spaced sites by a nuclear deoxyribonuclease. Biochem. Biophys. Res. Commun. *52*, 504–510.

van Holde, K.E. (1989). Chromatin (Springer, New York).

Hsieh, T.-H.S., Weiner, A., Lajoie, B., Dekker, J., Friedman, N., and Rando, O.J. (2015). Mapping Nucleosome Resolution Chromosome Folding in Yeast by Micro-C. Cell *162*, 108–119.

Hsieh, T.-H.S., Fudenberg, G., Goloborodko, A., and Rando, O.J. (2016). Micro-C XL: assaying chromosome conformation from the nucleosome to the entire genome. Nat Meth *13*, 1009–1011.

Hu, Z., Chen, K., Xia, Z., Chavez, M., Pal, S., Seol, J.-H., Chen, C.-C., Li, W., and Tyler, J.K. (2014). Nucleosome loss leads to global transcriptional up-regulation and genomic instability during yeast aging. Genes Dev. *28*, 396–408.

Huebert, D.J., Kuan, P.-F., Keleş, S., and Gasch, A.P. (2012). Dynamic Changes in Nucleosome Occupancy Are Not Predictive of Gene Expression Dynamics but Are Linked to Transcription and Chromatin Regulators. Mol. Cell. Biol. *32*, 1645–1653.

Hughes, A.L., and Rando, O.J. (2014). Mechanisms Underlying Nucleosome Positioning In Vivo. Annu. Rev. Biophys. *43*, 41–63.

Hughes, A.L., Jin, Y., Rando, O.J., and Struhl, K. (2012). A Functional Evolutionary Approach to Identify Determinants of Nucleosome Positioning: A Unifying Model for Establishing the Genome-wide Pattern. Mol. Cell *48*, 5–15.

Huisinga, K.L., and Pugh, B.F. (2007). A TATA binding protein regulatory network that governs transcription complex assembly. Genome Biol. *8*, R46.

Hwang, W.L., Deindl, S., Harada, B.T., and Zhuang, X. (2014). Histone H4 tail mediates allosteric regulation of nucleosome remodelling by linker DNA. Nature *512*, 213–217.

Imhof, A., and Bonaldi, T. (2005). “Chromatomics” the analysis of the chromatome. Mol. Biosyst. *1*, 112–116.

Ioshikhes, I.P., Albert, I., Zanton, S.J., and Pugh, B.F. (2006). Nucleosome positions predicted through comparative genomics. Nat. Genet. *38*, 1210–1215.

Ito, T., Tyler, J.K., Bulger, M., Kobayashi, R., and Kadonaga, J.T. (1996). ATP-facilitated chromatin assembly with a nucleoplasmin-like protein from Drosophila melanogaster. J. Biol. Chem. *271*, 25041–25048.

Jack, A.P.M., and Hake, S.B. (2014). Getting down to the core of histone modifications. Chromosoma *123*, 355–371.

Jenuwein, T., and Allis, C.D. (2001). Translating the Histone Code. Science *293*, 1074–1080.

Jha, S., and Dutta, A. (2009). RVB1/RVB2: Running Rings around Molecular Biology. Mol. Cell *34*, 521–533.

Jiang, C., and Pugh, B.F. (2009a). A compiled and systematic reference map of nucleosome positions across the Saccharomyces cerevisiae genome. Genome Biol *10*, R109.

Jiang, C., and Pugh, B.F. (2009b). Nucleosome positioning and gene regulation: advances through genomics. Nat. Rev. Genet. *10*, 161–172.

Jones, G.M., Stalker, J., Humphray, S., West, A., Cox, T., Rogers, J., Dunham, I., and Prelich, G. (2008). A systematic library for comprehensive overexpression screens in Saccharomyces cerevisiae. Nat. Methods *5*, 239–241.

Kagalwala, M.N., Glaus, B.J., Dang, W., Zofall, M., and Bartholomew, B. (2004). Topography of the ISW2–nucleosome complex: insights into nucleosome spacing and chromatin remodeling. EMBO J. *23*, 2092–2104.

Kaplan, N., Moore, I.K., Fondufe-Mittendorf, Y., Gossett, A.J., Tillo, D., Field, Y., LeProust, E.M., Hughes, T.R., Lieb, J.D., Widom, J., et al. (2009). The DNA-encoded nucleosome organization of a eukaryotic genome. Nature *458*, 362–366.

Keene, M.A., and Elgin, S.C.R. (1981). Micrococcal nuclease as a probe of DNA sequence organization and chromatin structure. Cell *27*, 57–64.

Klinker, H., Mueller-Planitz, F., Yang, R., Forné, I., Liu, C.-F., Nordenskiöld, L., and Becker, P.B. (2014a). ISWI Remodelling of Physiological Chromatin Fibres Acetylated at Lysine 16 of Histone H4. PLoS ONE *9*, e88411.

Klinker, H., Haas, C., Harrer, N., Becker, P.B., and Mueller-Planitz, F. (2014b). Rapid Purification of Recombinant Histones. PLoS ONE *9*, e104029.

Korber, P., and Barbaric, S. (2014). The yeast PHO5 promoter: from single locus to systems biology of a paradigm for gene regulation through chromatin. Nucleic Acids Res. *42*, 10888–10902.

Korber, P., and Horz, W. (2004). In Vitro Assembly of the Characteristic Chromatin Organization at the Yeast PHO5 Promoter by a Replication-independent Extract System. J. Biol. Chem. *279*, 35113–35120.

Kornberg, R.D. (1974). Chromatin Structure: A Repeating Unit of Histones and DNA. Science *184*, 868–871.

Kornberg, R.D., and Stryer, L. (1988). Statistical distributions of nucleosomes: nonrandom locations by a stochastic mechanism. Nucleic Acids Res. *16*, 6677–6690.

Korolev, N., Allahverdi, A., Yang, Y., Fan, Y., Lyubartsev, A.P., and Nordenskiöld, L. (2010). Electrostatic Origin of Salt-Induced Nucleosome Array Compaction. Biophys. J. *99*, 1896–1905.

Kouzarides, T. (2007). Chromatin Modifications and Their Function. Cell *128*, 693–705.

Krietenstein, N., Wippo, C.J., Lieleg, C., and Korber, P. (2012). Chapter Nine - Genome-Wide In Vitro Reconstitution of Yeast Chromatin with In Vivo-Like Nucleosome Positioning. In Methods in Enzymology, Carl Wu and C. David Allis, ed. (Academic Press), pp. 205–232.

Krietenstein, N., Wal, M., Watanabe, S., Park, B., Peterson, C.L., Pugh, B.F., and Korber, P. (2016). Genomic Nucleosome Organization Reconstituted with Pure Proteins. Cell *167*, 709–721.e12.

Krogan, N.J., Keogh, M.-C., Datta, N., Sawa, C., Ryan, O.W., Ding, H., Haw, R.A., Pootoolal, J., Tong, A., Canadien, V., et al. (2003). A Snf2 family ATPase complex required for recruitment of the histone H2A variant Htz1. Mol. Cell *12*, 1565–1576.

Kubik, S., Bruzzone, M.J., Jacquet, P., Falcone, J.-L., Rougemont, J., and Shore, D. (2015). Nucleosome Stability Distinguishes Two Different Promoter Types at All Protein-Coding Genes in Yeast. Mol. Cell *60*, 422–434.

Kulaeva, O.I., Gaykalova, D.A., and Studitsky, V.M. (2007). Transcription through chromatin by RNA polymerase II: Histone displacement and exchange. Chromatin Repair Remodel. Regul. *618*, 116–129.

Kunert, N., and Brehm, A. (2008). Mass Production of Drosophila Embryos and Chromatographic Purification of Native Protein Complexes. In Drosophila: Methods and Protocols, C. Dahmann, ed. (Totowa, NJ: Humana Press), pp. 359–371.

Langmead, B., Trapnell, C., Pop, M., and Salzberg, S.L. (2009). Ultrafast and memory-efficient alignment of short DNA sequences to the human genome. Genome Biol. *10*, 1–10.

Längst, G., Bonte, E.J., Corona, D.F.., and Becker, P.B. (1999). Nucleosome Movement by CHRAC and ISWI without Disruption or trans-Displacement of the Histone Octamer. Cell *97*, 843–852.

Lantermann, A.B., Straub, T., Stralfors, A., Yuan, G.-C., Ekwall, K., and Korber, P. (2010). Schizosaccharomyces pombe genome-wide nucleosome mapping reveals positioning mechanisms distinct from those of Saccharomyces cerevisiae. Nat Struct Mol Biol *17*, 251–257.

Lee, J.-S., Garrett, A.S., Yen, K., Takahashi, Y.-H., Hu, D., Jackson, J., Seidel, C., Pugh, B.F., and Shilatifard, A. (2012). Codependency of H2B monoubiquitination and nucleosome reassembly on Chd1. Genes Dev. *26*, 914–919.

Lee, W., Tillo, D., Bray, N., Morse, R.H., Davis, R.W., Hughes, T.R., and Nislow, C. (2007). A high-resolution atlas of nucleosome occupancy in yeast. Nat. Genet. *39*, 1235–1244.

Li, G., Levitus, M., Bustamante, C., and Widom, J. (2005). Rapid spontaneous accessibility of nucleosomal DNA. Nat Struct Mol Biol *12*, 46–53.

Li, M., Hada, A., Sen, P., Olufemi, L., Hall, M.A., Smith, B.Y., Forth, S., McKnight, J.N., Patel, A., Bowman, G.D., et al. (2015). Dynamic regulation of transcription factors by nucleosome remodeling. eLife *4*, e06249.

Lieb, J.D., Liu, X., Botstein, D., and Brown, P.O. (2001). Promoter-specific binding of Rap1 revealed by genome-wide maps of protein-DNA association. Nat Genet *28*, 327–334.

Lieleg, C., Krietenstein, N., Walker, M., and Korber, P. (2014). Nucleosome positioning in yeasts: methods, maps, and mechanisms. Chromosoma *124*, 131–151.

Lieleg, C., Ketterer, P., Nuebler, J., Ludwigsen, J., Gerland, U., Dietz, H., Mueller-Planitz, F., and Korber, P. (2015). Nucleosome Spacing Generated by ISWI and CHD1 Remodelers Is Constant Regardless of Nucleosome Density. Mol. Cell. Biol. *35*, 1588–1605.

Lopez-Perrote, A., Munoz-Hernandez, H., Gil, D., and Llorca, O. (2012). Conformational transitions regulate the exposure of a DNA-binding domain in the RuvBL1-RuvBL2 complex. Nucleic Acids Res. *40*, 11086–11099.

Lorch, Y., and Kornberg, R.D. (2015). Chromatin-remodeling and the initiation of transcription. Q. Rev. Biophys. *48*, 465–470.

Lorch, Y., Griesenbeck, J., Boeger, H., Maier-Davis, B., and Kornberg, R.D. (2011). Selective removal of promoter nucleosomes by the RSC chromatin-remodeling complex. Nat. Struct. Mol. Biol. *18*, 881–885.

Lorch, Y., Maier-Davis, B., and Kornberg, R.D. (2014). Role of DNA sequence in chromatin remodeling and the formation of nucleosome-free regions. Genes Dev. *28*, 2492–2497.

Lowary, P.T., and Widom, J. (1998). New DNA sequence rules for high affinity binding to histone octamer and sequence-directed nucleosome positioning. J. Mol. Biol. *276*, 19–42.

Luger, K. (2003). Structure and dynamic behavior of nucleosomes. Curr. Opin. Genet. Dev. *13*, 127–135.

Luger, K., Mäder, A.W., Richmond, R.K., Sargent, D.F., and Richmond, T.J. (1997). core particle at 2.8 A resolution. Nature *389*, 18.

Luger, K., Dechassa, M.L., and Tremethick, D.J. (2012). New insights into nucleosome and chromatin structure: an ordered state or a disordered affair? Nat. Rev. Mol. Cell Biol. *13*, 436–447.

Maeshima, K., Imai, R., Tamura, S., and Nozaki, T. (2014). Chromatin as dynamic 10-nm fibers. Chromosoma *123*, 225–237.

Maeshima, K., Rogge, R., Tamura, S., Joti, Y., Hikima, T., Szerlong, H., Krause, C., Herman, J., Seidel, E., DeLuca, J., et al. (2016a). Nucleosomal arrays self-assemble into supramolecular globular structures lacking 30-nm fibers. EMBO J.

Maeshima, K., Ide, S., Hibino, K., and Sasai, M. (2016b). Liquid-like behavior of chromatin. Genome Archit. Expr. *37*, 36–45.

Mavrich, T.N., Jiang, C., Ioshikhes, I.P., Li, X., Venters, B.J., Zanton, S.J., Tomsho, L.P., Qi, J., Glaser, R.L., Schuster, S.C., et al. (2008a). Nucleosome organization in the Drosophila genome. Nature *453*, 358–362.

Mavrich, T.N., Ioshikhes, I.P., Venters, B.J., Jiang, C., Tomsho, L.P., Qi, J., Schuster, S.C., Albert, I., and Pugh, B.F. (2008b). A barrier nucleosome model for statistical positioning of nucleosomes throughout the yeast genome. Genome Res. *18*, 1073–1083.

McKnight, J.N., Jenkins, K.R., Nodelman, I.M., Escobar, T., and Bowman, G.D. (2011). Extranucleosomal DNA Binding Directs Nucleosome Sliding by Chd1. Mol. Cell. Biol. *31*, 4746–4759.

Meluh, P.B., Yang, P., Glowczewski, L., Koshland, D., and Smith, M.M. (1998). Cse4p Is a Component of the Core Centromere of Saccharomyces cerevisiae. Cell *94*, 607–613.

Mizuguchi, G., Shen, X., Landry, J., Wu, W.-H., Sen, S., and Wu, Carl (2004). ATP-Driven Exchange of Histone H2AZ Variant Catalyzed by SWR1 Chromatin Remodeling Complex. Science *303*, 338–343.

Möbius, W., and Gerland, U. (2010). Quantitative Test of the Barrier Nucleosome Model for Statistical Positioning of Nucleosomes Up- and Downstream of Transcription Start Sites. PLoS Comput. Biol. *6*, e1000891.

Möbius, W., Osberg, B., Tsankov, A.M., Rando, O.J., and Gerland, U. (2013). Toward a unified physical model of nucleosome patterns flanking transcription start sites. Proc. Natl. Acad. Sci. *110*, 5719–5724.

Morse, R.H. (1999). Analysis of DNA Topology in Yeast Chromatin. In Chromatin Protocols, P.B. Becker, ed. (Totowa, NJ: Humana Press), pp. 379–393.

Moyle-Heyrman, G., Zaichuk, T., Xi, L., Zhang, Q., Uhlenbeck, O.C., Holmgren, R., Widom, J., and Wang, J.-P. (2013). Chemical map of Schizosaccharomyces pombe reveals species-specific features in nucleosome positioning. Proc. Natl. Acad. Sci. *110*, 20158–20163.

Narlikar, G.J., Sundaramoorthy, R., and Owen-Hughes, T. (2013). Mechanisms and Functions of ATP-Dependent Chromatin-Remodeling Enzymes. Cell *154*, 490–503.

Nishida, H., Katayama, T., Suzuki, Y., Kondo, S., and Horiuchi, H. (2013). Base composition and nucleosome density in exonic and intronic regions in genes of the filamentous ascomycetes Aspergillus nidulans and Aspergillus oryzae. Gene *525*, 5–10.

Öberg, C., Izzo, A., Schneider, R., Wrange, Ö., and Belikov, S. (2012). Linker Histone Subtypes Differ in Their Effect on Nucleosomal Spacing In Vivo. J. Mol. Biol. *419*, 183–197.

Ocampo, J., Chereji, R.V., Eriksson, P.R., and Clark, D.J. (2016). The ISW1 and CHD1 ATP-dependent chromatin remodelers compete to set nucleosome spacing *in vivo*. Nucleic Acids Res. gkw068.

Olins, A.L., Carlson, R.D., and Olins, D.E. (1975). Visualization of chromatin substructure: upsilon bodies. J. Cell Biol. *64*, 528–537.

Papamichos-Chronakis, M., Watanabe, S., Rando, O.J., and Peterson, C.L. (2011). Global Regulation of H2A.Z Localization by the INO80 Chromatin-Remodeling Enzyme Is Essential for Genome Integrity. Cell *144*, 200–213.

Park, D., Shivram, H., and Iyer, V.R. (2014). Chd1 co-localizes with early transcription elongation factors independently of H3K36 methylation and releases stalled RNA polymerase II at introns. Epigenetics Chromatin *7*, 1–11.

Parnell, T.J., Huff, J.T., and Cairns, B.R. (2008). RSC regulates nucleosome positioning at Pol II genes and density at Pol III genes. EMBO J. *27*, 100–110.

Parnell, T.J., Schlichter, A., Wilson, B.G., and Cairns, B.R. (2015). The chromatin remodelers RSC and ISW1 display functional and chromatin-based promoter antagonism. eLife *4*, e06073.

Patel, A., McKnight, J.N., Genzor, P., and Bowman, G.D. (2011). Identification of Residues in Chromodomain Helicase DNA-Binding Protein 1 (Chd1) Required for Coupling ATP Hydrolysis to Nucleosome Sliding. J. Biol. Chem. *286*, 43984–43993.

Petukhov, M., Dagkessamanskaja, A., Bommer, M., Barrett, T., Tsaneva, I., Yakimov, A., Quéval, R., Shvetsov, A., Khodorkovskiy, M., Käs, E., et al. (2012). Large-Scale Conformational Flexibility Determines the Properties of AAA+ TIP49 ATPases. Structure *20*, 1321–1331.

Pilpel, Y., Sudarsanam, P., and Church, G.M. (2001). Identifying regulatory networks by combinatorial analysis of promoter elements. Nat Genet *29*, 153–159.

Pointner, J., Persson, J., Prasad, P., Norman-Axelsson, U., Strålfors, A., Khorosjutina, O., Krietenstein, N., Svensson, J.P., Ekwall, K., and Korber, P. (2012). CHD1 remodelers regulate nucleosome spacing in vitro and align nucleosomal arrays over gene coding regions in S. pombe.

Raisner, R.M., Hartley, P.D., Meneghini, M.D., Bao, M.Z., Liu, C.L., Schreiber, S.L., Rando, O.J., and Madhani, H.D. (2005). Histone Variant H2A.Z Marks the 5′ Ends of Both Active and Inactive Genes in Euchromatin. Cell *123*, 233–248.

Rando, O.J. (2012). Combinatorial complexity in chromatin structure and function: revisiting the histone code. Curr. Opin. Genet. Dev. *22*, 148–155.

Rando, O.J., and Winston, F. (2012). Chromatin and Transcription in Yeast. Genetics *190*, 351–387.

Raveh-Sadka, T., Levo, M., Shabi, U., Shany, B., Keren, L., Lotan-Pompan, M., Zeevi, D., Sharon, E., Weinberger, A., and Segal, E. (2012). Manipulating nucleosome disfavoring sequences allows fine-tune regulation of gene expression in yeast. Nat. Genet. *44*, 743–750.

Reik, A., Schütz, G., and Stewart, A.F. (1991). Glucocorticoids are required for establishment and maintenance of an alteration in chromatin structure: induction leads to a reversible disruption of nucleosomes over an enhancer. EMBO J. *10*, 2569–2576.

Reja, R., Vinayachandran, V., Ghosh, S., and Pugh, B.F. (2015). Molecular mechanisms of ribosomal protein gene coregulation. Genes Dev. *29*, 1942–1954.

Rhee, H.S., and Pugh, B.F. (2011). Comprehensive Genome-wide Protein-DNA Interactions Detected at Single-Nucleotide Resolution. Cell *147*, 1408–1419.

Rhee, H.S., and Pugh, B.F. (2012). Genome-wide structure and organization of eukaryotic pre-initiation complexes. Nature *483*, 295–301.

Ricci, M.A., Manzo, C., García-Parajo, M.F., Lakadamyali, M., and Cosma, M.P. (2015). Chromatin Fibers Are Formed by Heterogeneous Groups of Nucleosomes In Vivo. Cell *160*, 1145–1158.

Richmond, T.J., Finch, J.T., Rushton, B., Rhodes, D., and Klug, A. (1984). Structure of the nucleosome core particle at 7 [angst] resolution. Nature *311*, 532–537.

Rippe, K., Schrader, A., Riede, P., Strohner, R., Lehmann, E., and Längst, G. (2007). DNA sequence-and conformation-directed positioning of nucleosomes by chromatin-remodeling complexes. Proc. Natl. Acad. Sci. *104*, 15635–15640.

Sadeh, R., Launer-Wachs, R., Wandel, H., Rahat, A., and Friedman, N. (2016). Elucidating Combinatorial Chromatin States at Single-Nucleosome Resolution. Mol. Cell *63*, 1080–1088.

Saha, A., Wittmeyer, J., and Cairns, B.R. (2005). Chromatin remodeling through directional DNA translocation from an internal nucleosomal site. Nat. Struct. Mol. Biol. *12*, 747–755.

Santisteban, M.S., Kalashnikova, T., and Smith, M.M. (2000). Histone H2A.Z Regulates Transcription and Is Partially Redundant with Nucleosome Remodeling Complexes. Cell *103*, 411–422.

Satchwell, S.C., Drew, H.R., and Travers, A.A. (1986). Sequence periodicities in chicken nucleosome core DNA. J. Mol. Biol. *191*, 659–675.

Schalch, T., Duda, S., Sargent, D.F., and Richmond, T.J. (2005). X-ray structure of a tetranucleosome and its implications for the chromatin fibre. Nature *436*, 138–141.

Schones, D.E., Cui, K., Cuddapah, S., Roh, T.-Y., Barski, A., Wang, Z., Wei, G., and Zhao, K. (2008). Dynamic Regulation of Nucleosome Positioning in the Human Genome. Cell *132*, 887–898.

Schwarz, P.M., and Hansen, J.C. (1994). Formation and stability of higher order chromatin structures. Contributions of the histone octamer. J. Biol. Chem. *269*, 16284–16289.

Segal, E., and Widom, J. (2009). Poly(dA:dT) tracts: major determinants of nucleosome organization. Curr. Opin. Struct. Biol. *19*, 65–71.

Segal, E., Fondufe-Mittendorf, Y., Chen, L., Thåström, A., Field, Y., Moore, I.K., Wang, J.-P.Z., and Widom, J. (2006). A genomic code for nucleosome positioning. Nature *442*, 772–778.

Sekinger, E.A., Moqtaderi, Z., and Struhl, K. (2005). Intrinsic Histone-DNA Interactions and Low Nucleosome Density Are Important for Preferential Accessibility of Promoter Regions in Yeast. Mol. Cell *18*, 735–748.

Sekiya, T., and Zaret, K.S. (2007). Repression by Groucho/TLE/Grg Proteins: Genomic Site Recruitment Generates Compacted Chromatin In Vitro and Impairs Activator Binding In Vivo. Mol. Cell *28*, 291–303.

Shen, C.-H., Leblanc, B.P., Alfieri, J.A., and Clark, D.J. (2001). Remodeling of Yeast CUP1 Chromatin Involves Activator-Dependent Repositioning of Nucleosomes over the Entire Gene and Flanking Sequences. Mol. Cell. Biol. *21*, 534–547.

Shen, X., Mizuguchi, G., Hamiche, A., and Wu, C. (2000). A chromatin remodelling complex involved in transcription and DNA processing. Nature.

Shim, Y.S., Choi, Y., Kang, K., Cho, K., Oh, S., Lee, J., Grewal, S.I.S., and Lee, D. (2012). Hrp3 controls nucleosome positioning to suppress non-coding transcription in eu- and heterochromatin. EMBO J. *31*, 4375–4387.

Shivaswamy, S., Bhinge, A., Zhao, Y., Jones, S., Hirst, M., and Iyer, V.R. (2008). Dynamic Remodeling of Individual Nucleosomes Across a Eukaryotic Genome in Response to Transcriptional Perturbation. PLoS Biol. *6*, e65.

Simic, R., Lindstrom, D.L., Tran, H.G., Roinick, K.L., Costa, P.J., Johnson, A.D., Hartzog, G.A., and Arndt, K.M. (2003). Chromatin remodeling protein Chd1 interacts with transcription elongation factors and localizes to transcribed genes. EMBO J. *22*, 1846–1856.

Simon, R.H., and Felsenfeld, G. (1979). A new procedure for purifying histone pairs H2A + H2B and H3 + H4 from chromatin using hydroxylapatite. Nucleic Acids Res. *6*, 689–696.

Siriaco, G., Deuring, R., Chioda, M., Becker, P.B., and Tamkun, J.W. (2009). Drosophila ISWI Regulates the Association of Histone H1 With Interphase Chromosomes in Vivo. Genetics *182*, 661.

Smith, C.L., and Peterson, C.L. (2003). Coupling tandem affinity purification and quantitative tyrosine iodination to determine subunit stoichiometry of protein complexes. Histone Modif. *31*, 104–109.

Smith, C.L., and Peterson, C.L. (2005). A Conserved Swi2/Snf2 ATPase Motif Couples ATP Hydrolysis to Chromatin Remodeling. Mol. Cell. Biol. *25*, 5880–5892.

Smolle, M., Venkatesh, S., Gogol, M.M., Li, H., Zhang, Y., Florens, L., Washburn, M.P., and Workman, J.L. (2012). Chromatin remodelers Isw1 and Chd1 maintain chromatin structure during transcription by preventing histone exchange. Nat Struct Mol Biol *19*, 884–892.

Song, F., Chen, P., Sun, D., Wang, M., Dong, L., Liang, D., Xu, R.-M., Zhu, P., and Li, G. (2014). Cryo-EM Study of the Chromatin Fiber Reveals a Double Helix Twisted by Tetranucleosomal Units. Science *344*, 376–380.

Soriano, I., Quintales, L., and Antequera, F. (2013). Clustered regulatory elements at nucleosome-depleted regions punctuate a constant nucleosomal landscape in Schizosaccharomyces pombe. BMC Genomics *14*, 813.

Soulard, A., Cremonesi, A., Moes, S., Schütz, F., Jenö, P., and Hall, M.N. (2010). The rapamycin-sensitive phosphoproteome reveals that TOR controls protein kinase A toward some but not all substrates. Mol. Biol. Cell *21*, 3475–3486.

Struhl, K., and Segal, E. (2013). Determinants of nucleosome positioning. Nat. Struct. Mol. Biol. *20*, 267–273.

Studitsky, V.M., Kassavetis, G.A., Geiduschek, E.P., and Felsenfeld, G. (1997). Mechanism of Transcription Through the Nucleosome by Eukaryotic RNA Polymerase. Science *278*, 1960–1963.

Swaney, D.L., Beltrao, P., Starita, L., Guo, A., Rush, J., Fields, S., Krogan, N.J., and Villen, J. (2013). Global analysis of phosphorylation and ubiquitylation cross-talk in protein degradation. Nat Meth *10*, 676–682.

Szenker, E., Ray-Gallet, D., and Almouzni, G. (2011). The double face of the histone variant H3. 3. Cell Res. *21*, 421–434.

Tagami, H., Ray-Gallet, D., Almouzni, G., and Nakatani, Y. (2004). Histone H3.1 and H3.3 Complexes Mediate Nucleosome Assembly Pathways Dependent or Independent of DNA Synthesis. Cell *116*, 51–61.

Thoma, F., Koller, T., and Klug, A. (1979). Involvement of histone H1 in the organization of the nucleosome and of the salt-dependent superstructures of chromatin. J. Cell Biol. *83*, 403–427.

Thomas, J.O., and Furber, V. (1976). Yeast chromatin structure. FEBS Lett. *66*, 274–280.

Tirosh, I. (2012). Computational Analysis of Nucleosome Positioning. In Chromatin Remodeling: Methods and Protocols, R.H. Morse, ed. (Totowa, NJ: Humana Press), pp. 443–449.

Tirosh, I., and Barkai, N. (2008). Two strategies for gene regulation by promoter nucleosomes. Genome Res. *18*, 1084–1091.

Tirosh, I., Sigal, N., and Barkai, N. (2010). Widespread remodeling of mid-coding sequence nucleosomes by Isw1. Genome Biol. *11*, 1–13.

Tolstorukov, M.Y., Colasanti, A.V., McCandlish, D.M., Olson, W.K., and Zhurkin, V.B. (2007). A Novel Roll-and-Slide Mechanism of DNA Folding in Chromatin: Implications for Nucleosome Positioning. J. Mol. Biol. *371*, 725–738.

Torigoe, S.E., Urwin, D.L., Ishii, H., Smith, D.E., and Kadonaga, J.T. (2011). Identification of a Rapidly Formed Nonnucleosomal Histone-DNA Intermediate that Is Converted into Chromatin by ACF. Mol. Cell *43*, 638–648.

Torigoe, S.E., Patel, A., Khuong, M.T., Bowman, G.D., and Kadonaga, J.T. (2013). ATP-dependent chromatin assembly is functionally distinct from chromatin remodeling. eLife *2*, e00863.

Tosi, A., Haas, C., Herzog, F., Gilmozzi, A., Berninghausen, O., Ungewickell, C., Gerhold, C.B., Lakomek, K., Aebersold, R., Beckmann, R., et al. (2013). Structure and Subunit Topology of the INO80 Chromatin Remodeler and Its Nucleosome Complex. Cell *154*, 1207–1219.

Tsankov, A., Yanagisawa, Y., Rhind, N., Regev, A., and Rando, O.J. (2011). Evolutionary divergence of intrinsic and trans-regulated nucleosome positioning sequences reveals plastic rules for chromatin organization. Genome Res. *21*, 1851–1862.

Tsankov, A.M., Thompson, D.A., Socha, A., Regev, A., and Rando, O.J. (2010). The Role of Nucleosome Positioning in the Evolution of Gene Regulation. PLoS Biol. *8*, e1000414.

Tsukiyama, T., Becker, P.B., and Wu, C. (1994). ATP-dependent nucleosome disruption at a heat-shock promoter mediated by binding of GAGA transcription factor. Nature *367*, 525–532.

Tsukiyama, T., Palmer, J., Landel, C.C., Shiloach, J., and Wu, C. (1999). Characterization of the imitation switch subfamily of ATP-dependent chromatin-remodeling factors in Saccharomyces cerevisiae. Genes Dev. *13*, 686–697.

Udugama, M., Sabri, A., and Bartholomew, B. (2011). The INO80 ATP-Dependent Chromatin Remodeling Complex Is a Nucleosome Spacing Factor. Mol. Cell. Biol. *31*, 662–673.

Valouev, A., Ichikawa, J., Tonthat, T., Stuart, J., Ranade, S., Peckham, H., Zeng, K., Malek, J.A., Costa, G., McKernan, K., et al. (2008). A high-resolution, nucleosome position map of C. elegans reveals a lack of universal sequence-dictated positioning. Genome Res. *18*, 1051–1063.

Valouev, A., Johnson, S.M., Boyd, S.D., Smith, C.L., Fire, A.Z., and Sidow, A. (2011). Determinants of nucleosome organization in primary human cells. Nature *474*, 516–520.

Varga-Weisz, P.D., Wilm, M., Bonte, E., Dumas, K., Mann, M., and Becker, P.B. (1997). Chromatin-remodelling factor CHRAC contains the ATPases ISWI and topoisomerase II. Nature *388*, 598–602.

Vary, J.C., Gangaraju, V.K., Qin, J., Landel, C.C., Kooperberg, C., Bartholomew, B., and Tsukiyama, T. (2003). Yeast Isw1p Forms Two Separable Complexes In Vivo. Mol. Cell. Biol. *23*, 80–91.

Venters, B.J., Wachi, S., Mavrich, T.N., Andersen, B.E., Jena, P., Sinnamon, A.J., Jain, P., Rolleri, N.S., Jiang, C., Hemeryck-Walsh, C., et al. (2011). A Comprehensive Genomic Binding Map of Gene and Chromatin Regulatory Proteins in Saccharomyces. Mol. Cell *41*, 480–492.

Verdin, E., and Ott, M. (2015). 50 years of protein acetylation: from gene regulation to epigenetics, metabolism and beyond. Nat. Rev. Mol. Cell Biol. *16*, 258–264.

Voong, L.N., Xi, L., Sebeson, A.C., Xiong, B., Wang, J.-P., and Wang, X. (2016). Insights into Nucleosome Organization in Mouse Embryonic Stem Cells through Chemical Mapping. Cell *167*, 1555–1570.e15.

Wal, M., and Pugh, B.F. (2012). Chapter Ten - Genome-Wide Mapping of Nucleosome Positions in Yeast Using High-Resolution MNase ChIP-Seq. In Methods in Enzymology, Carl Wu and C. David Allis, ed. (Academic Press), pp. 233–250.

Watanabe, S., Radman-Livaja, M., Rando, O.J., and Peterson, C.L. (2013). A Histone Acetylation Switch Regulates H2A.Z Deposition by the SWR-C Remodeling Enzyme. Science *340*, 195–199.

Watanabe, S., Tan, D., Lakshminarasimhan, M., Washburn, M.P., Hong, E.-J.E., Walz, T., and Peterson, C.L. (2015). Structural analyses of the chromatin remodeling enzymes INO80-C and SWR-C. Nat. Commun. *6*, 7108–7108.

Weber, C.M., and Henikoff, S. (2014). Histone variants: dynamic punctuation in transcription. Genes Dev. *28*, 672–682.

Weiner, A., Hughes, A., Yassour, M., Rando, O.J., and Friedman, N. (2010). High-resolution nucleosome mapping reveals transcription-dependent promoter packaging. Genome Res. *20*, 90–100.

Weiner, A., Chen, H.V., Liu, C.L., Rahat, A., Klien, A., Soares, L., Gudipati, M., Pfeffner, J., Regev, A., Buratowski, S., et al. (2012). Systematic Dissection of Roles for Chromatin Regulators in a Yeast Stress Response. PLoS Biol. *10*, e1001369.

Weiner, A., Hsieh, T.-H.S., Appleboim, A., Chen, H.V., Rahat, A., Amit, I., Rando, O.J., and Friedman, N. (2015). High-Resolution Chromatin Dynamics during a Yeast Stress Response. Mol. Cell *58*, 371–386.

Whitehouse, I., Rando, O.J., Delrow, J., and Tsukiyama, T. (2007). Chromatin remodelling at promoters suppresses antisense transcription. Nature *450*, 1031–1035.

Wippo, C.J., Israel, L., Watanabe, S., Hochheimer, A., Peterson, C.L., and Korber, P. (2011). The RSC chromatin remodelling enzyme has a unique role in directing the accurate positioning of nucleosomes. EMBO J. *30*, 1277–1288.

Woodcock, C.L. (1994). Chromatin fibers observed in situ in frozen hydrated sections. Native fiber diameter is not correlated with nucleosome repeat length. J. Cell Biol. *125*, 11–19.

Woodcock, C.L., Frado, L.-L., and Rattner, J.B. (1984). The higher-order structure of chromatin: evidence for a helical ribbon arrangement. J. Cell Biol. *99*, 42–52.

Wu, C. (1980). The 5' ends of Drosophila heat shock genes in chromatin are hypersensitive to DNase I. Nature *286*, 854–860.

Wu, R., and Li, H. (2010). Positioned and G/C-capped poly(dA:dT) tracts associate with the centers of nucleosome-free regions in yeast promoters. Genome Res. *20*, 473–484.

Wu, C., Wong, Y.-C., and Elgin, S.C.R. (1979). The chromatin structure of specific genes: II. Disruption of chromatin structure during gene activity. Cell *16*, 807–814.

Yamada, K., Frouws, T.D., Angst, B., Fitzgerald, D.J., DeLuca, C., Schimmele, K., Sargent, D.F., and Richmond, T.J. (2011). Structure and mechanism of the chromatin remodelling factor ISW1a. Nature *472*, 448–453.

Yen, K., Vinayachandran, V., Batta, K., Koerber, R.T., and Pugh, B.F. (2012). Genome-wide Nucleosome Specificity and Directionality of Chromatin Remodelers. Cell *149*, 1461–1473.

Yen, K., Vinayachandran, V., and Pugh, B.F. (2013). SWR-C and INO80 Chromatin Remodelers Recognize Nucleosome-free Regions Near +1 Nucleosomes. Cell *154*, 1246–1256.

Yu, L., and Morse, R.H. (1999). Chromatin opening and transactivator potentiation by RAP1 in Saccharomyces cerevisiae. Mol. Cell. Biol. *19*, 5279–5288.

Yuan, G.-C., Liu, Y.-J., Dion, M.F., Slack, M.D., Wu, L.F., Altschuler, S.J., and Rando, O.J. (2005). Genome-Scale Identification of Nucleosome Positions in S. cerevisiae. Science *309*, 626–630.

Zawadzki, K.A., Morozov, A.V., and Broach, J.R. (2009). Chromatin-dependent Transcription Factor Accessibility Rather than Nucleosome Remodeling Predominates during Global Transcriptional Restructuring in Saccharomyces cerevisiae. Mol. Biol. Cell *20*, 3503–3513.

Zentner, G.E., Tsukiyama, T., and Henikoff, S. (2013). ISWI and CHD Chromatin Remodelers Bind Promoters but Act in Gene Bodies. PLoS Genet *9*, e1003317.

Zhang, H., Roberts, D.N., and Cairns, B.R. (2005). Genome-Wide Dynamics of Htz1, a Histone H2A Variant that Poises Repressed/Basal Promoters for Activation through Histone Loss. Cell *123*, 219–231.

Zhang, Y., Moqtaderi, Z., Rattner, B.P., Euskirchen, G., Snyder, M., Kadonaga, J.T., Liu, X.S., and Struhl, K. (2009). Intrinsic histone-DNA interactions are not the major determinant of nucleosome positions in vivo. Nat. Struct. Mol. Biol. *16*, 847–852.

Zhang, Z., Wippo, C.J., Wal, M., Ward, E., Korber, P., and Pugh, B.F. (2011). A Packing Mechanism for Nucleosome Organization Reconstituted Across a Eukaryotic Genome. Science *332*, 977–980.

Zhao, J., Herrera-Diaz, J., and Gross, D.S. (2005). Domain-Wide Displacement of Histones by Activated Heat Shock Factor Occurs Independently of Swi/Snf and Is Not Correlated with RNA Polymerase II Density. Mol. Cell. Biol. *25*, 8985–8999.

Zhou, T., Yang, L., Lu, Y., Dror, I., Dantas Machado, A.C., Ghane, T., Di Felice, R., and Rohs, R. (2013). DNAshape: a method for the high-throughput prediction of DNA structural features on a genomic scale. Nucleic Acids Res. *41*, W56–W62.

Zhou, Y.-B., Gerchman, S.E., Ramakrishnan, V., Travers, A., and Muyldermans, S. (1998). Position and orientation of the globular domain of linker histone H5 on the nucleosome. Nature *395*, 402–405.

Zink, L.-M., and Hake, S.B. (2016). Histone variants: nuclear function and disease. Curr. Opin. Genet. Dev. *37*, 82–89.